



UNIVERSITÀ
DEGLI STUDI
DI PADOVA



Università degli Studi di Padova

Dipartimento dei Beni Culturali: Archeologia, Storia dell'Arte, del Cinema e della Musica

Corso di Studio Magistrale in
SCIENZE ARCHEOLOGICHE

Curriculum in
APPLIED SCIENCES TO CULTURAL HERITAGE MATERIALS AND SITES

Double Master Degree with the
Université Bordeaux Montaigne

Master Mention
ARCHEOLOGIE, SCIENCE POUR L'ARCHEOLOGIE
Parcours
ARCHÉOMETRIE

Archaeometrical study of mortars from public Roman structures in Verona

Co-supervisors:

Prof. Michele Secco,

Prof. Simone Dilaria

Prof. Caterina Previato

Prof. Rémy Chapoulie

Eliana Bridi

Candidate: Paula Stipanovic R.

Registr. number: 2039391

Academic Year 2022/2023

“Me inclino con nuevos ojos sobre las dos páginas blancas en las que mis números cuidadosos pusieron resultados de la sociedad. Y, con una sonrisa que guardo para mí, recuerdo que la vida, que tiene estas páginas con nombres de tejidos y dinero, con sus blancos, y sus trazos a regla y en letra, incluye también a los grandes navegantes, los grandes santos, los poetas de todas las épocas, todos ellos sin obra, la vasta prole expulsada de los que constituyen el valor del mundo.”

Fernando Pessoa (1985)

Libro del Desasosiego de Bernardo Soares.

Barcelona: Seix Barral.

List of Contents:

List of Contents:	1
List of Figures:	5
Acknowledgments	9
Abstract	11
1. Chapter I - Introduction	23
1.1. INTRODUCTION:	23
1.2. OBJECTIVES:	23
1.2.1. MAIN OBJECTIVE.....	23
1.2.2. SPECIFIC OBJECTIVES	24
1.3. BRIEF INTRODUCTION TO THE CONTEXT:	25
1.4. OUTCOMES:	25
1.5. DISSERTATION OUTLINE	26
2. Chapter II - State of art: Mortars	27
2.1. AN INTRODUCTION TO MORTARS: DEFINITIONS, COMPOSITION, AND PROPERTIES	27
2.1.1. INTRODUCTION TO MORTARS: AN OVERVIEW	27
2.1.2. KEY DEFINITIONS AND COMPONENTS	28
2.1.3. TYPES OF MORTARS	33
2.1.4. MORTARS' PROPERTIES.....	35
2.2. MORTARS THROUGHOUT HISTORY: AN INTRODUCTION TO ANCIENT MORTARS	38
2.3. PRODUCTION OF PROCESS OF LIME-BASED MORTARS IN ROMAN AGE	41
2.4. CURRENT APPROACH AND TECHNIQUES FOR MORTAR CHARACTERIZATION	50

2.4.1. MECHANICAL PROPERTIES OF MORTAR	52
2.4.2. CHEMICAL AND MINERALOGICAL PROPERTIES OF MORTAR.....	54
3. Chapter III - The city of Verona: history and architecture in the Roman age.....	57
3.1. POSITION AND HISTORY	57
3.2. THE ROMAN BUILDINGS OBJECT OF ANALYSIS.....	60
3.2.1. THE CITY WALLS AND GATES	60
3.3. THE FORUM AREA	64
3.3.1. THE CAPITOLIUM.....	65
3.4. THE BUILDINGS ON THE SAN PIETRO HILL	68
3.4.1. THE THEATRE	70
3.4.2. THE ODEON	76
3.4.3. THE TEMPLE IN CASTLE S. PIETRO	77
4. Chapter IV - Geological context of Verona.....	81
5. Chapter V - Population: an introduction to the Samples	85
5.1. AN INTRODUCTION TO MORTAR SAMPLES.....	85
5.2. SAMPLE SELECTION	99
6. Chapter VI - Methodology.....	105
6.1. ACTION PLAN OVERVIEW.....	105
6.1.1. COLORIMETRY	107
6.1.2. X-RAY DIFFRACTION (X.R.D.)	110
6.1.3. OPTICAL MICROSCOPY	112
6.1.4. SCANNING ELECTRON MICROSCOPY (S.E.M.).....	114
6.1.5. WET GRAVIMETRIC SEPARATION AND BINDER ANALYSIS.....	117
6.2. ANALYTICAL PROCEDURES.....	118
6.2.1. COLORIMETRY	118

6.2.2. X-RAY DIFFRACTION (X.R.D.)	118
6.2.3. THIN SECTION PRODUCTION	121
6.2.4. OPTICAL MICROSCOPY OBSERVATION	122
6.2.5. SCANNING ELECTRON MICROSCOPY (S.E.M.)	123
6.2.6. WET GRAVIMETRIC SEPARATION AND BINDER ANALYSIS	123
7. Chapter VII - Results:	129
7.1. COLORIMETRY	129
7.2. X-RAY DIFFRACTION (X.R.D.)	130
7.3. OPTICAL MICROSCOPY	133
7.4. SCANNING ELECTRON MICROSCOPY (S.E.M.)	144
7.5. BINDER ANALYSIS	151
7.5.1. X-RAY DIFFRACTION	151
7.5.2. SCANNING ELECTRON MICROSCOPY (S.E.M.)	154
8. Chapter VIII - Discussion and analysis of the results	157
9. Chapter IX - Conclusions.....	179
10. Chapter X - Bibliography	183
11. Chapter XI - Annex and Appendix	199

List of Figures:

FIGURE 1. THE BUILDING LIMES FORUM (2017) THE LIME CYCLE , THE BUILDING LIMES FORUM. AVAILABLE AT: HTTPS://WWW.BUILDINGLIMESFORUM.ORG.UK/WP-CONTENT/UPLOADS/2017/09/LIME-CYCLE-WEB-300X216.JPG (ACCESSED: 2023).....	42
FIGURE 2 LOCATION AND URBAN PLAN OF THE CITY OF VERONA (TAKEN FROM MARCHINI, G. P., 1978)	57
FIGURE 3 INITIAL SETTLEMENT IN SAN PIETRO HILL (BY G. DALLI. TAKEN FROM BOLLA, M. 2014.)	58
FIGURE 4 ROMAN URBAN SETTING (TAKEN FROM BOLLA, M. 2006)	59
FIGURE 5 URBAN PLAN. (TAKEN FROM CALCAGNI, A. C. 1999)	60
FIGURE 6 ILLUSTRATION OF PORTA LEONI (TAKEN FROM CAVALIERI MANASSE, G 1987).....	61
FIGURE 7 ACTUAL STATE OF PORTA LEONI. (TAKEN FROM CALCAGNI, A. C. 1999).....	62
FIGURE 8 ACTUAL STATE OF PORTA LEONI. (TAKEN FROM CALCAGNI, A. C., 1999).....	62
FIGURE 9 PORTA BORSARI. (TAKEN FROM BESCHI, L 1960)	63
FIGURE 10 FORUM AREA PLAN. (TAKEN FROM BASSO, P. 2019)	64
FIGURE 11 RECONSTRUCTION OF THE CAPITOLIUM (TAKEN FROM BOLLA, M. 2014).....	65
FIGURE 12 PLANNIMETRY OF THE ARCHAEOLOGICAL AREA OF THE CAPITOIUM (TAKEN FROM BOLLA, M. 2014).....	66
FIGURE 13 PRESERVED WALL OF "CATO" BUILDING (IMAGE TAKEN BY ELIANA BRIDI).....	66
FIGURE 14 FORUM AREA PLAN SHOWING THE LOCATION OF "CATO" BUILDING. (TAKEN FROM BASSO, P. ET AL 2019)	67
FIGURE 15 FORUM AREA PLAN. (TAKEN FROM BASSO, P. ET AL. 2019).	67
FIGURE 16 ILLUSTRATION OF SAN PIETRO HILL DURING ROMAN TIMES. (BY DALLI, G. TAKEN FROM BOLLA, M. 2016).....	68
FIGURE 17 CURRENT STATE OF SAN PIETRO HILL. (TAKEN FROM BOLLA, M. 2016).....	69
FIGURE 18 LOCATION OF THE ROMAN THEATRE (BASED ON THE PLAN IN BOLLA 2014)	70
FIGURE 19 ILLUSTRATION OF THE INTERIOR OF THE ROMAN THEATRE (BY MARCO CALDERINI, G. TAKEN FROM BOLLA, M. 2016)	71

FIGURE 20 ROMAN THEATRE AXONOMETRIC ILUSTRATION. (TAKEN FROM BOLLA, M. 2016)	72
FIGURE 21 ROMAN THEATRE ILLUSTRATION. (TAKEN FROM BOLLA, M. 2016)	73
FIGURE 22 AERIAL PICTURE OF ROMAN THEATRE (TAKEN FROM TRONCHIN, L. ET BEVILACQUA, A. 2022).	74
FIGURE 23 THEATRE SECTION. BY E. GUILLAUME (TAKEN FROM TRONCHIN, L. ET BEVILACQUA, A., 2022).	75
FIGURE 24 ROMAN THEATRE 1938. (TAKEN FROM BOLLA, M. 2016)	76
FIGURE 25 ODEUM SECTION. (TAKEN FROM CAVALIERI MANASSE, G., 1994).....	77
FIGURE 26 EXCAVATION IN CASTEL SAN PIETRO (TAKEN FROM CAVALIERI MANASSE, G., ET FRESCO, P. 2012).....	78
FIGURE 27. GEOLOGICAL PLAN OF VENETO	82
FIGURE 28. DIFFERENCE OF WAVELENGTH AND COLOR PERCEPTION. IMAGE TAKEN FROM: THE UNIVERSITY OF WAIKATO TE WHARE WĀNANGA O WAIKATO (2019) COLOURS OF LIGHT, SCIENCE LEARNING HUB. AVAILABLE AT: HTTPS://WWW.SCIENCELEARN.ORG.NZ/RESOURCES/47-COLOURS-OF-LIGHT	107
FIGURE 29. L*A*B* COORDINATE SYSTEM. IMAGE TAKEN FROM: GILCHRIST, A. AND NOBBS, J. (2017) ‘COLORIMETRY, THEORY’. FIG. 5. ENCYCLOPEDIA OF SPECTROSCOPY AND SPECTROMETRY, PP. 328–333. DOI:10.1016/B978-0-12-803224-4.00124-2.....	109
FIGURE 30. MOTIC AMERICA (2021) BIREFRINGENCE USING A MOTIC POLARIZING MICROSCOPE AND THE MICHEL-LÉVY CHART (PART I), MOTIC MICROSCOPES.	113
FIGURE 31 DAVIDSON, M.W. AND ABRAMOWITZ, M. (2002) ‘OPTICAL MICROSCOPY’, ENCYCLOPEDIA OF IMAGING SCIENCE AND TECHNOLOGY [PREPRINT]. DOI:10.1002/0471443395.IMG074.....	113
FIGURE 32. SHENG, Y. ET AL. (NO DATE) SCHEMATIC DIAGRAM OF SEM SETUP WITH VARIOUS COMPONENTS. SEM CONTAINS AN ..., A REVIEW OF COMPUTER MICRO-VISION-BASED PRECISIONMOTION MEASUREMENT: PRINCIPLES, CHARACTERISTICS ANDAPPLICATIONS. AVAILABLE AT: HTTPS://WWW.RESEARCH	115
FIGURE 33 ATRIA INNOVATION (2022) SOLUCIONES TECNOLÓGICAS PARA LA INDUSTRIA 4.0, ATRIA INNOVATION. AVAILABLE AT: HTTPS://WWW.ATRIAINNOVATION.COM/	116
FIGURE 34. SAMPLE MEASUREMENT BEFORE INITIAL GRINDING	118
FIGURE 35 FIG. XRD1. INSTRUMENTATION USED FOR INITIAL GRINDING	118

FIGURE 36. INITIAL GRINDING.....	119
FIGURE 37. XRD 3 AND 4. SECOND GRINDING PROCEDURE	120
FIGURE 38 XRD 5. SAMPLE MOUNTING INSTRUMENTATION.....	120
FIGURE 39. SAMPLES COS M2 AND COS M3 EMBEDDED IN RESIN ON ALUMINUM CONTAINER ..	121
FIGURE 40. CUT SAMPLES WITH GLUED GLASS ON THE HOT PLATE.	122
FIGURE 41 SAMPLES AR-M7 AND SG-M2 GENERAL OBVERVIEW OF DESCRIVED PROPERTIES	134
FIGURE 42 SAMPLES OD-M2 AND SGA-M3. SHOWING THE REPRESENTATIVE AGGREGATE FRACTION COMPOSITION OF GROUP N.1	135
FIGURE 43 SAMPLE LEO-M1 SHOWING THE PRINCIPAL CHARACTERISTICS OF SUB-GROUP 1A	137
FIGURE 44 SAMPLE AR-M3 SHOWING THE PRINCIPAL CHARACTERISTICS OF SUB-GROUP 1B	136
FIGURE 45 SAMPLE AR-M9 SHOWING THE PRINCIPAL CHARACTERISTICS OF SUB-GROUP 1C	136
FIGURE 46 SAMPLE LEO-M4 SHOWING THE DISTINCTIVE PROPERTIES OF GROUP N.2.....	137
FIGURE 47 SAMPLES COS-M4, COS-M3 AND COS-M2 SHOWING THE PROPERTIES AND CHARACTERISTICS OF SUB-GROUPS 2A, 2B AND 2C RESPECTIVELY.....	138
FIGURE 48 SAMPLES RED-M2, RM-M1 AND AR-M12.....	140
FIGURE 49 SAMPLE LEO-M5.....	141
FIGURE 50 SAMPLE AP-M1	¡ERROR! MARCADOR NO DEFINIDO.
FIGURE 51 SAMPLE COS-M5.....	142
FIGURE 52. SEM-EDS ANALYSIS OF SAMPLE AR-M13 DEMONSTRATING THE VARIATION IN THE CONPOSITION OF THE BINDER IN ANALYSED AREAS 6 AND 7.....	147
FIGURE 53 SAMPLE COS-M4 DEMONSTRATING THE CHARACTERISTIC PROPERTIES OF SEM GROUP II	148
FIGURE 54 SAMPLE AR-M12 DEMONSTRATING THE CHARACTERISTIC PROPERTIES OF SEM GROUP III.....	148
FIGURE 55 SAMPLE AR-M7 SEM-EDS ANALYSIS DEMONSTRATING A HIGH CONCENTRATION OF PHOSPHOROUS IN A ASH PARTICLE	149
FIGURE 56 SAMPLE CSP-M1 SEM ANALYSIS.....	150
FIGURE 57 SAMPLE COS-M7 SEM ANALYSIS	150
FIGURE 58 SAMPLE AP-M1 SEM ANALYSIS.....	150
FIGURE 59 SAMPLE COS-M5 SEM-EDS ANALYSIS DEMONSTRATING THE PRESENCE OF A DOLOMITIC BINDER	151

FIGURE 60. DIFRACTOGRAMS OF SAMPLES LEO-M5 AND AR-M7 DEMONSTRATING THE CLEAR DIFFERENCE BETWEEN THE IDENTIFIED MINERAL PHASES BETWEEN THE TWO BINDER..... 153

FIGURE 61 PCS ANALYSIS ON COLORIMETRY RESULTS DEPICTING MAIN GROUP, SUB-GROUPS, AND OUTLIERS. 158

FIGURE 62 PCA BIPLLOT OF XRPD RESULTS WITH IDENTIFIED CLUSTERS 159

Acknowledgments

I would like to express my deepest appreciation to my co-tutors; Prof. Michele Secco, Prof. Simone Dilaria, Prof. Caterina Previato, Prof. Rémy Chapoulie, and Ph.D. student Eliana Bridi, whose kindness, patience, and enthusiasms throughout this process are strongly appreciated. Without their disposition and will this endeavor would not have been possible.

I would like to extend my sincere thanks to Brigitte Spiteri and Giulia Ricci, who generously provided me with their gentle guidance and knowledge. I would also like to thank in a special way professor Lara Maritan for all her support and attention throughout these past two years.

Lastly, I'd like to thank my parents; Alberto and Camila, my siblings; Laina and Tingo, Tuttur and my friends. Without their support, kind words, and mostly their patience I could not have undertaken this journey. Thank you for your motivation and for guiding me when I felt lost.

Ringraziamenti

Vorrei esprimere il mio più profondo apprezzamento ai miei co-tutor; Prof. Michele Secco, Prof. Simone Dilaria, Prof. Caterina Previato, Prof. Rémy Chapoulie, e la studentessa di Ph.D. Eliana Bridi, la cui gentilezza, pazienza ed entusiasmo durante questo processo sono fortemente apprezzati. Senza la loro disposizione e volontà questo sforzo non sarebbe stato possibile.

Vorrei estendere i miei sinceri ringraziamenti a Brigitte Spiteri e Giulia Ricci, che mi hanno generosamente fornito la loro gentile guida e conoscenza. Vorrei anche ringraziare in modo speciale la professoressa Lara Maritan per tutto il suo sostegno e la sua attenzione in questi ultimi due anni.

Per concludere, vorrei ringraziare i miei genitori; Alberto e Camila, i miei fratelli; Laina e Tingo, Tuttur e i miei amici. Senza il loro supporto, le loro parole gentili e soprattutto la loro

pazienza non avrei potuto intraprendere questo viaggio. Grazie per la vostra motivazione e per avermi guidato quando mi sentivo perso.

Remerciements

Je voudrais exprimer ma plus profonde gratitude à mes co-tuteurs ; Professeur Michele Secco, Professeur Simone Dilaria, Professeur Caterina Previato, Professeur Rémy Chapoulie et l'étudiante du Ph.D. Eliana Bridi, leur gentillesse, patience et enthousiasme tout au long de ce processus sont fortement appréciés. Sans leur disposition et leur volonté, cet effort n'aurait pas été possible.

Je voudrais prolonger mes sincères remerciements à Brigitte Spiteri et Giulia Ricci, qui m'ont généreusement apporté leurs conseils et leurs connaissances. Je tiens également à remercier de manière particulière la professeure Lara Maritan pour tout son soutien et son attention tout au long de ces deux dernières années.

Pour finir, j'aimerais remercier mes parents ; Alberto et Camila, mes frères et sœurs ; Laina et Tingo, Tuttur et mes amis. Sans leur soutien, leurs paroles aimables et surtout leur patience, je n'aurais pas réussi à entreprendre ce voyage. Merci pour votre motivation et pour m'avoir guidé lorsque je me sentais perdu.

Abstract

The city of Verona, located in the Veneto region (north-eastern Italy), encountered an important urban development during the Roman age. The city's strategic location had a significant role in the Roman Empire's ability to rule the northern regions of Italy, providing it with a special status. Its growth and relevance were reflected in the public structures of the city. These structures demonstrate remarkable construction techniques and noteworthy durability. This endurance can attest to the high-quality materials and techniques implemented for its construction, one of them being the manufacturing process of mortars. Mortar production techniques are highly variable for several reasons, such as the available material, the magnitude of the construction, and both chronological and geographical aspects, to mention a few. The understanding of these procedures and techniques encompasses in this way an open window to the general knowledge of the construction processes and procedures (the general quality of the materials being used, the technical knowledge and techniques implemented, the relevance of the construction...).

However, the study of mortars, and more specifically their archaeometric analysis, is a topic developed only recently. The studies carried out on the analysis of these materials serve a great variety of purposes such as the identification of manufacturing techniques and recipes, understanding of mortar properties, or observation of degradation processes and restoration techniques, to mention a few. In this sense, these studies provide insightful information not only about past societies but also on the adequate preservation techniques that should be implemented for the conservation of structures. According to the specific objective of the individual studies, both *in-situ* and *ex-situ* analyses can be performed, and both destructive and non-destructive techniques are available, obtaining significantly different information.

The purpose of this dissertation is to perform an archaeometric assessment of the mortars employed in some of the most relevant Roman public constructions in the city of Verona. Mortar samples taken from significant archeological sites and buildings of the aforementioned city (including the Roman theatre, the Arena, Porta Leoni, and the Capitolium, to mention a few) were carefully analyzed throughout the implementation of a variety of techniques. The study was done

in order to comprehend the different mortars' composition, the manufacturing techniques, and the chemical processes and reactions involved in their production.

With this purpose in mind, the present project covered a series of topics, such as a literature review of mortar composition, properties, and manufacturing procedures. It also provided a general overview of the studied context. Through a bibliographical review, the general chronology and relevance of the studied constructions, as well as the city itself, has been established, to better comprehend the results obtained throughout the analysis according to the characteristics of each individual context.

Then, a multi-analytical procedure of characterization has been performed, on both the bulk samples (containing aggregates and binder) and the separated binder fractions of a certain number of selected samples. The study of the mortar samples has been carried out, as a general rule, from a general to a specific methodology, with the implementation of analytical techniques such as colorimetry, X-ray powder diffraction (XRPD), optical microscopy (OM) and scanning electron microscopy coupled with energy dispersive spectroscopy (SEM-EDS). The procedures here implemented followed the guidelines and methodologies already proposed and thoroughly described in literature by authors such as Arizzi, A., et Cultrone, G. (2021), Elsen, J. (2006), or Ergenç, D., et al. (2021).

Moreover, the results of the different techniques has been analyzed, statistically treated, and correlated with each other, to provide insightful information concerning the production techniques, the recipes used, and the related properties of mortars (also due to the possible presence of pozzolanic and parapozzolanic reactions).

The results obtained, and their corresponding interpretation and critical analysis, provided key information regarding both the manufacturing process, the raw materials used for production, and the reaction processes taking place in the mortars. On one hand, it was possible to observe a clear relation between the mineralogical profile of the analyzed samples, their chronology, and their purpose. In this sense, it was possible to hypothesize the implementation of different recipes, with different ingredients, being used according to the function of the mortar. In other words, the process of mortar production took into account the final purpose of this material in order to use a particular mixture that would satisfy the materials' requirements. Furthermore, its relation to the chronological contexts demonstrated a "learning curve" for mortar manufacturing. On it, it was

possible to observe a clear process of mastering mortar production techniques presenting hydraulic properties, and a subsequent loss of knowledge.

Additionally, due to the observed reactivity of the material and the presence of dedolomitization, it was possible to postulate the presence of alkaline carbonate reactions (ACR) taking place in the sampled mortars and responsible for the high levels of hydraulicity (attested by the presence of both C-S-H and M-S-H phases). This reaction was also favored by the manufacturing technique implemented in the production of the mortars. Indeed, according to the observations made, it was possible to hypothesize the implementation of a hot-lime mixing technique. Furthermore, the constant presence of phosphorous in mortar samples (likely derived from volcanic particles), as well as the presence of potassium (leached from K-feldspar microlites and the amorphous glass of the same volcanic particles), provided the means for C-S-H and M-S-H phase formation as a consequence of ACR.

Finally, the presence of secondary calcite in the voids of several of the mortar samples attested the occurrence of a decalcification phenomenon. However, as a consequence of the high amount of active magnesium derived from the dissolution of dolomite or dolomitic limestones by ACR, leading to the relevant precipitation of M-S-H, no increase of porosity was perceived.

Sommario

La città di Verona, situata nella regione del Veneto (Italia nord-orientale), conobbe un importante sviluppo urbano durante l'età Romana. La posizione strategica della città ebbe un ruolo significativo nella capacità dell'Impero Romano di governare le regioni a nord della penisola, conferendole uno status speciale. La sua crescita e rilevanza si riflettevano nelle strutture pubbliche della città. Queste strutture mostrano notevoli tecniche costruttive e rilevante durabilità. Questa resistenza può essere dovuta all'alta qualità dei materiali e alle tecniche implementate per la sua costruzione, una dei quali è il processo di produzione delle malte. Le tecniche di produzione delle malte sono molto variabili per diversi motivi, come la materia prima disponibile, l'importanza della costruzione e i fattori sia cronologici che geografici, per citarne alcuni. La comprensione di queste procedure e tecniche fornisce una chiave di lettura rilevante per conoscenza generale dei processi di costruzione (la qualità generale dei materiali utilizzati, la conoscenza diffusa e le tecniche implementate, la rilevanza della costruzioni...).

Tuttavia, lo studio delle malte, e più specificamente la loro analisi archeometrica, è un argomento sviluppato relativamente di recente. Gli studi condotti sull'analisi di questi materiali servono a una grande varietà di scopi come l'identificazione di tecniche e ricette di fabbricazione, la comprensione delle proprietà della malta o l'osservazione dei processi di degrado e delle tecniche di restauro, per citarne alcuni. In questo senso, questi studi forniscono informazioni approfondite non solo sulle società del passato ma anche sulle tecniche di restauro adeguate che dovrebbero essere implementate per la conservazione delle strutture. A seconda dell'obiettivo specifico dei singoli studi, possono essere eseguite analisi sia *in-situ* che *ex-situ*, e sono disponibili sia tecniche distruttive che non distruttive, ottenendo informazioni significativamente diverse.

Lo scopo della presente tesi è quello di effettuare uno studio archeometrico delle malte impiegate in alcune delle più rilevanti costruzioni pubbliche romane della città di Verona. Campioni di malta prelevati da siti archeologici ed edifici di significativa rilevanza della suddetta città (tra cui il teatro romano, l'Arena, Porta Leoni e il Capitolium, per citarne alcuni) sono stati attentamente analizzati attraverso l'implementazione di una varietà di tecniche. Ciò è stato fatto per comprendere la diversa composizione delle malte, le tecniche di produzione, i processi chimici e le reazioni instauratesi nelle fasi di presa ed indurimento.

Il progetto è consistito in una fase iniziale di revisione della letteratura sulla composizione, le proprietà e le procedure di produzione delle malte. È stata inoltre effettuata una panoramica generale del contesto in questione. Attraverso revisione bibliografica, si è definita la cronologia generale e la rilevanza delle costruzioni studiate, nonché della città stessa, per comprendere meglio i risultati ottenuti nel corso delle analisi a seconda delle caratteristiche di ciascun contesto.

Quindi, si è svolta una procedura di caratterizzazione multi-analitica dei materiali, sia sui campioni totali (contenenti aggregati e legante) che sulla frazione legante separata di un certo numero di campioni selezionati. Lo studio dei campioni di malta si è effettuato, di norma, da un punto di vista generale a quelle più specifici, con l'implementazione di tecniche analitiche quali colorimetria, diffrazione ai raggi X delle polveri (XRPD), microscopia ottica (OM), e microscopia elettronica a scansione accoppiata a spettroscopia a dispersione di energia (SEM-EDS). Le procedure qui implementate seguono le linee guida e le metodologie già proposte e ampiamente descritte in letteratura da autori come Arizzi, A., et Cultrone, G. (2021), Elsen, J. (2006), o Ergenç, D., et al. (2021).

I risultati delle diverse tecniche sono stati analizzati, trattati statisticamente e correlati tra loro, per fornire informazioni approfondite riguardanti le tecniche di produzione, le ricette utilizzate e le conseguenti proprietà delle malte (legate alla possibile presenza di reazioni pozzolaniche e parapozzolaniche).

I risultati ottenuti, e la loro corrispondente lettura e analisi critica, hanno fornito informazioni chiave riguardanti sia i processi di fabbricazione, sia le materie prime utilizzate per la produzione, sia i processi di reazione avvenuti nelle malte. Da un lato è stato possibile osservare una chiara correlazione tra il profilo mineralogico dei campioni analizzati, la loro cronologia e la loro destinazione d'uso. In questo senso è possibile ipotizzare la realizzazione di ricette diverse, con ingredienti diversi, da utilizzare a seconda della funzione della malta. In altre parole, il processo di produzione della malta teneva conto dello scopo finale di questo materiale per utilizzare una miscela particolare che soddisfacesse i requisiti finali del contesto costruttivo. Inoltre, la sua relazione la cronologia costruttiva ha mostrato una “curva di apprendimento” per la produzione delle malte, con una rilevante padronanza delle tecniche di produzione di malte dopo una fase iniziale di sperimentazione, seguita da una successiva perdita di conoscenza.

Inoltre, alla luce della reattività osservata nei materiali e della presenza di fenomeni di dedolomitizzazione, è stato possibile postulare la presenza di reazioni alcali-carbonato (ACR) nelle malte campionate, responsabili degli elevati livelli di idraulica (attestati dalla presenza di entrambe di fasi C-S-H e M-S-H). Queste reazioni sono state favorite dalle tecniche produttive adottate. Infatti, alla luce delle osservazioni effettuate, è stato possibile ipotizzare l'implementazione della tecnica della miscela a calce calda. Inoltre, la presenza costante di fosforo nei campioni di malta (probabilmente derivato dai materiali vulcanici presenti), così come la presenza di potassio (come conseguenza della lisciviazione dai microliti di K-feldspato e dalle matrici silicatiche amorfe dei materiali vulcanici stessi), hanno fornito gli attivanti chimici per la formazione di fasi C-S-H e M-S-H come conseguenza dell'ACR.

Infine, la presenza di calcite secondaria in numerosi vuoti dei campioni di malta attesta il verificarsi di fenomeni di decalcificazione. Tuttavia, la precipitazione di rilevanti aliquote di fasi M-S-H come conseguenza dell'elevata quantità di magnesio attivo per dedolomitizzazione di dolomie e calcari dolomitici non ha prodotto alcun aumento rilevante di porosità.

Résumé

La ville de Vérone, située dans la région de Vénétie (nord-est de l'Italie), a connu un développement urbain important à l'époque romaine. L'emplacement stratégique de la ville a joué un rôle important dans la capacité de l'Empire romain à gouverner les régions du nord de l'Italie, lui conférant un statut particulier. Sa croissance et sa ampleur se reflétaient dans les structures publiques de la ville. Ces structures font preuve de techniques de construction maîtrisées et d'une durabilité remarquable. Cette endurance atteste de la qualité des matériaux et des techniques mises en œuvre pour la construction, parmi lesquelles le processus de fabrication des mortiers. Les techniques de production de mortier sont très variables pour plusieurs raisons, telles que le matériau disponible, l'ampleur de la construction et les aspects chronologiques et géographiques, pour n'en citer que quelques-unes. La compréhension de ces procédés et techniques ouvre ainsi une fenêtre sur la connaissance générale des processus et procédures de construction (la qualité générale des matériaux utilisés, le savoir-faire et les techniques mises en œuvre, la pertinence de la construction...).

Cependant, l'étude des mortiers, et plus particulièrement leur analyse archéométrique, est un sujet développé récemment. Les études réalisées sur l'analyse de ces matériaux servent à des fins très diverses telles que – entre autre - l'identification des techniques et recettes de fabrication, la compréhension des propriétés des mortiers ou l'observation des processus de dégradation et des techniques de restauration. En ce sens, ces études fournissent des informations pertinentes non seulement sur les sociétés passées, mais également sur les techniques de préservation adéquates qui devraient être mises en œuvre pour la conservation des structures. Selon l'objectif spécifique de chaque étude, des analyses *in situ* et *ex situ* peuvent être effectuées, et des techniques destructives et non destructives sont disponibles, obtenant des informations significativement différentes.

Le but de cette thèse est de réaliser une évaluation archéométrique des mortiers utilisés dans certaines des constructions publiques romaines les plus importantes de la ville de Vérone. Des échantillons de mortier prélevés sur des sites archéologiques et des bâtiments importants de la ville susmentionnée (notamment le théâtre romain, les arènes, la Porta Leoni et le Capitole, pour n'en citer que quelques-uns) ont été soigneusement analysés tout au long de la mise en œuvre de diverses techniques. L'étude a été réalisée afin de comprendre la composition des différents

mortiers, les techniques de fabrication ainsi que les processus et réactions chimiques impliqués dans leur production.

Dans cet objectif, le présent projet a couvert une série de sujets, tels qu'une revue de la littérature sur la composition, les propriétés et les procédures de fabrication du mortier. Il donne également un aperçu général du contexte en question. À travers une revue bibliographique, la chronologie générale et la pertinence des constructions étudiées, ainsi que de la ville, seront établies, pour mieux comprendre les résultats obtenus tout au long de l'analyse en correspondance avec les caractéristiques de son contexte individuel. De plus, la reconstruction d'un contexte géographique aura lieu, puisqu'elle définit dans une large mesure les résultats possibles obtenus.

Additionallement, une procédure multi-analytique aura lieu, à la fois sur l'échantillon global (contenant des granulats et du liant) et sur la fraction de liant séparée d'un certain nombre d'échantillons sélectionnés. L'étude des échantillons de mortier sera réalisée, en règle générale, d'une méthodologie générale à une méthodologie spécifique, avec la mise en œuvre de techniques analytiques telles que la colorimétrie, la diffraction des rayons X sur poudre (XRPD), la microscopie optique (OM) et la microscopie électronique à balayage couplé à la spectroscopie à dispersion d'énergie (MEB-EDS). Les procédures mises en œuvre dans le présent travail suivent les lignes directrices et méthodologies déjà proposées et largement décrites dans la littérature par des auteurs comme Arizzi, A., et Cultrone, G. (2021), Elsen, J. (2006), ou Ergenç, D., et al. (2021).

De plus, les résultats des différentes techniques ont été analysés, traités statistiquement et corrélés entre eux, pour fournir des informations pertinentes sur les techniques de production, les recettes utilisées et les propriétés associées des mortiers (également en raison de la présence possible de matières pouzzolaniques et réactions parapouzzolaniques).

Les résultats obtenus, ainsi que leur interprétation et analyse critique correspondante, ont fourni des informations clés sur le processus de fabrication, les matières premières utilisées pour la production et les processus de réaction se déroulant dans les mortiers. D'une part, il a été possible d'observer une relation claire entre le profil minéralogique des échantillons analysés, leur chronologie et leur destination. En ce sens, il était possible d'émettre l'hypothèse de la mise en œuvre de différentes recettes, avec différents ingrédients, utilisés en fonction de la fonction du mortier. En d'autres termes, le processus de production du mortier a pris en compte la destination finale de ce matériau afin d'utiliser un mélange particulier qui satisferait aux exigences du

matériau. De plus, sa relation avec les contextes chronologiques a démontré une « courbe d'apprentissage » pour la fabrication du mortier. On y a pu observer un net processus de maîtrise des techniques de production de mortiers présentant des propriétés hydrauliques, et une perte de connaissances qui en a résulté.

D'abondant, en raison de la réactivité observée du matériau et de la présence de dédolomitisation, il a été possible de postuler la présence de réactions carbonatées alcalines (ACR) se produisant dans les mortiers échantillonnés et responsables des niveaux élevés d'hydraulicité (attestés par la présence de phases C-S-H et M-S-H). Cette réaction a également été favorisée par la technique de fabrication mise en œuvre dans la fabrication des mortiers. En effet, d'après les observations réalisées, il a été possible d'émettre l'hypothèse de la mise en œuvre d'une technique de malaxage à chaud-chaux. De plus, la présence constante de phosphore dans les échantillons de mortier (probablement dérivé de particules volcaniques), ainsi que la présence de potassium (lixiviés des microlites de feldspath potassique et du verre amorphe de ces mêmes particules volcaniques), ont fourni les moyens pour le C-S-H et le M-S-H. formation de phase suite à l'ACR.

Finalement, la présence de calcite secondaire dans les vides de plusieurs échantillons de mortier atteste de l'apparition d'un phénomène de décalcification. Cependant, en raison de la quantité élevée de magnésium actif dérivée de la dissolution de la dolomite ou des calcaires dolomitiques par ACR, conduisant à la précipitation correspondante de M-S-H, aucune augmentation de la porosité n'a été perçue.

1. Chapter I - Introduction

1.1. INTRODUCTION:

The city of Verona, located in the Veneto region (north-eastern Italy), encountered an important urban development during the Roman age. Its strategic position contributed to the relevant importance of the city, as its location constituted a key point in the control of the northern territory of the Roman Empire. It is because of the high status and relevance that a series of public structures of great significance were constructed during this period. Some of these constructions, such as the Arena and the theatre, are partially standing up to this day, demonstrating the remarkable construction techniques and noteworthy durability. Several different aspects can attest to this aforementioned durability, being the implementation of resistant mortars one of them. Mortar is an anthropogenic composite material that serves as the binding agent between masonry units. In this sense, the properties of the mortar used will deeply impact the durability of the construction, conferring monolithic properties to the individual pieces.

Within this framework, the present work aims to perform an archaeometric characterization of the mortars used in some of the most relevant Roman public constructions of Verona. For this purpose, mortar samples were extracted from the Capitolium, the Roman Theatre, the Odeum, the Curia, the Arena, and from the city walls surrounding Roman Verona. The samples were then analyzed through colorimetry, X-ray powder diffraction (XRPD), optical microscopy, and scanning electron microscopy coupled with energy dispersive spectroscopy (SEM-EDS). Observations and analyses were performed on the mortar samples to better comprehend mortar composition, the manufacturing techniques and pozzolanic or parapozzolanic processes carried out for as a consequence of specific compositional and technological factors.

1.2. OBJECTIVES:

1.2.1. MAIN OBJECTIVE

Within the outlined scope, the primary objective of the present academic dissertation is to perform an archaeometric assessment of the mortars employed in some of the most relevant Roman

public constructions in the city of Verona. This analytical endeavor involves the investigation of mortar samples derived from key archeological sites and buildings by the implementation of different analytical techniques. The research will systematically observe the physical properties, mineralogical profiles, and chemical composition of both the binder-aggregate and the isolated binder fraction of the collected mortar samples to gain a comprehensive understanding of mortar composition, manufacturing techniques, and the chemical processes and reactions involved in its production.

1.2.2. SPECIFIC OBJECTIVES

In order to achieve the previously established objective, the study project will consist of six (6) specific aims to be carried out throughout this project.

- Assess a literature review of mortar composition, properties, manufacturing procedures, and the corresponding applicable analytical techniques. Explore current approaches and procedures taking place in mortar characterization.
- Reconstruct, through a bibliographic revision, the historical and geographical context in which the construction of the previously mentioned Roman buildings is established.
- Observe, through the use and implementation of different analytical techniques, the general composition of the mortars, and determine, if observed, the nature of the interaction between the binder and the aggregate fraction within them.
- Identify the chemical and mineralogical compositions of the binder fractions of mortar samples.
- Determine, according to the analysis of the obtained result, different recipes used for mortar production.
- Define, according to the observations, some of the possible variations in the manufacturing processes of mortars taking place in Verona throughout the Roman age, through the analysis and correlation of the different obtained results and the previously established context.

1.3. BRIEF INTRODUCTION TO THE CONTEXT:

The archaeometrical analysis of mortars is a relatively recently developed topic that has been currently seen an uprising. The studies carried out on the analysis of this material serve a great variety of purposes such as the identification of manufacturing techniques and recipes, understanding of mortars properties, or observation of degradation processes and restoration techniques, to mention a few. In this context, both in-situ and ex-situ analyses can be performed according to the purpose or objective of the individual study. In the case presented in this dissertation, samples extracted from Roman public structures are carefully studied and analyzed in the lab through a series of well-established analytical techniques to obtain a full physicochemical characterization. For this reason, the physical properties, mineralogical and chemical profiles of the aforementioned samples will be studied and defined for both the mortar as an integral unit and the binder fraction. Moreover, the results of the different techniques will be analyzed and correlated, providing insightful information concerning the production techniques, the recipes used, and the subsequent properties of the mortars (related to the possible presence of pozzolanic and parapozzolanic reactions).

1.4. OUTCOMES:

The present dissertation seeks to provide as a final outcome the identification of mortar recipes and manufacturing techniques developed in the Roman era in Verona for the construction of the most significant public structures. For this purpose, an integrated study of the physical-chemical properties of the different types of sampled mortars will be performed. In order to achieve this goal, two main objectives are set. In the first instance, a clear definition of the physical-chemical properties of the microstructure of the mortar samples will be performed through the determination of certain physical and aesthetical properties, and the identification of both the mineralogical and chemical profiles of the samples. Within this outcome, it is sought not only to describe the observed properties and characteristics but to establish general tendencies through the comparison and correlation of the obtained results and their possible relation with their context. On the other hand, mineralogical and chemical profiles will be obtained also from the sole binder fractions. This process will allow for a better understanding of the techniques and processes

adopted for mortar production, and the latter interaction between the binder and aggregate fraction constituting the mortar. The results will provide a general overview of different methodologies adopted, which, correlated to the context, will be able to provide insightful information in the development of manufacturing techniques.

1.5. DISSERTATION OUTLINE

Chapter one (1) provides an introduction to the performed study, providing a general context to the research in question. It also comprehends the general and specific objectives, a brief introduction to the research context, and the final expected outcomes. Chapter two (2) lays out an introduction to mortars, dealing with their definition, contextualization, function types, and properties, as well as their evolution throughout history, a general overview of the manufacturing process, and the common current approaches adopted for their analysis. Chapter three (3) seeks to provide a comprehensive introduction to the context of the study case, describing relevant information about the chronology of the development of both the city and the individual sampled buildings. Chapter four (4) establishes the geological context in which the city is located, in order to better comprehend the possible sources utilized for mortar production. Chapter five (5) displays the methodology used for the present study. It includes an overview of the methodology, a brief introduction to each of the techniques used for the analysis, and the specifications or details of the procedures of implementation. Chapter six (6) presents the raw data obtained as a result of the different analyses carried out. Moreover, chapter seven (7) provides a careful and thorough discussion, and analysis, including statistical analysis of the results presented in chapter six (6) and their correlation to the individual context. It also describes the key findings regarding the mortar's composition and the possible binder-aggregate reactions. Chapter eight (8) summarizes the findings and imparts the conclusions, describing the possible discoveries and evaluating the process carried out during the analysis. To finalize, chapters ten (10) and eleven (11) provide both the relevant bibliography and the annex and appendix.

2. Chapter II - State of art: Mortars

2.1. AN INTRODUCTION TO MORTARS: DEFINITIONS, COMPOSITION, AND PROPERTIES

2.1.1. INTRODUCTION TO MORTARS: AN OVERVIEW

The definition of mortar, according to Artioli, G. et al. (2019), Ergenç, D., et al. (2021), and Rispoli, C., et al. (2020) refers to a hardened composite made from geological materials (both passive and reactive), such as binders, aggregates and additives. It has been described as a complex and variable material, precisely because of variations presented on the nature of the raw materials and aggregates, their proportions, and the manufacturing procedures used. Any alteration in these factors will result in significant changes of mortar products with distinct physical and chemical characteristics (Donais, M. K., et al. 2020). The evolution and alterations of the manufacturing technology throughout history, as attested by Arizzi, A., et Cultrone, G. (2021) will lead to different types of mortars (with different properties and behaviors). The addition of additives and admixtures will also influence in a determinative way the properties of both the final product and the mortar paste before hardening (Arizzi, A., et Cultrone, G. 2021). In this sense, the resulting mortar would be influenced by the technological advances and the depth of the knowledge regarding its production, the available materials, the nature of the construction project (public or private, monumental or small scale, economical background...), and the particular use of the mortar within the construction (as a plaster, as a binding agent...).

Mortar in construction is most used as a binding agent between masonry units and as a filling agent for empty spaces in structural elements. It can also be used, as mentioned by Adam, J. P. (2005), for foundation purposes, for pointing and rendering of walls and floors, as plasters, or for decorative purposes. According to Vitti, P. (2021): “In traditional construction, structural mortars improve the adhesion and cohesion of single units of bricks or stone and contribute to the formation of structures that can stand the pressure of (a) dead loads (i.e. the permanent loads generated by the structure itself), (b) live loads (i.e those imposed loads generated by the use of the structure) and (c) environmental loads (i.e those accidental loads caused by wind pressure, earthquakes, snow, thermal expansion or contraction and settlements). The more the mortar has a

binding capacity, the more it will improve the structural behavior of the structure.” In this sense, the structural behavior of a building depends to a large extent on the mortar, since it is the one bringing cohesion between the single units. Or, as better explained by Pineda, P., et al. (2022): “Moreover, the static and dynamic structural behavior is strongly related to the mechanical, chemical, and microstructural properties of mortars”. This structural stabilization provided by mortars can be explained both by the proper adhesion of the individual units and as an immediate effect caused by the proper distribution of charges along the vertical field (Adam, J. P. 2005). Furthermore, the plasticity and durability of this material allow as well for its use as a covering or protective surface, where it serves both a decorative purpose and a protection one. In this one, walls and floors are covered with mortar in order to avoid possible damage caused by water infiltration and salt growth, among others (Ergenç, D., et al. 2021; Artioli, G. et al. 2019). In this sense, mortar becomes one of the most important materials in the construction, being a guarantor of not only the structural stability of the building, but also of its aesthetics (Oliveira, M., et al. 2022).

2.1.2. KEY DEFINITIONS AND COMPONENTS

In order to provide a more profound understanding of mortar types, it is necessary to provide some further definitions, as proposed by Ergenç, D., et al. (2021). The following terms pretend to provide a better background for the understanding of concepts that will be approached throughout this work. It should be mentioned that the list of terms is based on the definition provided in the previously mentioned article by Ergenç, D., et al. (2021).

- Binder: The term binder according to Ergenç, D., et al. (2021) refers to “the binding medium that, after hardening, holds the aggregate particles together. It can be defined as a material with adhesive and cohesive properties capable of binding aggregates into a coherent mass”. In this sense, a binder is a substance that, due to its cohesive nature, holds elements together.

- Lime: can be defined as the product obtained after the firing, at high temperatures, of limestone. It consists of a white powder composed of oxides of calcium and magnesium, or a slurry paste composed of hydroxides if it has been slaked (Ergenç, D., et al. 2021).

- Aerial mortar: This is a carbonate-based solid material, formed as a consequence of the hardening of a slaked lime (or lime putty). It is considered a porous and permeable material and does not have hydraulic properties (Veiga, R. 2017; Nogueira, R., et al. 2020).

- Aggregate: As its name suggests, an aggregate is a material, most commonly from geological origin (mineral aggregates, sands, gravels, and crushed stones), that is added to the slaked lime. The addition of the aggregate provides several benefits, such as better mechanical stability, durability, and workability and it limits the shrinkage phenomena during the hardening process (Ergenç, D., et al. 2021).

- Additives: “The term additive refers to a constituent usually added in small quantities to a mix to bind or modify its manufacture or properties (e.g. air-entraining agents and setting accelerators)” (Ergenç, D., et al. 2021). In other words, the term additive refers to an external constituent that, when added to the mortar mixture, modifies its properties. This is done to obtain certain benefits, such as better mechanical strength or to diminish the amount of pores.

- Pozzolan: The term pozzolan is given to various siliceous and aluminous materials such as volcanic ashes, fired clays, or ashes added to the mortar in order to obtain a hydraulic mortar. The mixing of the added pozzolans with the slaked lime will create a chemical reaction where aluminosilicates and Ca(OH)_2 recombine forming the C-S-H phases (Malhotra, V. M., et Kumar Mehta, P. 2017).

- Quicklime: Refers to the white unstable powder that results from the calcination and further grinding of limestone, it is composed, as previously mentioned, of oxides of calcium (CaO) (Ergenç, D., et al. 2021).

- Slaked lime: slaked lime or lime putty is the slurry viscous paste resulting from the addition of water to quicklime (or lime hydration). “The composition may differ depending on the mineralogical composition of the quicklime. If the quicklime is calcitic (CaO), calcium hydroxide (Ca(OH)_2)—the mineralogical name of which is portlandite—is produced. Dolomitic limes, which are rich in magnesium, produce Mg(OH)_2 in addition to Ca(OH)_2 . The mineralogical name of Mg(OH)_2 is brucite, and it is obtained by hydrating (or slaking) dolomitic quicklime (CaO and MgO) with water to produce a paste or powder.” (Ergenç, D., et al. 2021).

- Setting: Setting refers to the cohesive process in which the already hydrated lime (the slaked lime) hardens, and turns into a carbonate. The environmental conditions in which the paste solidifies will affect in a great manner the resulting mortar (modifying its porosity, resistance, and durability. (Ergenç, D., et al. 2021)

Mortar, as previously mentioned, is a highly variable material, due to changes in the production technique, the geological nature of aggregates, and the binding material. Any variation on the initial mixture will derive in significantly different mortar products with different working properties. The three main components present in a mortar, as described in the definitions, are the binder, the aggregates, and the additives.

The type of aggregate added to the mix will affect greatly the final product. The main function of the aggregates, as previously mentioned, is to reduce the presence of cracks formed during the hardening process and to increment the overall volume of the binder (Artioli, G. et al. 2019). Nevertheless, their variability will have such a deep impact on the resulting mortar. Its variable nature is due to the fact that local material was more commonly employed, due to the logistic reasons. In other words, the aggregates used are highly dependable on the geological context of the construction. However, it should be mentioned that artificial aggregates were also employed in some cases, as remarked by (Moropoulou, A., et al. 2005). Those aforementioned are not the only factors that determine the selection of certain materials as aggregates; indeed, the final purpose or function of the mortar and the economical background of the construction will greatly contribute to their utilization. (DeLaine, J. 2021).

It is also because of their variable nature that aggregates can be classified in several ways, such as size (or dimension), natural or artificial, passive or active (hydraulic) among others. Concerning the dimension of the aggregates, they can be classified into different categories, ranging from fine sands, or even clays up to coarse gravels (Artioli, G. et al. 2019). Natural aggregates refer mostly to rock fragments (such as pebbles, gravel, or sands) coming from a geological origin and being naturally formed, while artificial aggregates are manmade materials, such as ceramic fragments (Ergenç, D., et al. 2021). Passive or active, refer mostly to the reaction of the aggregates to the binder, where active refers to aggregates having a reaction to the binder enhancing in this way certain properties of the mortar. On the other hand, passive aggregates do not present any type of reaction to the binder and maintain their original properties (Theodoridou,

M., et al. 2013; Ergenç, D., et al. 2021). All of these properties of the aggregates will eventually lead to the determination of the properties of the mortar, representing an essential key for its good performance (Pavía, S., et Caro, S. 2007; Veiga, R. 2017; Stukovnik, P., et al. 2020).

The most common types of reactive aggregates are the pozzolans, aluminosilicate materials that, in the presence of water, react with the calcium hydroxide present in the lime binder to form hydration products with higher resistance and better mechanical properties (Malhotra, V. M., et Kumar Mehta, P. 2017; Elsen, J. 2006). The resulting hydration products are both C-S-H phases (calcium silicate hydrates) and C-A-H phases (calcium aluminate hydrates). This is better described by Sagin, E. U., et al. (2021) when mentioning: “Pozzolans are siliceous or siliceous-aluminous materials that also contain amorphous silica or alumina. They react with lime ($\text{Ca}(\text{OH})_2$) in the presence of water or moisture to form calcium silicate hydrate (C-S-H) or calcium aluminate hydrate (C-A-H). Higher contents of amorphous silica and alumina increase the hydraulic properties of lime mortars”. The resulting material is, therefore, more resistant, stronger, and durable and have better waterproofing effects (Vitti, P. 2021; Pavía, S., et Caro, S. 2007). It is for this reason that they were commonly employed since Hellenistic times (Artioli, G. et al. 2019) for the construction of aqueducts, building foundations or bridges (Bakolas, A., et al. 2008). This material was then adopted by the Romans, whose biggest contribution to mortar production and technology was the systematic use of pozzolan (Sagin, E. U., et al. 2021). This can be evidenced in the prescriptions for mortar production in historical sources and treaties such as *De Architectura* written by Vitruvius or *Naturalis Historia* by Pliny (Sagin, E. U., et al. 2021). In these sources, pozzolans are commonly associated with volcanic ashes, more specifically the volcanic ash coming from Naples’s Bay. Nonetheless, other materials could be used as well as pozzolans, such as crushed terracotta or vegetable (plant) ash (Vitti, P. 2021). These other pozzolans were artificially made and were used when natural ones were not available in the construction site (Moropoulou, A., et al. 2005). The same factor of viability determines the type of artificial pozzolan used, where “waste terracotta products were more abundant in urban situations, manure and crops in rural ones” (DeLaine, J. 2021).

The last mentioned ones, the *terracotta* or fired clay fragments, are commonly named *cocciopesto*. This material was used since early Hellenistic times, according to Elsen, J. (2006). It was used due to the mechanical properties acquired by the mortar when present and was commonly

used for the construction in high humidity environments such as cisterns or aqueducts, or in normal conditions to improve the mortar's performance (Pineda, P., et al. 2022; Böke, H. D., et al. 2006; Moropoulou, A., et al. 2005). Their pozzolanic nature can be explained due to the presence of amorphous silica and alumina as a consequence of the firing process, or as explained by Bakolas, A., et al. (2008): "Clay minerals, composed mainly by silica and alumina, present a sharp pozzolanic activity when heated at temperatures in the range of 600–900°C and ground in sufficient fineness. During the thermal treatment, silica and alumina loses the combined water, leading to a demolition of the crystalline network. Silica and alumina remain in an unstable amorphous phase that could react with hydrated lime and water".

It is due to their reactivity that additives were implemented in mortar production techniques. As mentioned before, the main purpose of the additives is to enhance certain attributes of mortars, such as durability, mechanical resistance, water permeability, or drying speed, to mention some. This variation in the mortar is the result of the addition of certain elements to the admixture that react with the binder, leading in this way to the desired working characteristics. In this sense, the reactivity of the binder was exploited in different occasions by the addition of both aggregates and additives to acquire the desired properties in mortars. Or as explained by Moropoulou, A., et al. (2005): "Mortars and concretes employed in ancient structures concern composite materials comprised of binding material (or a mixture of binders), of natural or artificial aggregates or a mix of them and pozzolanic additions (natural or artificial), in order to ameliorate lime-based mortars and prolong their longevity. Sometimes, to improve rheological and mechanical characteristics, some organic additives and vegetable and animal materials as reinforcement were used". Among the organic compounds, it is possible to find Arabic gum, animal glue, bee wax, or egg yolk to mention a few (Artioli, G. et al. 2019).

All of the previously described factors play a decisive role in the mortar products, deriving in significantly different mortars. In this way, the production process of mortar becomes a design choice, which needs to take into consideration all the different factors that could influence the final product and the limitations or opportunities presented by the context in which the construction takes place.

2.1.3. TYPES OF MORTARS

One of the most defining properties of a mortar is the composition of its binder. This material can be produced from different sources, leading to radically different results. It is precisely because of this that mortars' main classification arises from the composition of the binder. In this, the nature of the original material used as a binder will determine the general characteristics of the mortar. According to Artioli, G. et al. (2019) and Vitti, P. (2021) mortars can be classified into earthen mortars, lime mortars, gypsum mortars, and Portland-cement mortars, which are produced by the mixture of lime and clay (Artioli, G. et al. 2019). These different types of binders have been widely used since ancient times, as described by (Moropoulou, A., et al. 2005) when stated: “For the preparation of mortars and concretes various materials were employed; gypsum and lime were used for rendering since ancient times, but in structural mortars and concretes lime use dominated”.

Gypsum binder is the resulting binder made out of both hydrous and non-hydrous calcium sulfates after the thermal treatment of gypsum. According to Artioli, G. et al. (2019) gypsum can be defined as “a sulfate and evaporite mineral, most commonly found in layered sedimentary deposits in association with halite, anhydrite, sulfur, calcite, and dolomite”. After firing, depending on the firing conditions (especially temperature), the initial gypsum will be transformed into anhydrite or basanite. These phases are characterized by structural variability, leading to the possible presence of α , β , or γ forms, which would present different characteristics, such as crystal size, density, and solubility, to mention a few (Vitti, P. 2021). Gypsum binder regardless of its classification (anhydrite or basanite) counts with certain advantages and disadvantages. As mentioned by Vitti, P. (2021), gypsum shows good mechanical properties, being very resistant to stress, and an increment of volume as it sets, which will result in a better cohesion of the bonded materials, good protection to humidity, due to its fire resistance, and a quick setting time, which starts after 2 – 6 minutes from hydration and finalizes after 2 hours (Vitti, P. 2021). However, it can also show a lower resistance to compression and a higher solubility in water.

Similarly, lime binder refers to, as its name suggests, a binder resulting from the calcination of limestone. It is, as mentioned by Sagin, E. U., et al. (2021) “among the most frequently used building materials for thousands of years, starting with the discovery of pyrotechnology”. Due to the nature of the source material, the limestone, the resulting material is composed mainly of calcite and quartz, with the possible presence, at significantly lower amounts, of feldspars, micas,

or plagioclase (among others) (Maravelaki-Kalaitzaki, P., et al. 2003). The use of dolomite as a source for lime-based mortars will influence the mineralogical profile of the binder, however, it can still be considered as a lime-based mortar, due to the carbonate base of the stone (Ergenç, D., et al. 2021). This can be observed as well due to the presence of magnesium in the binder, as dolomite chemical composition is $\text{CaMg}(\text{CO}_3)_2$ (Artioli, G. et al. 2019; Vitti, P. 2021), or through the possible presence of brucite as a result of the reaction. These dolomitic lime mortars show a higher mechanical strength, nonetheless, they exhibit slower hydration in comparison to calcitic lime binders (Vitti, P. 2021; Veiga, R. 2017). Taking this into consideration, the selection of the limestone was of the utmost importance since the resulting mortar will be highly influenced by the presence of clay within the stone.

These lime mortars, as is the case of the gypsum ones, can be further classified into different groups according to their composition and properties. They can be classified, as proposed by Nogueira, R., et al. (2020), into fine mortars and coarse mortars, according to their microstructure. However, the most commonly used and accepted classification system groups them into hydraulic and non-hydraulic (or aerial). These mortars can be recognized through their composition; however, their properties or characteristics are a key component for their distinction. In this, non-hydraulic mortars, show lower mechanical strength, low elasticity, and high water permeability (Ergenç, D., et al. 2021), due to their higher porosity (<20%) (Ergenç, D., et al. 2021). Aerial mortars, as remarked by Ergenç, D., et al. (2021) tend to contain as well a higher presence of lime nodules (lumps) within the matrix. Another method of distinction is, according to Adam, J. P. (2005), the proportion of clay present in the limestone. Where the presence of clay from 0.1% to 8% can be referred to as aerial limestone (or even pure limestone when the clay presence is lower than 1%). On the other hand, when the percentage of clay present in the limestone varies from 8% to 20%, it can be described as hydraulic lime. Nevertheless, a limestone with more than 20% of clay presence will not be considered suitable for mortar production (Adam, J. P. 2005).

In addition, hydraulic binders can be further classified into aerial-lime mortars mixed with pozzolans, hydraulic lime, formulated lime, natural cement, Portland cement, and white cement (Arizzi, A., et Cultrone, G. 2021). The first group, as described by its name, is composed of both aerial lime binders and pozzolans. Due to the presence of pozzolans, as seen before, the mixture acquires new properties, increasing its mechanical resistance and durability, turning in this way

the aerial lime mortar into a hydraulic one. These are the most common hydraulic mortars found during the Roman period due to the tendency to use pure limestone, as suggested by Vitruvius in *'De Architectura'*. The second and third ones are modern products and they are referred to, by Arizzi, A., et Cultrone, G. (2021), hydraulic limes resulting from the firing of both pure limestone and clay and a “modern hydraulic binder consisting of mainly air-hardening or natural hydraulic lime with added hydraulic and/or pozzolanic materials” (Arizzi, A., et Cultrone, G. 2021), correspondingly. In addition to these modern products, we can find natural cement, which is also called Roman cement. The aforementioned product was developed during the 19th century, and its production includes the process of calcination of naturally argillaceous limestone below sintering temperature (Arizzi, A., et Cultrone, G. 2021; Artioli, G. et al. 2019). It is precisely in this last factor that it differs from the manufacturing process of Portland cement, in which temperatures can reach up to 1450 °C (Arizzi, A., et Cultrone, G. 2021). In this last procedure, gypsum is also added to the final mix. Further steps and additions to the mixture of Portland cement can lead to de production of white cement.

2.1.4. MORTARS' PROPERTIES

The properties of mortars have a notable variation according to the mortar type, the nature of the aggregates and additives, and the production process. This variation could drastically change the working characteristics of each mortar, providing it with a higher mechanical resistance, and durability, as mentioned before. These properties can be used to define the quality of the mortar. As better expressed by Adam, J. P. (2005) “The quality of mortar depended on the evenness of the burning of the stone, the proportion and nature of the aggregate, and the care taken in mixing (which must be as uniform as possible)”. The slaking process or hydration of the mixture is also mentioned by Pavía, S., et Caro, S. (2007) when mentioning that a longer slaking period will improve the physical and working properties of lime binders. Another significant factor of the production process in the resulting mortar is the conditions to which the mortar is exposed during carbonation (Izaguirre, A., et al. 2010). Fusade, L. et Viles, H. A. (2019) highlight the following, regarding the carbonation process of lime mortars: “Environmental conditions have an impact on the early days of lime mortar, during the setting and hardening process of the fresh mortar. Research has shown that this hardening process, also called carbonation, is governed by the temperature and relative humidity (RH) of the environment. This combination of temperature and

relative humidity in the environment in which lime mortar will harden is called the curing condition”. This is due to the interaction of the matrix and the environment, as this can affect the reaction in which the matrix interacts with CO₂ from the environment and liberates water from the mixture to obtain the desired results. These curing conditions will also determine the carbonation rate, profoundly impacting the microstructure of the binder (Pineda, P., et al. 2022).

2.1.4.1. MECHANICAL PROPERTIES

The mechanical properties of mortars are mainly characterized by the porosity of the structure, the type and amount of aggregates present, and the type of binder (either gypsum, earthen, lime... or aerial vs. hydraulic). The mechanical strength of a binder can be determined by its resistance to compression, tensile, and torsion, in other words to its cohesion and plasticity. A strong cohesion in mortar is created when mortar and aggregates are tightly bonded together. According to Pavía, S., et Caro, S. (2007) this is the effect of the reaction between the aggregates and the binder, which can be detected due to the presence of a reaction rim when observed under the microscope. This aggregate-binder reaction denotes, in this sense, the level of hydraulicity of the mortar. This level of hydraulicity is a key element for the determination of the working mechanical properties of lime-based mortar, since, as mentioned by Maravelaki-Kalaitzaki, P., et al. (2003) “tensile strength values of the mortars are directly proportional to their level of hydraulicity”. In the same way, and as previously commented, aerial mortar shows “low mechanical strength, high deformation capacity (plasticity), low elasticity modulus and high permeability to water” (Ergenç, D., et al. 2021) when compared to hydraulic mortars. In this sense, the nature of the aggregate and additive has a deep impact on the mechanical strength of the mortar. Its abundance in the mixture will play an essential role as well, since a binder-rich mix will have higher compression resistance, according to Fusade, L. et Viles, H. A. (2019). Moreover, the presence of the right proportions of aggregates within the mixture will derive in shrinkage control during the carbonation.

2.1.4.2. POROSITY

Porosity is defined as the total amount of pores (both open and closed) present in a material. They play an essential role in the identification of manufacturing procedures since their morphology and abundance reflects this (Pineda, P., et al. 2022). The pore morphology testifies how water was leaving the system and air was entering and being entrapped during the hardening process (carbonation). However, the amount of water inside the mortar mixture will also be a determining factor, since a higher amount of water will need to be evacuated from the system (Arizzi, A., et Cultrone, G. 2021). Finally, the type and amount of aggregate present in the sample can influence as well the porosity of the resulting material, especially for non-hydraulic mortars. The crack pattern of the binder can also attest to the curing conditions and the initial mixture design of the mortar (Pineda, P., et al. 2022). Cracks present due to shrinkage can indicate as well the use of certain aggregates, or the temperatures employed for the calcination of the limestone (Pineda, P., et al. 2022).

The mechanical properties of mortars are deeply influenced by their porosity. According to Pineda, P., et al. (2022) “The role of porosity is essential in mechanical performance, despite the type of binding system and small pore size and low porosity are desirable. The pore size is also related to durability, as pore dimensions should be large enough to prevent condensation inside structural elements (a small pore has a water condensation effect) and, at the same time, small enough to provide a water-proof barrier”. This water-proof barrier refers essentially to the open porosity, which is the porosity connected to the surface of the mortar, and it is in this one that water can access the sample (Fusade, L. et Viles, H. A. 2019). As this process occurs, water will generally transport salts, which will then crystallize inside the pores and can eventually cause detrimental effects (Fusade, L. et Viles, H. A. 2019; Nogueira, R., et al. 2020). In this sense, the pore structure of the mortar is strictly related to its durability. This fact is also noted by Pineda, P., et al. (2022) when observing the effects of pozzolans in the matrix. This author mentions that this presence, and further reaction with the binder, will create a continuous microcrystalline matrix that, due to its compactness, will delay the fluid diffusion and lead in this way to a lower porosity and a higher hydraulicity. Therefore, it is possible to identify the type of mortar according to the average pore type or the total porosity of the sample (Pineda, P., et al. 2022). A good example of this is demonstrated by Ergenç, D., et al. (2021), that observed that “Historic aerial lime mortars have

high porosity (>20%) with a small volume of pores with diameters <1 μm . High-quality mortar shows a low volume of micro-pores and a small volume of larger pores ($\leq 50\text{-}\mu\text{m}$ diameter)”.

2.1.4.3. WATER RETENTION AND CAPILLARY COEFFICIENTS

The water-proofing properties of mortars are among their key properties, causing it to be employed in the construction of cisterns, aqueducts, and baths. This property, as previously explained, depends on a high measure of the open porosity of the mortar, since it is directly related to its capillary coefficients and the amount of water entering the material (Izaguirre, A., et al. 2010). The water-proof properties of mortars are indicators of the original mixture design, where the use of certain aggregates and additives will modify the microstructure and therefore the mortar itself. In a first instance, the use of pozzolans will improve radically the resistance to water on mortars (Pineda, P., et al. 2022). On the other hand, Stukovnik, P., et al. (2020) remarks that the use of dolomite in the mixture will increase the alkalinity of the mortar and therefore its strength, resulting in better water resistance. Under this objective, it becomes evident the way in which the mortar mixture plays an essential role in the final properties of the material. The addition of materials such as aggregates will result in significant variations in the microstructure, in other words in different kinds of mortars.

2.2. MORTARS THROUGHOUT HISTORY: AN INTRODUCTION TO ANCIENT MORTARS

Pyrotechnology has been defined on several occasions as a turning point in the history of humanity, since it not only allowed change in the human diet and relationship with its environment, but also provided the basis for the development of other manufacturing techniques. Among these innovations, it is possible to observe the development of mortars, as mentioned by Sagin, E. U., et al. (2021) who said “Lime mortars have been among the most frequently used building materials for thousands of years, starting with the discovery of pyrotechnology”. This material, as previously mentioned, has several applications in construction from finishing walls and decoration to infillings and foundations (Elsen, J. 2006), which lead to its extensive use and development. In the same way, this led to extensive variability throughout time and the different geographical areas where it was applied (Arizzi, A., et Cultrone, G. 2021). Traditionally, the most commonly used

binders have been mud, gypsum, and lime (Elsen, J. 2006), where lime and gypsum were the first artificial binders created according to Ergenç, D., et al. (2021). The author mentions as well that these man-made mortars “were employed widely in the Middle East in the seventh and eighth millennia BC” (Ergenç, D., et al. 2021). However, Adam, J. P. (2005) argues that the use of these binders not developed until the sixth millennium b.C. in the town of Çatal Hüyük, and not in the eighth century. Adam, J. P. (2005) and Elsen, J. (2006) highlight as well the use of gypsum binders as a mortar in Egypt and in the Middle East since the third millennium. On the other hand, due to the nature of binder, mud or clays were used since Neolithic times, being employed in different ways, such as mudbricks or infillings (Artioli, G. et al. 2019; Moropoulou, A., et al. 2005). Among the artificial binders, lime mortars were the most extensively used (Theodoridou, M., et al. 2013; Veiga, R. 2017; Fusade, L. et Viles, H. A. 2019). According to Ergenç, D., et al. (2021) this repetitive use is due to the availability of limestone, the relatively simple production procedures, and the high quality of the results, being this a durable mortar with good mechanical resistance.

The first known appearance of lime mortar is not completely clear, as Elsen, J. (2006) states that it is around 4000 b.C. in Egypt, while Sagın, E. U., et al. (2021) argue that it was in the 6th millennium b.C. However, it is accepted by various authors that it is in the Greek world where lime mortar is systematically used. Furthermore, it is highlighted on several occasions the first use of pozzolans within this specific context. Thanks to the repeated use of lime binders, mortar mixtures counted with different local recipes, some of which used special aggregates (called pozzolans) to enhance certain properties of mortars (Artioli, G. et al. 2019). Among these, the use of volcanic dust and crushed ceramic was adopted in Greece during the bronze age (Arizzi, A., et Cultrone, G. 2021). The specific date of its appearance is, once again, not given precisely, with authors debating between the first and the second millennium BC (Artioli, G. et al. 2019; Ergenç, D., et al. 2021). This technological advance in the production of hydraulic mortars was then adopted by the Romans, who established its use throughout its territory (Arizzi, A., et Cultrone, G. 2021).

The addition of pozzolanic materials to mortar first appeared in the Roman empire in areas near volcanoes, such as the Bay of Naples, where natural pozzolana existed (Moropoulou, A., et al. 2005). Then, due to the hydraulic properties of the resulting mortar, the use of this material was spread throughout the empire, creating a systematic use of pozzolans (Sagın, E. U., et al.

2021). This constant use of reactive material from terracotta and volcanic sands led to the construction of high-quality buildings, that are enduring over time (Artioli, G. et al. 2019). This is remarked by Vitti, P. (2021) when mentioning: “Under Augustus (end of 1st c. b.C.), some buildings in the capital show a greater expertise in the selection of materials. Mortars began to have higher binding capacity and durability”. The construction of buildings saw, in this way, an era of development, benefiting from the hydraulic properties of mortars and high-quality materials. This led in the same way to the development of construction techniques such as concrete masonry, the so-called *opus caementicium* (Artioli, G. et al. 2019). The mastering of vault constructions, as a result of mortar development in this period, should also be highlighted. According to Vitti, P. (2021) the cohesion and durability of these architectural elements rely predominantly upon the properties of the mortar used. This can be observed when the author mentions “Romans were already experimenting with what would have turned out to be a major revolution in vaulting. In imperial Rome (1st–4th c. CE), the caementa were layered in horizontal courses from the impost to the crown, a marked departure from earlier vaulting. Mortar played a major role in achieving the necessary cohesiveness. Horizontal layering improved compactness since *caementa* could be set one by one in the mortar, with appropriate density and avoiding cavities. These extraordinary vaults were made possible by the exceptional mechanical resistance of the pozzolanic mortars, and proved to be long-lasting”.

In this framework, the recipes or mixture design for mortar production in the Roman empire were of the utmost importance, being the ones that will lead to high-quality results. It is for this reason, and the extensive use of this material, that treaties were written with the ideal formulas for mortar production (Ergenç, D., et al. 2021). One good example of this is ‘*De Architectura*’ written by Vitruvius, where he states that the selection of pure limestone and good pozzolans are a key component during this process. As a consequence of this, it was prescribed the preferred use of pure limestone, without inclusions, and the use of pozzolans, especially in Rome and in the areas around Naples, during the Roman period. This selection of materials created a need to establish sourcing centers and commercial routes for the transport of high-quality materials, especially to urban areas (DeLaine, J. 2021). However, local sources that did not require complicated supply were always preferable. This fact can be observed when Vitti, P. (2021) mentions “Outside Rome, pozzolanic mortars were produced taking advantage of materials different from volcanic ash (if not available locally), such as crushed terracotta or plant ash”.

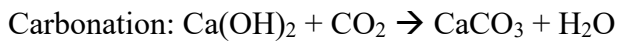
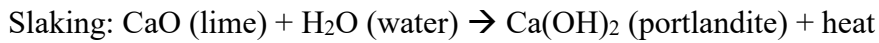
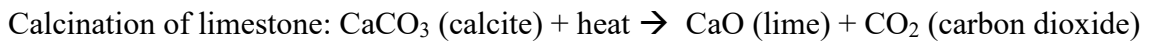
Despite the mastering of techniques for mortar production leading to durable construction, the late Roman Empire saw a decline in the quality of mortar production (Vitti, P. 2021). Knowledge regarding material selection, required times, techniques, and proportions were lost, up to the point where “building techniques developed in the Late Empire were inferior relative to the dry-stone or brick masonry made by the Greeks” (Vitti, P. 2021). It is for this reason that during the Middle Ages there is no evidence of high-quality mortars, being these “unaged and poorly slaked” (Artioli, G. et al. 2019). The author mentions as well a description given by Viollet le-Duc, referring to these mortars as brittle, due to inappropriate firing. Nonetheless, as remarked by Artioli, G. et al. (2019), some techniques of mortar production prevailed in areas such as Homra, Surkhi, and certain parts of Italy.

On the other hand, the abandonment of the Roman recipes during the Middle Ages led to the production of new hydraulic lime-based mortars. In these, impure limestone was selected (which can be seen as a clear sign of the loss of knowledge from the Roman treaties) and passed through the process of calcination. The firing of clay embedded within the limestone will produce a new type of reactive material, with a similar reaction to the one observed by the use of *cocciopesto*. However, the resulting mortar did not have a standardized level of hydraulicity (Artioli, G. et al. 2019; Vitti, P. 2021). An exception to this trend can be seen with the technological advance observed in the construction of Gothic churches. The construction of these buildings, as described by Vitti, P. (2021), “was based on mortared stone blocks to form walls, arches and vaults. While walls were built with stones with a fill of mortared rubble, structural elements such as columns, arches, flying buttresses, and vaults were built in solid stone. [...] Thinner structural architectural parts, such as columns or ribs, had thinner joints, which resulted in stiffer structural elements”. Apart from this, gypsum mortars encountered a peak of use, especially in the areas of northern Germany and Paris.

2.3. PRODUCTION OF PROCESS OF LIME-BASED MORTARS IN ROMAN AGE

The production of lime mortars is constituted by three major steps: calcination of limestone, slaking and mixing, and finally carbonation process. In the first instance, calcium hydroxide, a reactive compound is obtained from the thermal decomposition of limestone (Artioli, G. et al. 2019; Oliveira, M., et al. 2022). The resulting material is ground, and water is added to the resulting

compound, by a process called slaking (Ergenç, D., et al. 2021; Vitti, P. 2021). The interaction between water and quicklime will cause an exothermic reaction, forming portlandite ($\text{Ca}(\text{OH})_2$), a workable paste or putty (lime putty) to which the aggregates are added. Finally, the lime putty is left to dry and harden, reacting with carbon dioxide from the atmosphere, through a process called carbonation. The resulting product after carbonation is completed (if there is no chemical reaction between the binder and the aggregates) is CaCO_3 (Ergenç, D., et al. 2021; Vitti, P. 2021). Since the resulting material has the same composition as the initial limestone, this process is referred to as the ‘lime cycle’, and it has been thoroughly explained in literature. Adam, J. P. (2005) provides an example of this, mentioning the chemical reactions taking place in each step



A graphical representation of the process can also be observed in figure 01:

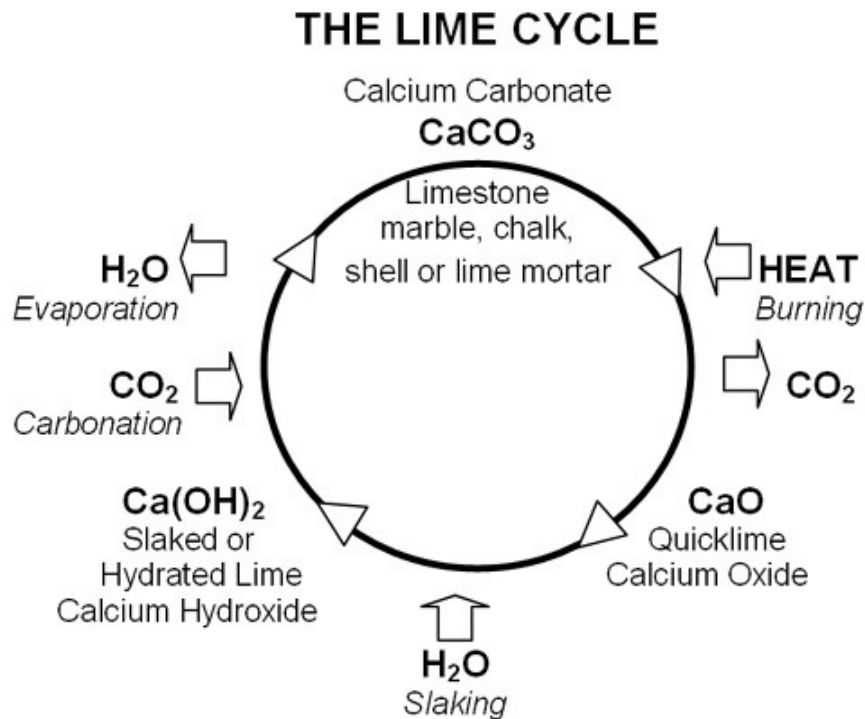


Figure 1. The Building Limes Forum (2017) The Lime Cycle , The Building Limes Forum. Available at: <https://www.buildinglimesforum.org.uk/wp-content/uploads/2017/09/Lime-Cycle-web-300x216.jpg> (Accessed: 2023).

Therefore, the first steps of mortar production involve the identification and extraction of raw materials. The identification of sources was a key element since good quality mortars depended in great measure on the selection of their constituents. During the Roman period, there was a clear establishment of criteria for the sourcing of materials. In a first instance, pure limestone was generally used for binder production, as described by Vitruvius (Delgado Rodrigues, J., 2020). This was identified by its whiteness and hardness, and, according to Adam, J. P. (2005), it was then tested by firing and slaking it. However, this strict criterion made it necessary, in some cases, to source limestone from a considerable distance, and transport it to the construction site (DeLaine, J. 2021). In certain cases, pozzolans were also imported, being this a different process with respect to standard aggregates, which were locally sourced. These were commonly extracted in areas near the construction site, without extensive criteria for their selection, as their selection criteria were based on their abundance and viability of extraction (DeLaine, J. 2021). In some cases, a volumetric separation was done by sieving the aggregates, and some further washing could also have been done.

The transport of the raw materials posed new challenges, due to the increase in the costs of construction. Regarding this, DeLaine, J. (2021) comments: “It has been estimated that one of the major elements in the cost of construction was the transport of building materials, but this depended on the weight and volume to be transported, the distance, the form of transport and the available infrastructure”. It is precisely for this reason that a logical solution to lower the costs was to increase the amount of material transported having the same weight. For this reason, the firing of the limestone was commonly done in the quarry, which according to DeLaine, J. (2021) “reduces the weight by about 44%”. Costs of transport depended as well on the means of it, being this by land, by river (with a different price for upstream or downstream) or by sea. Each of these had different requirements and characteristics. For instance, in the case of sea transport, a much higher amount of material was required in order to be profitable. For land transport, “wagons, drawn by oxen or mules, were the usual mode for overland transport” (DeLaine, J. 2021), carrying between 1-2 tonnes of material on average. The transport of aggregates, on the other side, presented some clear differences. As previously mentioned, these materials were locally sourced, so the required transport encompassed only short distances. It is for this reason that it was common to use carts for this activity (DeLaine, J. 2021).

Once the construction started onsite, the materials used for mortar production needed to be present simultaneously. In this sense, and as remarked by DeLaine, J. (2021), “establishing and maintaining a supply of lime may have been one of the priorities”. This is because mortar is required in all various stages of construction, from the building of foundations to the construction of walls and craftsmanship of finishes, which meant that continuous production of mortar would have taken place all throughout the construction time. It should be remarked as well that this was especially true due to the time frame it takes for the mortar to dry and harden, which meant that it was not possible to produce lime and store it for later use. In this sense, an “efficient use of manpower in construction requires that all the necessary materials are at hand. Depots of building materials are therefore a normal feature of construction sites” (DeLaine, J. 2021). Moreover, since different recipes of mortar were required for different uses, a further classification of the aggregates was required. It is for this reason that it would have been possible to find deposits of aggregates with different characteristics (DeLaine, J. 2021).

As outlined above, the firing of limestone was commonly performed in or near limestone quarries (Adam, J. P. 2005), since it reduced significantly the volume of the product, making it more efficient for transport. This procedure was commonly carried out in kilns, as the burning of limestone in open spaces, although possible, would “result in an incomplete calcination, and the lime produced was contaminated by ash and charcoal from the fuel” (DeLaine, J. 2021). These kilns, as described by Cato the Elder (DeLaine, J. 2021) were “a circular construction resembling a truncated cone in section, varying greatly in size, with the kilns observed ranging from 2 to 7m in both diameter and height, the size generally being related to the length of the process” (Adam, J. P. 2005). They were usually built over a slope, to have easier access to the opening of the combustion chamber in the lower part of the kiln and for loading and unloading purposes (Adam, J. P. 2005). According to DeLaine, J. (2021) the kilns had a cyclical procedure, consisting of filling, firing and unloading, and cleaning. The aforementioned author mentions as well that previous studies suggest that due to the required times for each of the steps of the firing procedure, only three firings could be carried out each month. The mastering of the temperature inside the kiln was necessary, since as argued by Artioli, G. et al. (2019) “the temperature of the firing process controls the quality and reactivity of the starting binder”. According to Pavía, S., et Caro, S. (2007) lower temperatures, or the so-called ‘soft burning’ was preferable, since higher temperatures would lead to a higher tendency of shrinkage in the resulting binder. The operational

temperatures of the kilns ranged between 920 - 1000 °C, which provides the perfect conditions for calcination to take place (which occurs around 850 °C) (Artioli, G. et al. 2019). It should be highlighted however that these conditions could have only been achieved by controlling the fire, for which a constant amount of fuel was required, as remarked before in literature (Artioli, G. et al. 2019; DeLaine, J. 2021).

The resulting material after the calcination has taken place in the kiln are blocks of oxide of calcium of a crumbly texture (Adam, J. P. 2005). According to Adam, J. P. (2005), these quicklime blocks have the same dimensions as the initial limestone, however, their weight is significantly lower. These are then ground, in order to obtain the desired highly reactive quicklime powder, which then is subjected to the slaking process (Artioli, G. et al. 2019). It should be mentioned that some fragments of poorly fired limestone can be found within the resulting material. These fragments, according to Ergenç, D., et al. (2021) “preserve internal geological features characteristic of the original limestones”, which can be useful for source identification.

The quicklime was transported to the site and slaked. This process, as described by DeLaine, J. (2021) involved the gradual addition of water to the reactive quicklime powder. The mixture had to be constantly mixed with the help of a long handle hoe until lime lumps disintegrated completely (Adam, J. P. 2005). Slaking generally took place in the ‘lime-slaking pits’ dug in the building site, which was later used as rubbish pits, commonly found in archeological surveys (DeLaine, J. 2021). It is necessary to highlight the relevance of this procedure, regarding both the input material and the technique used, since it “govern properties such as lime reactivity, shrinkage, density, and water retention capacity, which in turn determine workability, plasticity, and carbonation speed” (Pavía, S., et Caro, S. 2007) of the final product. It is for this reason that longer slaking periods were preferable, resulting in better physical properties due to the gradual addition of water and careful mixture (Moropoulou, A., et al. 2005).

After the slaking procedure is finalized, lime putty could be either stored or used immediately. In the first case, as mentioned by Veiga, R. (2017) “Lime putty can be stored for many years remaining in perfect conditions (in fact it gets better with time), without carbonation and the consequent loss of reactivity”. This was done in order to ensure that the slaking process was finished, avoiding the appearance of lime lumps due to poor slaking or mixing (DeLaine, J. 2021; Ergenç, D., et al. 2021). The addition of aggregates and additives would have taken place

right after slaking was done. The addition of these elements, as previously explained in the present work, had different purposes, such as reducing the shrinkage, adding volume, and modifying the general properties of the binder, such as “improve their carbonation speed, mechanical strength, and waterproofing performance” (Ergenç, D., et al. 2021). The amount or type of aggregates added to the mix could vary significantly according to the available material, the socio-economical context of the building, and the purpose of the mortar within the structure (bedding mortar, foundation, finishes...). Despite this variability, some recipes for mortar production, described in the literature, were commonly followed (DeLaine, J. 2021). In these, the amount of material used was given as a ratio of binder to aggregate (1:2, 1:3), which was commonly measured by volume using baskets. The function of mortar played an important role when deciding these amounts since different purposes or functions required different mortar characteristics. As a general condition, good workability and plasticity of the mortar were required. However, it was essential for when the mortar was intended for decorative purposes (Veiga, R. 2017). This required the mortar to have a specific mixture of aggregates and binders, as well as proper sorting since a coarser fraction would not allow the desired soft finishes (DeLaine, J. 2021). This can be evidenced when DeLaine, J. (2021) provided the description for wall finishes, mentioning “The first (anchorage) layer was the thickest, as much as 50 mm in some cases, as it had to even out the face of the wall. The mortar was applied to the wall using a trowel, with the surface left rough to help the second layer adhere; the large particles of poorly sorted aggregate in the mix encouraged this further. The second layer usually contained smaller and better-sorted aggregate and was given a fat finish probably using a float, as was the very thin final layer composed of lime with little or no aggregate, which could be left plain or painted”. The contrary case can be observed when the mortar was used for foundations or as structural elements. In this case, the rubble fraction and the presence of coarser aggregates were necessary for the proper functioning of the building. The use of certain reactive aggregates depends, in the same way, on the function of the mortar and its location in the building. The use of pozzolans was most commonly used in structural elements, however, some of them could have been employed on mortars used for decoration and finishes. One good example of this is the use of crushed ceramics for flooring since it provided them a better resistance.

After the mortar is properly slaked and mixing is completed, it is carried with baskets and used for construction. It is at this moment that the third and final phase of mortar production will take place; the hardening or carbonation. According to Delgado Rodrigues, J., (2020) “lime

carbonation can be described as a reaction of two reactants, an external reactant A (carbon dioxide dissolved in water), with an internal one B (dissolved calcium hydroxide) to produce an intermediate product C (amorphous calcium carbonate – ACC), an unstable product that will convert to calcite, the most stable polymorph of calcium carbonate”. In other words, during the process of carbonation, CO₂ (carbon dioxide) from the environment, when in contact with Ca(OH)₂ (portlandite), forms crystals of calcite (CaCO₃) and modifies the microstructure of the mortar (Arandigoyen, M., et al. 2006; Veiga, R. 2017). This provides a general idea of the carbonation process, however, this simplified explanation encompasses several phases or stages. According to Oliveira, M., et al. (2022) carbon dioxide must enter into the mortar, where it will be dissolved in water accumulated in the pores. Then, the contact between the dissolved CO₂ and the Ca(OH)₂ will cause the precipitation of CaCO₃. As a result of the reaction, aragonite and vaterite can also precipitate, nonetheless, these phases will eventually convert into calcite since it is the most stable polymorph (Arandigoyen, M., et al. 2006). This reaction will involve H₂O as well, which will flow from the matrix through the now hardened pores.

In this way, the process by which mortars harden will depend on both intrinsic and external factors. On one side, the composition of the mortar will influence in a great measure the factors affecting carbonation such as the carbonation rate and the resulting microstructure (Fusade, L. et Viles, H. A. 2019). On the other, the curing conditions in which this process occurs will have a deep impact on the process itself. Environmental conditions such as temperature, relative humidity, and wind velocity will affect the final product. The most evident explanation for this is the case of relative humidity, since, as previously mentioned, a certain amount of water is required for the dissolution of CO₂ (Veiga, R. 2017; Delgado Rodrigues, J., 2020). According to Fusade, L. et Viles, H. A. (2019) a “higher RH allows a higher rate of carbonation”, and therefore a higher calcite content. Fusade, L. et Viles, H. A. (2019) suggest that the ideal moisture conditions for carbonation of lime binder happen between a relative humidity of 55 – 75%. In this way, the final phase of mortar production will condition the final product, developing a higher level of variability.

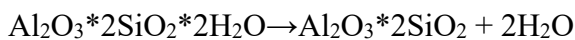
2.3.1.1. PRINCIPLE OF CHEMICAL REACTION IN THE PRODUCTION PROCESS

As it has been highlighted on several occasions, mortar is a highly variable material, due to the different mixture of binders, aggregates, and additives. This is due to the use of different recipes, proportions, and production techniques implemented for each of the steps of mortar manufacturing. In this way, the mechanical properties and durability of the resulting material are a reflection of its chemical composition and fabrication procedure. This fact is clearly described by Vitti, P. (2021) when mentioning: “The mechanical and cohesive qualities of the mortar, as well as its durability, depend on the lime: its composition, porosity, inclusions in the carbonate rock as well as the dimensions of the carbonate rock clasts and the firing temperature and process. Other factors, such as the composition and dimension of aggregates, the amount of water, appropriate immersion into water of masonry units proportionately to their porosity, and external temperature at the time of the masonry production also contribute to durability.”. On the other hand, as previously marked, the environmental conditions during the setting of mortar, meaning the curing conditions, play as well an essential role in the definition of the outcome (Fusade, L. et Viles, H. A. 2019). Therefore, it is logical to state that the chemical composition of mortar is also highly variable since it depends on all the aforementioned factors.

Lime-based binders in mortars are constituted in this way by two main categories; dolomitic binder and lime binder. Dolomitic binder, as its name suggests, is the product of the calcination of dolomitic limestone (or magnesian limestone) (Maravelaki-Kalaitzaki, P., et al. 2003). According to Veiga, R. (2017) the fired products are both magnesia (MgO) and calcium oxide (CaO), which form brucite ($Mg(OH)_2$) after slaking. In this way, the outcome is composed mainly of $MgCO_3$, and the possible presence of hydromagnesite. The lime binder, as previously mentioned, is primarily composed of $CaCO_3$, which is as well the final composition of the binder. However, a series of phases can be identified within the binder, as clearly described by Arizzi, A., et Cultrone, G. (2021). Among these it is possible to identify portlandite, C-S-H (calcium silicate hydrates), C-A-H (calcium aluminate hydrates), AFm, belite, and alite phases, to name a few. The formation of these phases responds to factors such as the firing conditions of the raw material, the setting speed, the slaking technique, or the presence of certain elements.

On the other hand, the aggregate fraction of the mortar plays an essential role in the chemical composition of the final product. As has been claimed by Veiga, R. (2017) the addition

of certain elements to the mixture will lead to a modification of the matrix, due to the interaction between the aggregates or additives and the binding material. Regarding this matter, the author states: “The use of additions, both mineral (pozzolans, microsilica, fillers, etc.) and organic (water retention, water-repellent or plastifier agents, organic fibers, etc.) induce changes in characteristics and may (or may not) improve performance and durability” (Veiga, R. 2017). A clear example of this is the use of reactive materials commonly called pozzolans, which have been observed in several occasions in literature. This, as described by Sagın, E. U., et al. (2021) “are siliceous or siliceous-aluminous materials that also contain amorphous silica or alumina”. The mentioned materials, when in contact with portlandite and water will produce calcium silicate (C-S-H) and calcium aluminate (C-A-H) hydrates, which will lead to a higher resistance in the mortar, due to the presence of “interlocking crystals” (Böke, H. D., et al. 2006; Arizzi, A., et Cultrone, G. 2021)). This reaction can be observed in the description provided by Böke, H. D., et al. (2006):



Although this phenomenon is more common to occur with pozzolans, as it has been remarked, some non-reactive aggregates may react as well with the binder. A clear example of “inert” aggregates reacting with the binder is the so-called dedolomitization process (Stukovnik, P., et al. 2020). This process, as described by Stukovnik, P., et al. (2020) consists of the interaction of dolostones reacting to the binder due to its alkalinity, commonly referred to as an alkali carbonate reaction. This dedolomitization is best described by the author when mentioning that “During the dedolomitization reaction, dolomite crystals in the grains interact with the hydroxide ions that originate from dissolved portlandite in the binder, causing the decomposition of the crystals and the intergrowth of calcite and brucite. Consequently, the carbonate ions are released, and they diffuse into the binder. In the binder, they react with the Ca^{2+} ions that originate from the dissolved portlandite and form secondary CaCO_3 (carbonate halo) around slowly decaying dolomite grains” (Stukovnik, P., et al. 2020).

A similar case of an intentional addition of a certain material or substance can be observed for the case of additives in the mixture. This action although it is not a result of a conscious decision or the understanding of chemistry, is done in principle to alter the binder composition to obtain desired results in the mortar. For this purpose, and as it has been previously commented, the use

of both organic and inorganic materials was added to the already slaked lime putty, where it reacts with the binder before setting or carbonation occurs. One example of this can be seen in the intentional addition of vegetable ash or bone residues, as can it be seen in the study carried out by Secco, M. et al. (2020). In this, the identification of the aforementioned additives was achieved thanks to the presence of “cryptocrystalline particles, mainly siliceous-aluminous in composition with associated calcium, magnesium, phosphorous, alkalis, iron, chlorine and titanium” (Secco, M. et al. 2020) interacting with the binder, and producing a pozzolanic reaction.

2.4. CURRENT APPROACH AND TECHNIQUES FOR MORTAR CHARACTERIZATION

The scientific study of mortars used in historical contexts has been an uprising topic since the 1990s (DeLaine, J. 2021). As it is commonly the case for archaeometrical studies, the information that can be obtained from these studies derives directly from the analysis of the finished product (DeLaine, J. 2021). In this way, and following the common tendency, new in situ studies can be carried out that could proportion valid information from the analyzed structure without damaging or harming it (Donais, M. K., et al. 2020). However, due to the complex nature of the material, a series of analyses that provide key insights into historical mortars are necessarily destructive. This factor depends in great measure on the objective of the study carried out. According to Arizzi, A., et Cultrone, G. (2021) the study of historical mortars can provide the following information: “The nature of the mortar, i.e. whether it is air-hardening or hydraulic, the type and grading of the aggregates, the binder-to-aggregate (B/A) ratio and the presence of secondary components, among others; The manufacturing process, i.e. where the raw materials come from and how they were processed, for example during firing, slaking or mixing; The building techniques applied, to find out more about ancient and traditional methods of applying and curing mortars, and to recognize when subsequent interventions have been performed; And the state of conservation, in order to understand the decay processes suffered by the mortar and its resistance to alteration factors.”.

According to this, and as it has been established by several authors, one of the most relevant information that can be obtained is the general composition of the mortar: the understanding of the raw materials used and the interaction between them (DeLaine, J. 2021). For this purpose, it is common to identify the geological origin of the aggregates used for the manufacturing of this

material regarding its mineralogy (Rispoli, C., et al. 2020). The proportions of the binder and aggregates should also be studied, providing in this way a complete understanding of the recipe used (Lindqvist, J. E., et Sandström, M. 2021; Veiga, R. 2017). In this way, it is possible not only to obtain information regarding the source of the materials implemented but also to “draw socio-economic conclusions on the provenance of the raw materials and the production processes” (Elsen, J. 2006). In the same way, studies regarding the interaction between aggregates and matrix can provide an idea of the working properties of the analyzed mortar. This can also be confirmed throughout a series of analyses that would test the mortar's overall performance, resistance, and durability (Oliveira, M. L. S., et al. 2020).

Another essential point in the study of mortars, as it has been previously mentioned, is its possibility to provide a relative or absolute chronology and the understanding of the different construction techniques (Vitti, P. 2021). Due to the high variability of mortars as a result of small changes in their manufacturing processes, it is possible to characterize the relative chronology of a structure by “understand their construction sequence and phasing through comparisons of the mortars’ elemental compositions” (Donais, M. K., et al. 2020). On the other hand, mortars can provide as well exact dates, as they are a reliable source for absolute dating through carbon 14 and optically stimulated luminescence dating (Ergenç, D., et al. 2021).

Due to the historical context from which the analyzed mortars are obtained, degradation and further restoration-related investigations are commonly addressed. The aging characteristics of mortars under specific conditions have been addressed in literature (Izaguirre, A., et al. 2010; Nogueira, R., et al. 2020). On the other hand, the identification of the nature of a mortar (the understanding of the production techniques, and the identification and quantification of the aggregates used) is commonly required for the proper restoration of a structure (Maravelaki-Kalaitzaki, P., et al. 2003). Moropoulou, A. et al. (2005) address this subject when mentioning: “Therefore, there is a demand for proper restoration mortars and building materials compatible with the original structures.” In this way, it is precisely through the understanding of the material that an analogous mortar used for restoration purposes can be produced.

The study of historical mortars provides a clear characterization of both physical and chemical aspects of the analyzed materials. In this way, it encompasses a series of analytical techniques that can provide different answers to the questions posed by the specific investigation.

In this sense, the selection of the technique and the analytical plan is of the utmost importance, as mentioned by Elsen, J. (2006) “The choice of the appropriate analytical technique depends mainly on the questions that have to be answered and on the amount of material available”.

Most of the studies on mortars begin, in a first instance, with the observation and description of the macroscopic features of each sample. This procedure can be done either with the naked eye of a trained professional or with the help of a magnification loupe (or stereomicroscope) (Arizzi, A., et Cultrone, G. 2021; Ergenç, D., et al. 2021). The recorded information should encompass aspects such as a detailed description of the aggregates present in the samples, the description of the binder, its texture, and color, the differentiation between layers (if there are present), the degree of cohesion of the material, degradation processes taking place (if any), and the chromatic characteristics, among others (Arizzi, A., et Cultrone, G. 2021).

After the macroscopic observation is done, other chemical and mechanical techniques can be applied in order to obtain the desired responses, according to the investigation's purposes. The physical aspects of mortars can be evaluated through a series of mechanical tests; whose aim is to assess their working conditions. The study of porosity and the general properties of the pore system will provide as well some key information concerning the physical aspects of mortars and will provide certain clues regarding the production techniques implemented. Furthermore, the hydric properties of mortars can also be tested through a series of analytical techniques. Finally, colorimetry or color measurement can be performed to evaluate the aesthetical aspects of the mortar samples. On the other hand, the chemistry and mineralogy of mortars can be studied through the implementation of other techniques, such as optical microscopy, x-ray powder diffraction (XRD), thermogravimetric analysis (TGA), x-ray fluorescence (XRF), scanning electron microscopy (SEM), cathodoluminescence or Fourier-transformed infrared spectroscopy (FTIR). Mortar dating can also be assessed by two different techniques: radiocarbon dating (^{14}C) and optically stimulated luminescence (OSL).

2.4.1. MECHANICAL PROPERTIES OF MORTAR

The mechanical properties of mortars play an essential role, as previously mentioned, in the working conditions of the entire structure (Ergenç, D., et al. 2021). This materials not only

allow the cohesion of the single units in a masonry building, but they also play an essential role in weight or load distribution. Similarly, and as mentioned by Ergenç, D., et al. (2021), “the strength of an aerial lime mortar is proportional to the strength of the weakest component—the binder”. However, the aggregate fraction of the mortar will define a lot of the specific characteristics of this binder (due to the interaction between one another) (Veiga, R. 2017). In this way, “mechanical characterization includes measuring the strength of the mortar (compression, tensile and shear strength), the drilling resistance, hardness and modulus of elasticity” (Ergenç, D., et al. 2021). Hardness can be addressed through the use of a mechanical press (Arizzi, A., et Cultrone, G. 2021), the rebound hardness test (Ergenç, D., et al. 2021), the Schmidt hammer, and the indentation hardness (Arizzi, A., et Cultrone, G. 2021). On the other hand, the resistance of the material can be tested through the micro-drilling test, which according to Ergenç, D., et al. (2021), can also provide different values according to the depth of the sample. It should be mentioned, however, that all of the mentioned analyses require direct contact with the material and can be harmful to it. It is necessary to remark that some of the tests require a minimal amount of testing material.

Moreover, the comprehension of the pore system of the analyzed material is crucial for the understanding of its mechanical properties. This is due to the fact that the amount and types of pores present in the sample affect directly the strength of the mortar and its durability, usually being inversely proportional (the higher the amount of pores, the lower the strength and durability) (Pineda, P., et al. 2022). According to Elsen, J. (2006) “the following three values are fundamental for the description of porous materials: total porosity (TP), pore size distribution (PSD) and specific surface (SS)”, which can be obtained from several tests and analyses. Most of the tests implemented for porosity analysis (except for mercury intrusion porosimetry) are non-destructive and encompass a variety of pore types and sizes. These techniques are observation of porosity in thin sections, mercury intrusion porosimetry (MIP), air permeability test, capillarity water test, x-ray computed tomography (CT), and ultrasonic pulse velocity (UPV) (Ergenç, D., et al. 2021).

In the same way, porosity determines in a great measure the hydric behavior of the mortar, or as mentioned by Arizzi, A., et Cultrone, G. (2021) “It is important to study the porosity of historic mortars in order to find out more about their hydric behavior”. Arizzi, A., et Cultrone, G. (2021) defines hydric behavior as the reaction of the material concerning water, which determines the durability of the mortar. However, not all mortars are suitable for testing, since this test requires

a minimal amount of sampled material and its proper cohesion. The hydric properties of a mortar can be studied through the implementation of the following tests: water absorption at atmospheric pressure, water absorption by the pipe method, water permeability, and water vapor test (Arizzi, A., et Cultrone, G. 2021).

2.4.2. CHEMICAL AND MINERALOGICAL PROPERTIES OF MORTAR

Optical microscopy is a technique commonly used for mortars' characterization, as it allows for the observation of “the main textural and compositional features of these materials” (Arizzi, A., et Cultrone, G. 2021). This technique, used as well in petrography, is usually carried out in transmitted light (TL) and requires observation under the trained eye since prior knowledge or expertise is essential to obtain the desired results (Ergenç, D., et al. 2021). From this technique, information such as the type of binder, the type (or nature) and amount of aggregate, the use of pozzolans or additives, and the pore system can be observed. Furthermore, according to Lindqvist, J. E., et Sandström, M. (2021), combination with chemical methods can provide valuable information concerning the properties of the sample”. The observations done throughout this procedure could provide useful information regarding not only the material itself, but the manufacturing process since this leaves traces in the analyzed final product. One clear example of this that has been addressed in the literature is the presence of lime lumps, which according to their nature (underburned, overburned, or lime lumps *sensu stricto*) are a consequence of carbonation or slaking conditions (Elsen, J. 2006).

X-ray diffraction is a technique often used for the identification of crystalline mineral phases (Ergenç, D., et all. 2021; Pineda, P., et al. 2022). This provides key knowledge of the mortar, which according to Arizzi, A., et Cultrone, G. (2021) “can highlight the presence of hydraulic limes, pozzolanic admixtures, or cement”. However, the technique has certain limitations such as the inability to distinguish between carbonate binder or aggregates, C-S-H phases due to their amorphous nature, and the presence of phases under the detection limits.

Thermogravimetric analysis (TGA), according to Ergenç, D., et all. (2021) is used to “perform chemical characterization and analyze the crystallographic thermal stability of mortar components”. With this in mind, the samples' behavior, mainly its weight loss, when subjected to

temperature changes will determine the amount of hydrated phases in a mortar (Pineda, P., et al. 2022). In this way, when the sample is subjected to thermal variations, and the weight is monitored, it is possible to observe the drying properties of the analyzed mortar (being this represented in the weight loss as a function of time) (Ergenç, D., et al. 2021).

On the other hand, x-ray fluorescence (XRF) is an analytical technique used to determine the chemical or elemental composition of a sample (Arizzi, A., et Cultrone, G. 2021). This technique allows the identification of and quantification of both major and minor elements, as remarked by Ergenç, D., et al. (2021). Portable options of the machine are also available, to avoid sampling.

Furthermore, scanning electron microscopy (SEM), one of the most common techniques for mortar characterization, is a non-destructive technique that coupled with energy dispersive spectroscopy (EDS) “provides significant qualitative and semi-quantitative information about crystal morphology and the chemical composition” (Ergenç, D., et al. 2021). According to Tenconi, M., et al. (2018), it allows for the microtextural and microchemical characterization of the matrix. In this way, key important features such as the pore structure, reaction rims, or the presence of aggregates can be observed and analyzed. The SEM-EDS allows in this way for the identification of both C-S-H and C-A-H phases present in mortars (Arizzi, A., et Cultrone, G. 2021).

Cathodoluminescence, in the study of historical mortars, is commonly used for the identification of certain components and processes that carbonate rocks went through during their transformation (Ergenç, D., et al. 2021). In this way, and as mentioned by Ergenç, D., et al. (2021), it is “possible to differentiate calcium carbonate (CaCO_3) of geological/natural origin (original grains) from that generated by the pyrogenic process”.

Fourier-transform infrared spectroscopy (FTIR) is, as its name mentions, a spectroscopic technique that has been used for the identification of chemical compounds (Arizzi, A., et Cultrone, G. 2021). This permits, during the characterization process of historical mortars, the observation of organic compounds added to the matrix and compounds from a mineralogical context such as calcite, quartz, aluminum silicate aggregates, portlandite, and gypsum, to mention a few (Ergenç, D., et al. 2021).

Finally, laser ablation inductively coupled plasma mass spectrometry (LA-ICP-MS), although not commonly used, provides useful information concerning the provenance of raw materials, due to the possibility of detection of trace elements in the analyzed mortar (Arizzi, A., et Cultrone, G. 2021).

3. Chapter III - The city of Verona: history and architecture in the Roman age

3.1. POSITION AND HISTORY

The city of Verona is located in the north of the Italian territory, more specifically in the region of Veneto. It is situated in the Po Valley, between the cities of Padua (40 km approx.) and Milan (160 km approx.). The city is strategically situated in the valley of the Adige River, where it could execute control over its navigation and as a consequence to a significant part of the territory.



Figure 2 Location and urban plan of the city of Verona (taken from Marchini, G. P., 1978)

It is precisely because of its location that the city itself originates. During the middle and recent Bronze Age, as mentioned by Bonetto (2009), the area that now constitutes the city of Verona was subjected to intense frequentation, due to its geographical position and natural characteristics. This frequentation eventually leads to the first settlement to be established. The initial nucleus was located on the left side of the Adige River, on the hill of San Pietro. However, the settlement did not last long and was then abandoned. The area later encountered another period of occupation during the Iron age. In this period, as in the previous one, the settlement was located in the southern area, over the hill of San Pietro. Nonetheless, the settlement was abandoned during the 7th and the 6th centuries BC (deduced from the lack of archeological data for this period). The final settlement, once again taking place on the left side of the river, was around the 3rd and 2nd

centuries BC by the Celtic tribe of the Cenomani, as mentioned by Bonetto (2009). It is important to mention that this series of settlements occurred on the hill due to its geographical and natural characteristics. On one hand, the strategic position over the Adige River provided not only control over the territory but also a mandatory passage through this area, which translated into the possibility of connection with other parts of the region. On the other hand, the natural properties of the land allowed as well the practical and easy creation of a ford around the river or in the hill itself, providing protection to its citizens and reinforcing the control of the territory. It is precisely for this reason that the settlement was later incorporated into the Roman territories (Marchini 1978).



Figure 3 Initial settlement in San Pietro hill (by G. Dall'i. Taken from Bolla, M. 2014.)

After the Romanization of the territory took place, the strategic connectivity was strengthened by the creation of the important route of the Via Postumia, which according to Bolla (2014) crossed all of northern Italy, as it connected Genoa to Aquileia. This route crossed the Adige River on a wooden bridge that will later be replaced by the Pietra bridge, which provided better means for the integration of the two banks of the river (Marchini 1978). The Romanization of Verona was also testified by the Legal status obtained by the city in the year 84 BC when the city became a colony. This legal status was mentioned by Bolla (2014) as “different from that of other northern Italian centers transformed into municipalities”. The Romanization process continued as well with the construction of a new settlement on the right side of the river and the program of monumentalization of the city. One of the most relevant effects of the Romanization of the city is the formulation of a new city plan.

In the year 49 BC Verona was subjected to a radical transformation ordered by Caesar. A new urban layout was designed on the right side of the Adige, with the appropriate spaces required for the Roman people of Verona to “exercise the rights and duties of citizenship” (Marchini 1978). The city followed the colonial Roman model for the formulation of the city plan. It was constituted by an orthogonal grid of streets, with two main axes (the decumanus maximus and the cardo maximus). These two main routes or axes of development intersected in the Forum, where the public life of the city took place. It is in the forum, as can be seen in other Roman cities, where the most important buildings, such as the Capitolium, the curia, temples, and some commercial structures, could be found. The construction of the new city involved as well the location of the artisan quarters, which according to Cavalieri Manasse (1987) were found in the suburbs, and the cemeteries, located outside the city walls. At the same time, the movement of the general location of the city nucleus left the area of the hill of San Pietro free of buildings. This was taken as an advantage for the planners, who established the monumentalization of the hill and scenic backdrop of the city by constructing the theatre, the Odeon, and a temple on the top of the hill. This led as well to the construction of the Postumio bridge, which (as did the Pietra bridge), functioned not only to connect both banks of the river but also to allow the construction of the two aqueducts that would supply water to the city (Bonetto, J. 2009).



Figure 4 Roman urban setting (Taken from Bolla, M. 2006)

barbarians in the year 102 – 101 BC, establishing in this way the importance of Verona as a strategic point of protection in the Alpine border (Marchini, G. P. 1978).

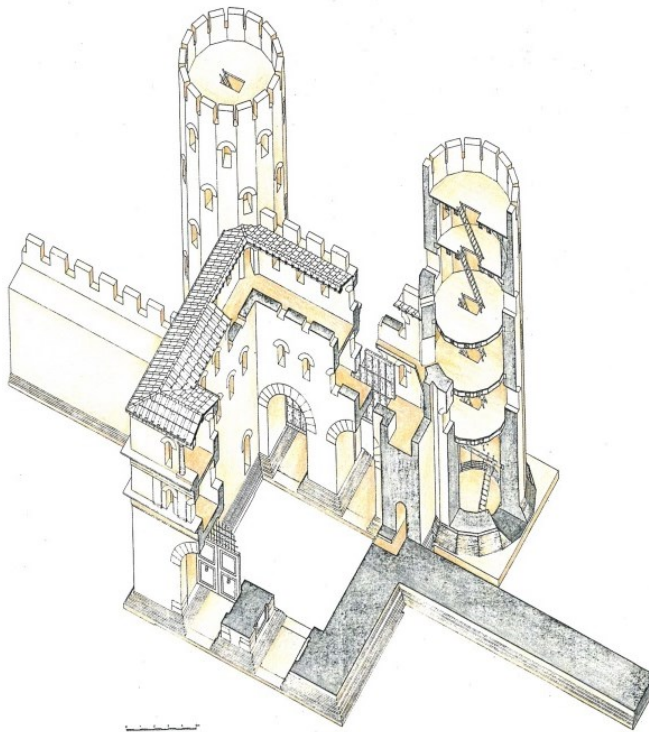


Figure 6 Illustration of Porta Leoni (Taken from Cavalieri Manasse, G 1987).

Later on, around 49 BC, a new defensive wall was built, protecting the southern and eastern sides of the city (the other two were already protected by the presence of the Adige River). It was a “massive brick walls, 3.60 m wide at the base, which narrowed with a series of offsets towards the top, located about eleven meters in height, and were interrupted by two gates, today called ‘Porta Leoni’ and ‘Porta Borsari’” (Bolla 2014). This building technique of sesquipedalian brick walls was, according to Cavalieri Manasse, G. (2003) applied common construction techniques for defensive walls in the Po Valley. In it, a conglomerate of pebbles was used for the

foundation, and bricks were joined by lime mortar for its elevation. It had a height of 3.60 m. with a base wider than the top of the wall (providing better stability) (Bonetto, J. 2009). The two gates that constituted the entrance to the city were located one along the southern side, the ‘Porta Borsari’ (also called ‘Porta Lovia’ due to its proximity to the temple of Jupiter Lustral) which crossed the via Postumia, and the other, the so-called ‘Porta Leoni’ along the south-eastern side of the wall.

This defensive system presented a series of changes, even its partial destruction and reconstruction throughout the history of the city. During the Augustan age, the city encountered a period of peace and stability, that led to the disuse of the walls. For this reason, the defensive system was partially dismantled, in favor of residential buildings and the growth of the city (Bolla 2014). However, during the Claudian age (as a consequence of the stability and peace that characterize this period), and more specifically in the year 44 AD (according to an epigraph) the walls were reconstructed this time with a greater emphasis on aesthetic values. During this time,

the walls were not subjected to any variations regarding their position or dimensions, but rather their materiality and aesthetic. Some sections were demolished and reconstructed using white limestone (Bolla, M. 2014). The two gates were altered as well to respond to the aesthetical needs (Marchini, G. P. 1978). This operation did not encompass the destruction of the previously existing gates, but rather its “covering” or juxtaposition of a new façade with the same white limestone, or as better described by Bolla, M. 2014: “In reality, the old brick doors were not touched, but their sober brick facades were juxtaposed (a real "image operation" with no functional significance) with new elevations in light and shiny stone with rich architectural ornaments”.



Figure 7 Actual state of Porta Leoni. (Taken from Calcagni, A. C. 1999)

However, this period of peace did not last for long and the city saw once again the need to recover its defensive purpose. During the period of Gallienus, the city of Verona was once again threatened due to rivalry between the emperor Julius Philip the Arab and Decius and the attacks on the city's proximity by the Alamanni (Marchini, G. P. 1978). It is for this reason that the reconstruction of the municipal walls took place under the orders of emperor Gallienus, as

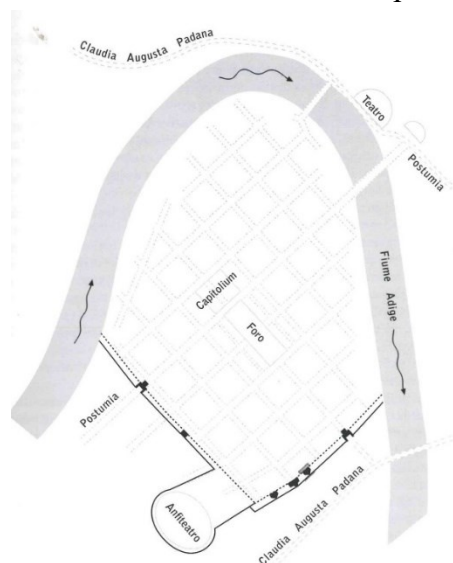


Figure 8 Actual state of Porta Leoni. (Taken from Calcagni, A. C., 1999)

mentioned in the inscription found in “Porta Borsari” (Bonetto, J. 2009). The new walls, as expressed by Bolla, M. (2014) were extended to include the amphitheatre, which, if taken by the enemies could constitute a clear threat to the city (due to the height of the structure). In this period, the construction technique used, opposite to the one of the Claudian period, was disorganized and unaesthetic. The use of poor mortars and reused stones, mainly from funerary origin in such a disorganized way caused the definition of this technique as “tumultuous” (Bolla 2014; Bonetto 2009).

These same walls were later strengthened and elongated during the Theodoric period (493 – 526 AD) (Marchini, G. P. 1978). This was done due to the decision of the Ostrogothic king to establish its residence in the city of Verona, which led to the evident need for the fortification of the city (Bonetto, J. 2009). The new defensive system had a series of changes regarding the previous one; in the first instance, the walls reached a new height of 14 m (from 8-10 m in the previous walls) (Bolla, M.

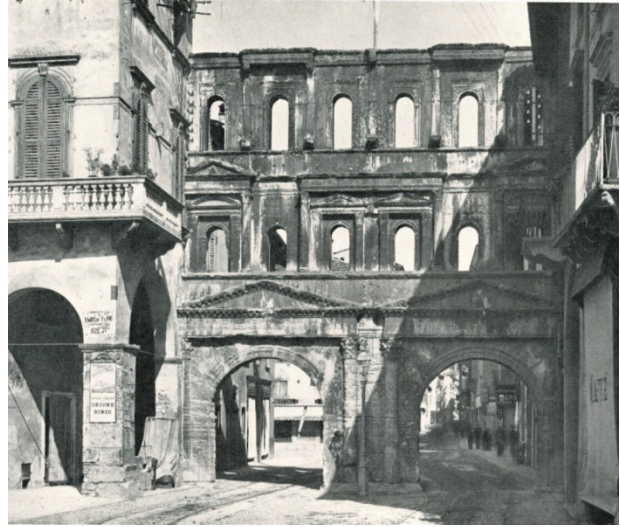


Figure 9 Porta Borsari. (Taken from Beschi, L 1960)

2014). On the other hand, the new system included the fortification of San Pietro Hill, which according to Marchini, G. P. (1978) and Bolla, M. (2014) was called castrum in Medieval times. Finally, even though the construction of the walls required the re-use of materials (mainly recovered from the Arena (Bonetto, J. 2009)) their disposition showed an organized plan differentiated from the “tumutuos” one (Bolla, M. 2014).

3.3. THE FORUM AREA

An area of the city heavily impacted by the monumentalization of the second half of the 1st century BC, as previously mentioned, is the forum. Its construction testified not only the importance of the city itself but also its wealth (achieved due to its location as a crossroad and the healthy climate of the region). For this reason, in the Augustan age, the decision of its construction took place. Being the center of public life, it represented the most important expressions of political, economic, and religious power. It was located at the crossroads between the decumanus maximus and the Cardo maximus and had dimensions of 74 x 76.50 m. On its north-western side stood the Capitolium, whose construction stood at the end of the forum. The square was surrounded as well by a portico, shops, and minor roads. Furthermore, on the western side of the forum, the curia and the basilica were located. Both buildings occupied the same area, being symmetrical and in this way, demonstrating careful planning of the city center.

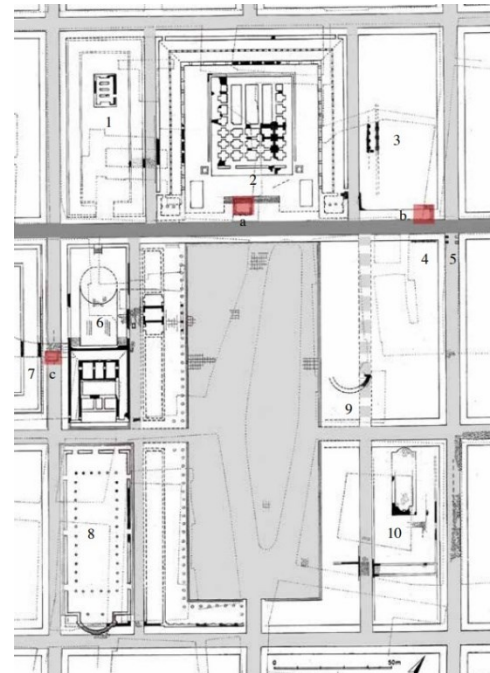


Figure 10 Forum area plan. (Taken from Basso, P. 2019)

During the Claudian Age, and more specifically in the year 44 AD, the forum was transformed by paving its floor with white and pink Valpolicella slabs, as mentioned by (Bonetto 2009; Cavalieri Manasse 1987). At the same moment, most streets were paved in Valpolicella limestone, except for the main roads where black basalt was used due to its higher resistance. Another change in the forum area occurred in the Hadrian age, with the rebuilding or restoration of the basilica (Cavalieri Manasse 1987). However, like most Roman buildings, it saw its downturn, and by the fourth and fifth century AD it had already shown a state of abandonment and decline (Cavalieri Manasse 2003; Bolla 2014). Nonetheless, the memory of the site as the center of the city stood long after its decline, now with the Piazza delle Erbe.

3.3.1. THE CAPITOLIUM

As previously mentioned, the area of the forum included buildings such as the Capitoliium (also called the Capitoline complex), the Basilica, the Curia, and commercial buildings. It constituted the center of city life, where all the most important activities would take place, and where “political, administrative, judicial and



Figure 11 Reconstruction of the Capitoliium (Taken from Bolla, M. 2014)

commercial functions” (Bolla 2014) would be exercised. In this sense, the area comprehended by the forum and the buildings within it were the reflection of the city itself, therefore, it should reflect the wealth and the political relevance achieved by the city (Marchini 1978). As mentioned by Cavalieri Manasse 2003: “Among the achievements of the municipal system there was also the construction of the urban complex of greatest political and ideological value, the Capitoline one”. It was located in the northern area of the forum, occupying its entire flank. The proposed construction chronology, as described by (Bolla 2014) began with the monumentalization plans of the city (49 BC) and ended around the year 20 BC Unlike in other Roman forums, the Capitoliium in the Veronese one was not directly adjacent to the forum area due to the interruption caused by the presence of the decumanus maximus. However, this disruption was overcome by the perfect alignment of the building with the forum and by locating it over a platform to virtually reunite them. These terraces provided the building with a base of 22 meters over the street (Bolla 2014) and it could be accessed by a centralized series of stairs located on the main façade (according to recent reconstructions). On it, a three-sided portico (80 meters long) stood on its perimeter, with the main building being centered in this area. According to Cavalieri Manasse (1987) and Bonetto (2009), it had a rectangular plan with dimensions of 35.5 m. width and 42.2 m of depth. The main building had as well two pronaos divided by three rows of columns (Bonetto 2009). Its construction implemented mainly the use of bricks and tuffaceous stones as mentioned by

(Cavalieri Manasse 2003). Its decoration, which was on the Tuscan order, was mainly done with stucco and crowning with terracotta slabs (Cavalieri Manasse 2003). Furthermore, it should be mentioned that the building was never subjected to significant changes, which lead to its already noticeable deterioration of the structure by the 4th-century AD, and its eventual demolition (Bolla 2014; Marchini 1978).

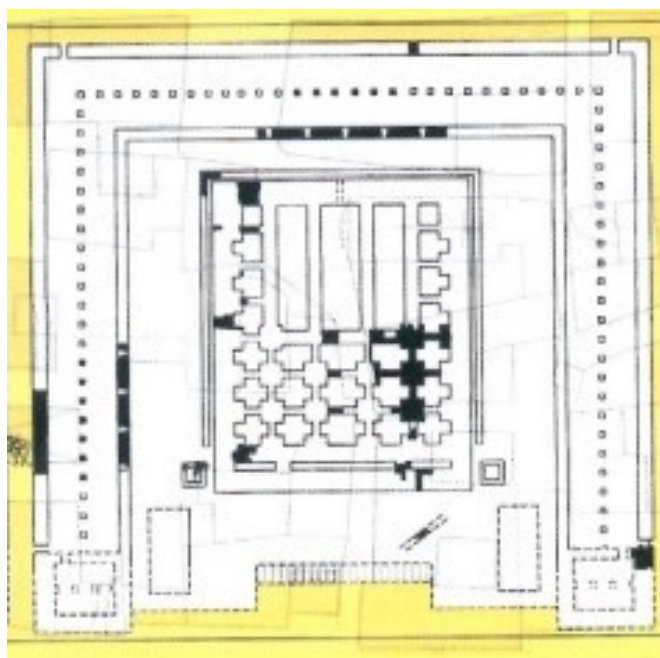


Figure 12 Planimetry of the archaeological area of the Capitolium (Taken from Bolla, M. 2014)

3.3.1.1. THE “CATO” BUILDING

There is little to no information regarding the “Cato” building. The only information that can be presented about this structure is its location and some procedure. It is located on the southwestern corner of the forum, by the side of the Capitolium and the Curia complex. The remaining wall, observed thanks to archeological surveys consists of a concrete core with alternating layers of bricks. In addition, it is possible to observe the implementation of blocks of tuff of small dimensions on its façade.



Figure 13 Preserved wall of “Cato” building (Image taken by Eliana Bridi)

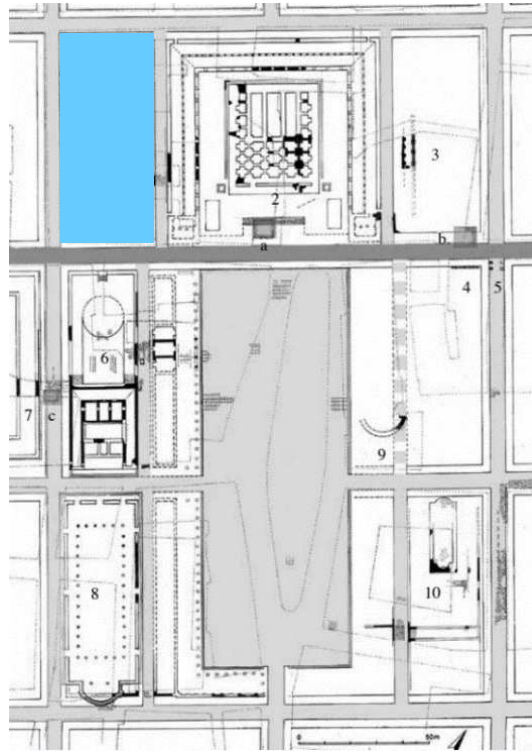


Figure 14 Forum area plan showing the location of "Cato" building. (Taken from Basso, P. et al 2019)

3.3.1.2. THE CURIA

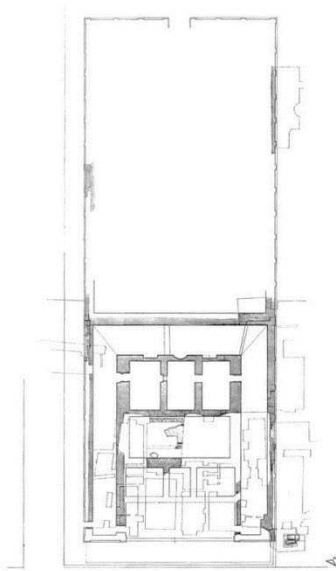


Figure 15 Forum area plan. (Taken from Basso, P. et al. 2019).

As part of the monumentalization plan that took place in Verona at the beginning of the first century BC, and within the epicenter of the monumental area, the construction of the curia took place (Cavaliere Manasse, G. 2003). This public structure erected in the heart of Verona (in the forum), provided the appropriate space for the assembly of the decurions and the highest magistrates (Bolla, M. 2014), showing in this way the political influence of the city. It was located in the southern area of the porticoed space, with a similar area (29 x 80 m. and 27.5 x 78 m.) to that of the basilica (Bonetto, J. 2009). The two buildings were placed side by side, being separated only by a minor road with traffic

restrictions (Cavalieri Manasse, G. 1987; 2003; Bolla, M. 2014). On the other side, by the west, the curia faced an elevated or raised square with porticos (Cavalieri Manasse, G. 2003).

There is little information regarding the general design and morphology of this building. However, the hypothesis of its resemblance to the Curia Julia in Rome was proposed by Bolla, M. (2014), who also provided a small description of the structure as follows: “The curia was accessed by a stairway; flanked by porticoes, it was a single hall, with side benches and a podium at the back”.

3.4. THE BUILDINGS ON THE SAN PIETRO HILL



Figure 16 Illustration of San Pietro hill during Roman times. (By Dalli, G. Taken from Bolla, M. 2016)

The monumentalization of San Pietro Hill was one of the most significant changes in the city. As mentioned before, the design of the new city in the year 49 BC shifted the location of the city from the hill to the right side of the river. This change provided an option for a new use of the San Pietro hill as the backdrop of the new city. The area was therefore destined for the construction

of the theatre complex. During the last decades of the first century BC some preliminary preparations had to take place for the construction of the grandiose building. First, the expropriation of private buildings had to take place, to obtain the construction area. Then, the colossal works on the hill had to be performed in order to prepare the terrain for the construction. The first step to take place was the construction of the embankment of the river. This provided the stabilization of the area not only for the proper construction of the bridges (previously mention to connect both banks of the river) but also to protect the hill area from possible erosion due to the action of the river itself (Bolla



Figure 17 Current state of San Pietro hill. (Taken from Bolla, M. 2016).

2014; Marchini 1978). The construction of the embankment-reinforced walls, which stood parallel to the theatre's later façade, was done in 'opus reticulatum' (Bonetto 2009; Marchini 1978). Further actions for the theatre's construction involved the terracing of the slope of the hill. The terracing system involved the extraction of rocks from the hill itself, which would be later used for the construction of the theatre. This provided the opportunity to observe the underwater activity and redirect its course to protect the theatre from further damage due to water action (Marchini 1978). The terracing system also made it possible for the hill to provide better support for the theatre and the connected public buildings (the Odeon and the temple at the top of the hill) to prevent possible landslides.

After the preliminary works were done the construction of the theatre took place. It consisted of a monumental building of 150 x 108 m. as suggested by (Bonetto 2009). Then, as a part of the complex and even conceived as one project, the construction of the Odeon was carried on. The construction of the Promenades of the Theatre was part of the project as well. In this sense, as mentioned by (Marchini 1978): "all the monumental arrangement of the hill of San Pietro depended on a single project". As part of the same project, the construction of the temple crowning the top of the hill took place in the same period.

3.4.1. THE THEATRE

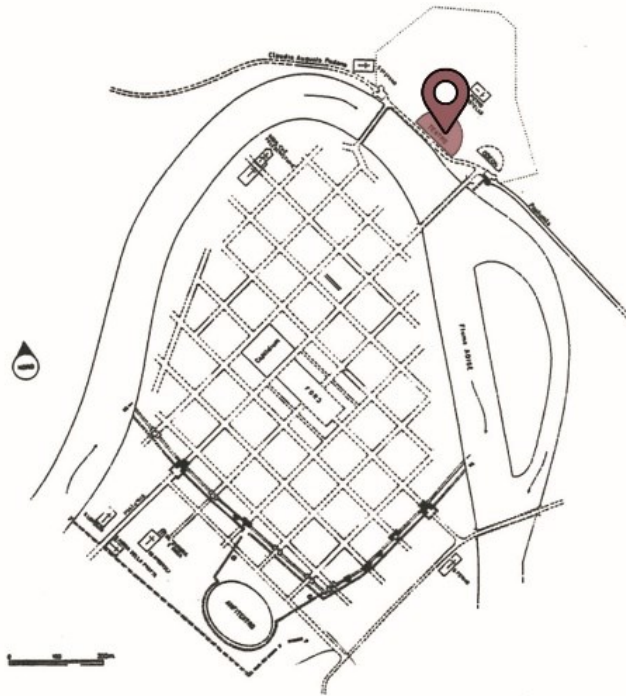


Figure 18 Location of the roman theatre (Based on the plan in Bolla 2014)

The theatre, as previously mentioned, was built on the left side of the Adige River during the Augustan Period. At this time, the city of Verona encountered a period of wealth and prosperity, which led to the construction of the new city center, which moved from the hillside of San Pietro to the right side of the Adige (where the course of the water and the construction of defensive walls would protect the city). During this same period, a clear effort for the construction of theatres, an impulse by the emperor Augustus himself, marked the urban development of Roman cities. In

Verona, the convergence of these two

previous movements or characteristics leads to the construction of the grandiose theatre complex on the hill of San Pietro. The construction began with the rising of the theatre itself (and all the respective preliminary works on the terrain) in the first century BC. The location of the grandiose building was carefully analyzed, selecting the point in which the terrain could partially be used as a support for the theatre building itself, as well as providing a proper backdrop for the city. The presence of the theatre complex on the hill San Pietro gave the city a scenic view, which could be accessed through the axial perspective of the *Decumanus maximus*. At the same time, the hill offered both a practical solution, for the structural support of the *cavea* and the quarrying of construction material, and a symbolic one, providing the complex some sort of “*arce* or *acropolis* (but the definition is improper) concerning the new urban system”, as mentioned by Bolla (2014). Finally, the selected position was located, as many of the Roman theatres from the Augustan period, were near an important road (*via Postumia*), which provided the perfect opportunity for the residents of the city to showcase their most majestic constructions.



Figure 19 Illustration of the interior of the Roman theatre (By Marco Calderini, G. Taken from Bolla, M. 2016)

However ideal the location could have seen, it imposes a series of challenges to overcome in order to adapt it to the proper series of construction works of the theatrical complex (which involved the theatre, the Odeon, a series of terraces, and sacred spaces like the temple located on the hilltop). An enormous effort took place to stabilize the slope of the hill, to prevent possible future landslides. This involved the formation of a series of terraces, as well as the construction of an embankment in front of the Adige River (Bolla 2016). The embankment wall had as its purpose to provide protection from the river erosion action on the base of the hill, and to provide the base of the building structure with a stable terrain (Marchini 1978). The construction of the embankment walls, as mentioned by Cavalieri Manasse (1987) constituted a protection of 71 m alongside the river, built in a technique called *opus quadratum*. On the other hand, the terracing of the slope involved managing the steepness through a series of excavations (from which materials were quarried for further construction purposes. This “cutting” of the hill allowed the builders a clear view of the underground water flow. With this information, it was possible to propose a system for water drainage that would protect the theatrical structures from the damages water would course, as well as protect the hill from possible landslides due to erosion (Marchini 1978; Bolla 2016; Dal Forno 1975). For this reason, the construction of a series of a deep paved system of

ditches took place in different places of the theatrical complex (such as around the top part of the cavea or the orchestra).

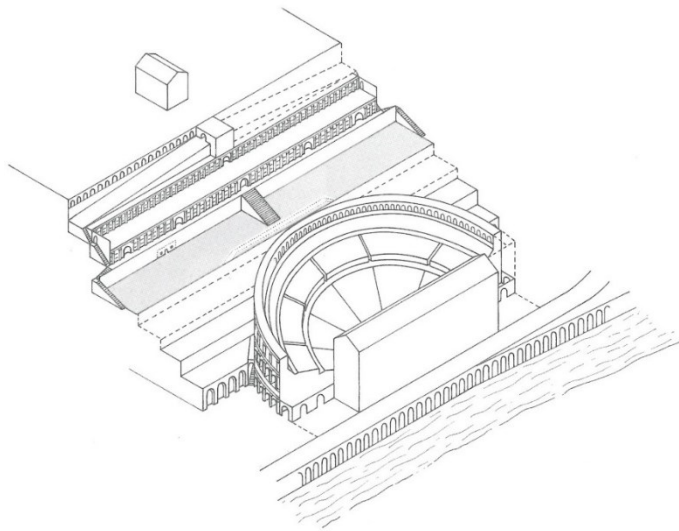


Figure 20 Roman theatre axonometric illustration. (Taken from Bolla, M. 2016)

those northern Italy theatres and could accommodate up to three thousand spectators, according to Tosi (1994). As mentioned by Bolla (2016) the overall dimensions of the building were 150 meters (including the lateral annex) and a diameter of 108 m. These grandiose dimensions gave a distinction to the building, being considered one of the most important in northern Italy (together with the theatre in Trieste).

The scenic building, which stood 10 m. from the riverbank was described by Sear (2006) as the most spectacular part of the building, due to the rich decoration and careful design. It consisted of the scaenae frons, the post-scaene, two parascaene and a pro-scaene. The scaenae frons, with a height of 27m and a plan of 6 x 72 m, had three niches with doors to access the stage. The center had a curvilinear shape and the two later ones a rectilinear one, giving the building a sense of symmetry. It was, as mentioned before, richly decorated, with marble, colonnades (from three different orders) spectacular statues, and ornaments. It is today one of the most well-preserved parts of the monumental building. The proscenium, located between the parascaenae and the orchestra consisted of a table, which rises 1.4m above the orchestra. The front to the elevation is counted as well with some rich decoration in carved marble (Tronchin et Bevilacqua 2022).

The theater design, in accordance with the style of the Augustan period, had the characteristics of a purely Roman theatre. Nonetheless, the theatre's cavea partially rested on the hill slope, giving it a mixed form, since this characteristic corresponds to the Greek theatres. It consisted of a completely closed body, that, as described by (Cavaliere Manasse 1987) "was connected to the hill through monumental elevations". The scenic building was one of the largest among

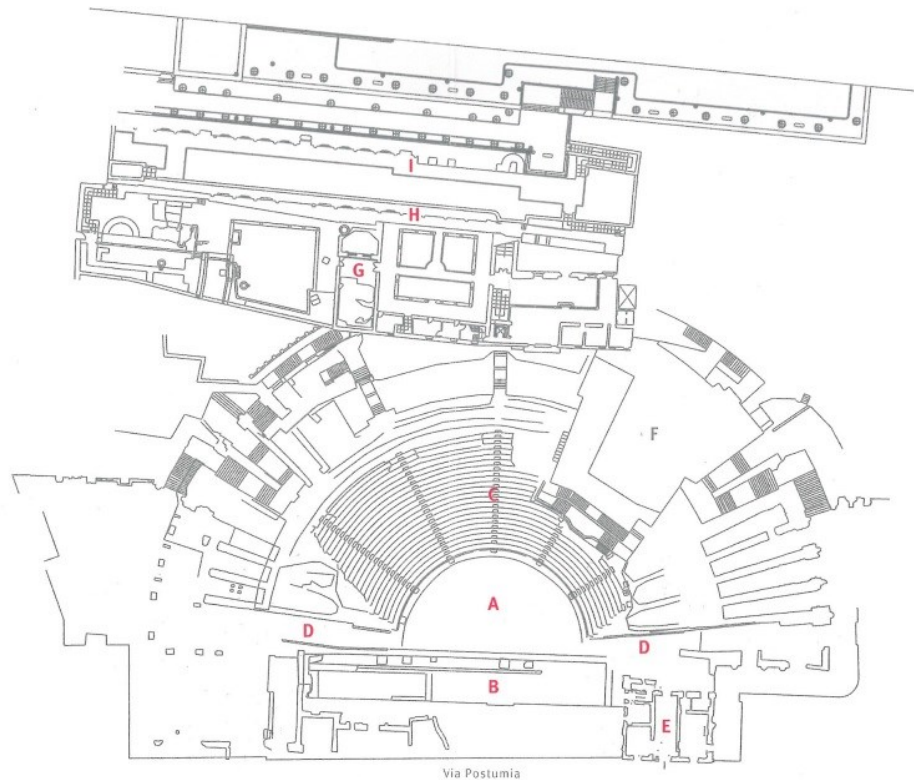


Figure 21 Roman theatre illustration. (Taken from Bolla, M. 2016)

The orchestra, which is defined by Dal Forno (1975) as “the semicircular space between the auditorium and the scene” was occupied by movable seats for the aristocracy. According to Bolla (2016) it had a diameter of 100 Roman feet, which is equivalent to 30 m. approximately. Due to the nature of the space it was not possible to decorate it, still, it was ornamented by the use of colored marble to pave the floor. In the same way, two marble leaders were situated at the sides in order to access the parascenae. However, the main access to the orchestra was through the two galleries located on the sides (Tronchin et Bevilacqua 2022). From the orchestra, it was possible to access the cavea, where, citing Sear (2006) “The seating was arranged in a semicircle around the orchestra as in the Greek theatre”. It partially rested on the hill slope, on its central part, and the two lateral ones were supported by radial vaulted walls (Marchini 1978) built-in opus cementitium (Cavalieri Manasse 1987). These walls were isolated from the underground water through the use of the previously described channel system created by the Romans (with a variable height of 18 m approximately, according to Dal Forno (1975). With its height of 30 m. (Bolla 2016), it was horizontally divided into three parts, the summa (upper), the media, and the ima (lower) cavea, and vertically in 6 sections divided by 7 stairways (counting the two lateral ones)

(Bonetto 2009; Dal Forno 1975). The ima cavea was paved with white stone and would accommodate, on its 23 steps, the upper class. The media cavea, on the other hand, would be used essentially for plebians and the summa cavea would be for poor people and women (Sear 2006). It is hypothesized as well the presence of a tribuna of 4.05 x 2.55 m. on the center of the third step (Tronchin et Bevilacqua 2022).

However, as mentioned by Marchini 1978 a true comprehension of the cavea is difficult due to further interventions and restoration works. At the top of the summa cavea, it is possible to find the semicircular ambulatory, which according to Tronchin et Bevilacqua 2022, was 2,95 m large x 2.3 m in height. It is possible to find as well the two “promenades” and the three terraces which



Figure 22 Aerial picture of Roman Theatre (Taken from Tronchin, L. et Bevilacqua, A. 2022).

connected to the hill giving a sense of unity to the theatrical complex itself (Marchini 1978; Bolla 2016). It should be mentioned as well the presence of a velerium, which was used to protect spectators from climatic conditions (Tronchin et Bevilacqua 2022).

Regarding the construction materials, as previously commented, the building was mainly done in local tuff quarried from the San Pietro hill itself (although the use of Ammonite limestone from the Valpolicella quarries was also mentioned by Bolla (2016)). This yellowish sandstone offers satisfactory compressive strength but it is prone to degradation due to environmental actions. According to Dal Forno 1975 this decision “greatly reduced the cost of erection and that of using precious marble, but increased the cost of maintenance and restoration over the centuries”, which lead to the covering or protection with an external layer of mortar. Another technique widely used for its construction is the opus cementitium for the construction of vaults and walls (Scaparro 1994). Bricks were also used on the roofs, especially after some of the restoration works took

place. Finally, as mentioned before, there was wide use of marble for aesthetical purposes. This marble, coming from different locations (including Italy, Greece, and Asia Minor) (Bolla 2016), was present and could be found mainly in the scenic building and the orchestra. Finally, the use of metal also testifies to the ornamentation of the construction (Bolla 2016).

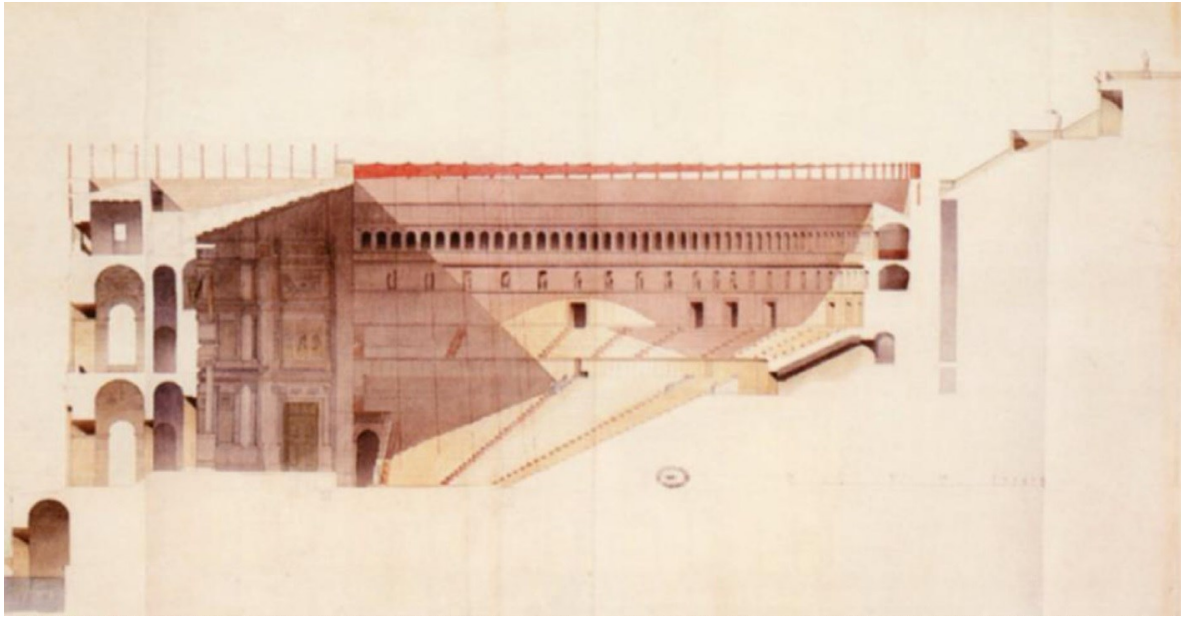


Figure 23 Theatre section. By E. Guillaume (Taken from Tronchin, L. et Bevilacqua, A., 2022).

The theatre, after its construction, was subjected to a series of alterations. Some of them were performed in order to embellish and renovate it, however, the main ones were due to the disuse and the downfall of the monumental structure. During the Neronian age, more specifically in the year 69, a series of works were done on the scenic front to embellish it (from where a series of columns can be identified) (Cavaliere Manasse 1987). The restoration efforts continued once again during the Hadrian and the Severan age, with the embellishment of the scenae frons, the reconstruction of the roofs, and the construction of a small temple dedicated to Isis (Cavaliere Manasse 1987). Nonetheless, a fire provoked by the Alemanni in the year 258 caused some serious devastation to the building, leading to its lack of use and posterior detriment (Tronchin et Bevilacqua 2022). After, it suffered as well from damages caused by a river flooding in 589 and a heavy earthquake in 1117. However, its most significant degradation was due to the change of use of the land into a necropolis and the authorization to quarry materials (especially marble) from the theatre complex (Bolla 2016; Tronchin et Bevilacqua 2022). This resulted as well in the erection of a series of religious buildings in the area during the Carolingian era (including the construction

of the San Siro church in 880 AD and the former convent S. Gerolamo (Dal Forno 1975; Bolla 2014)).

The theatre, however, was not deemed to be hidden forever, it saw the light once again after the excavation works done by the Venetian merchant Andrea Monga in 1834 (Bolla 2014). After the founding of the western area of the cavea and the eastern staircase, the municipality decided to



Figure 24 Roman theatre 1938. (Taken from Bolla, M. 2016)

buy the land in 1904 and perform the excavation works to complete the demolitions (respecting the presence of some of the buildings, such as the church of San Siro and Libera and the convent of Saint Gerolamo) (Dal Forno 1975). This provided a clear path to exalt the majestic building and bring it back to life. Further excavations have been performed on the site ever since, by different archeologists and researchers (Tronchin et Bevilacqua 2022).

3.4.2. THE ODEON

Once the construction of the theater was finalized, by the Augustan age, the construction works for the Odeon took place (Cavalieri Manasse, G. 2003; Bolla, M. 2016; Tosi, G. 1994). It was located on the San Pietro hill, to the southeast of the theatre in the current piazza Martiri della Libertà, where a small part of it is still visible (Bolla, M. 2012; 2016). According to Bolla, M. (2012; 2014) the function of this structure was to held musical auditions, poetry recitals, and prose readings for a small number of spectators. Due to the poor state of conservation of the building, there is little information regarding its layout. Nonetheless, it is hypothesized to be a semicircular space of 60.00 m long (Tosi, G. 1994), covered by a wooden roof (Bolla, M. 2012). Having a similar spatial distribution and style of the theatre, with the proscenium built in opus quadratum

and facing the hill (Tosi, G. 1994). Cavalieri Manasse, G. (1994) described this structure as follows: “It consists of a robust conglomerate foundation with a maximum thickness of 5.20 m, bordered towards the mountain by two white limestone steps, the upper one slightly set back.

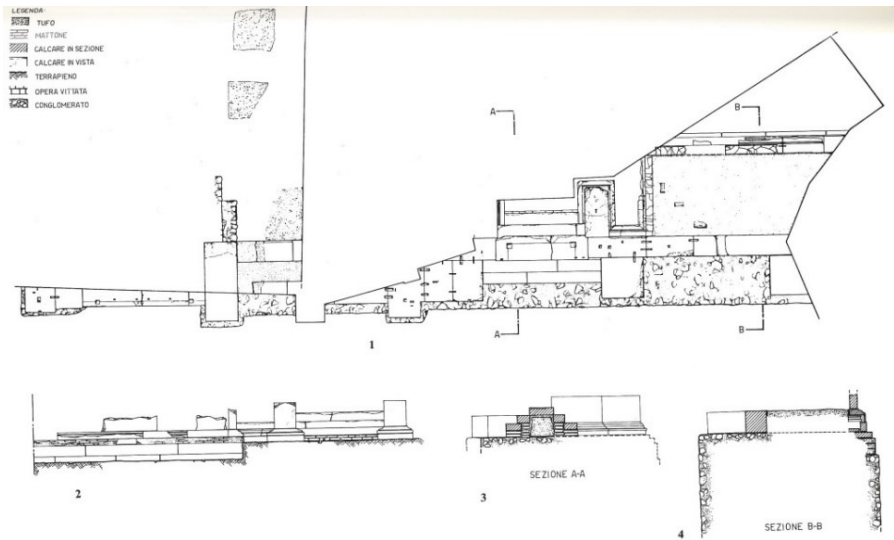


Figure 25 Odeum section. (Taken from Cavalieri Manasse, G., 1994).

Upstream (east) the staircase is framed by two protruding bodies profiled by elegant plinths in soft stone supported by slabs of white marble with gray veins.” Cavalieri Manasse, G. (1994), also highlights the presence of some conserved areas of this structure in via del Redentore where the use of bricks and “tuffaceous” stone can be observed. Furthermore, towards the river, a course of white limestone blocks is conserved, which constitutes the lower part of the external face of the building, marked by dice, at regular intervals of 3.70 m. (Cavalieri Manasse, G. 1994). The des-use of the building occurred at the same period as the theatre, after suffering irreparable damages due to fire (Bolla, M. 2016). The structure was later located in 1960 thanks to the works done on the piazza Martiri della Libertá.

3.4.3. THE TEMPLE IN CASTLE S. PIETRO

The construction of a temple crowning the top of San Pietro Hill took place after the extensive works for the terracing were finished, during the monumentalization of the area (Cavalieri Manasse, G. 1987; Bonetto, J. 2009; Bolla, M. 2014). There is limited information concerning the morphology, design, and construction of this structure, due to the level of destruction it has been subjected to. The initial reason for its dismantling was the construction of the palace in the area previously occupied by the temple during the Greek-Gothic war, or as attested by Bolla, M. 2014: “Later, during the Greek-Gothic war (between Goths and Byzantines)

Verona continued to be considered an important stronghold; in this period the area on the top of the hill, around the temple now transformed into a church, became a fortified place, called castrum in Medieval documents”. Cavalieri Manasse, G. 1987 regarding the construction techniques implemented in this building it is hypothesized that “one of the building techniques present in the monument is the opus reticulatum, implemented in Rome and the Lazio and Campania area, between the middle of the first century. BC and the Augustan age and Julius Claudius, but which, like the more ancient opus incertum, is extremely rare in northern Italy”. It is also known that the material used for its construction was the so-called “tuffaceous” stone present on the hill of San Pietro. It is a yellowish limestone of average mechanical properties, which was implemented for the rising of the building (since the foundation was the rock present on the mountain itself) (Cavalieri Manasse, G., & Fresco, P. 2012). After, the building was excavated and observed once again during 1851, due to the presence of Austrian barracks in the area (Bonetto, J. 2009). Finally, the structure was once again excavated in 2007 by Cavalieri Manasse, G., & Fresco, P., however, due to the presence of the new structure it is not possible to investigate thoroughly.



Figure 26 Excavation in Castel San Pietro (Taken from Cavalieri Manasse, G., et Fresco, P. 2012).



- 1 Torre della porta
- 2 Odeum
- 3 Castello S. Pietro
- 4 Capitolium and area della Corte

- 5 Curia
- 6 Porta Leoni
- 7 walls on San Cosimo
- 8 Arena (amphitheater)
- 9 Roman theatre

Figure 27 Location of sampled sites in urban context

4. Chapter IV - Geological context of Verona

Mortar is a complex composite material resulting from the admixture and thermal treatment of geological materials. In this sense, the resulting mortar largely depends on the local geological settings where the construction took place (Ergenç, D., et al. 2021). Or, as (DeLaine, J. 2021) mentioned: “Local geological settings, the physical environment especially the ready availability of fuel and their relation to the building site in terms of transport routes, appear to have been primary factors affecting choice”. In this way, the comprehension of the geological context of the analyzed area represents valuable information for the understanding of production techniques and material sources used in mortar production. In literature, this relationship between mortar and its geological contexts has been used to obtain information regarding the provenance of raw materials, mainly through the identification of aggregates in mortars. As explained by Elsen, J. (2006): “The mineralogy of these aggregates reflects their geological origin and thus can give valuable information about their provenance”. This information is also proven to be extremely valuable when doing restoration, since “A detailed chemical and mineralogical characterization of historic mortar components should prove extremely useful in the correct choice of materials for the restoration of Roman masonry” (Schiavon, N., et Mazzocchin, G.A. 2009). It is for this reason that it is possible to find scientific works such as the one by Rispoli, C., et al. (2020), where the question of the use of volcanic ash from the Bay of Naples is addressed, or by Pineda, P., et al. (2022) to identify the source or materials used in mortars. In this case, a description of the geological context is included in order to better comprehend the nature of the aggregates and their possible interaction with the binder, providing a more profound comprehension of the production processes and the resulting materials.

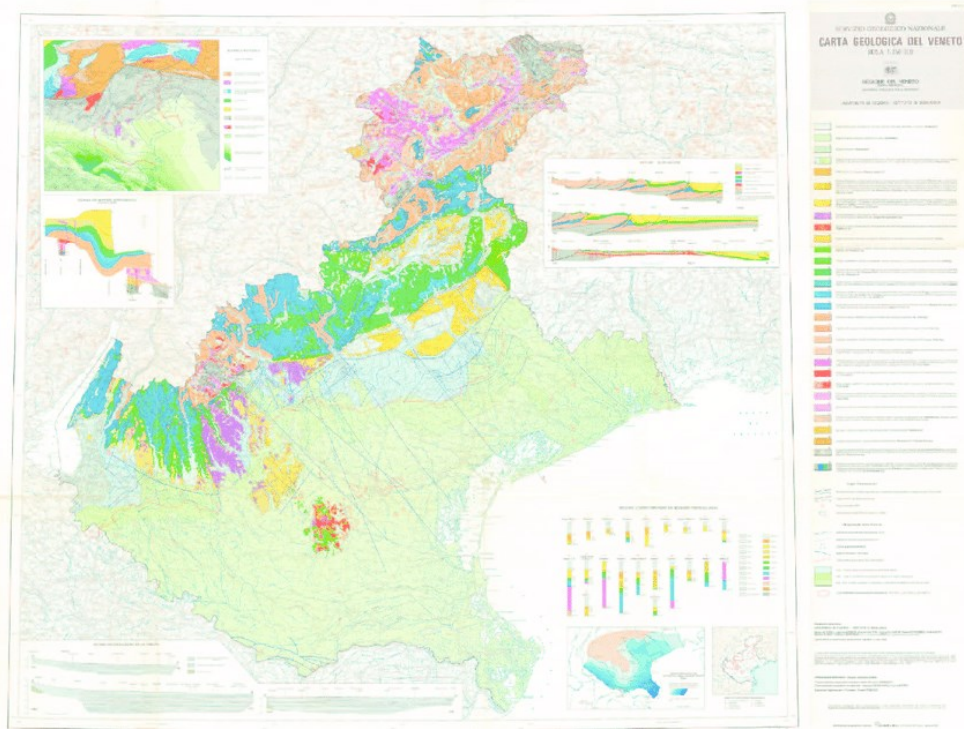


Figure 28. Geological plan of Veneto

As mentioned in the previous chapter, the city of Verona is located in the north of Italy, in the region of Veneto. It is situated on the valley of the river Adige, near the border to the region of Trentino, which is characterized by the presence of the Dolomites, where the river Adige is born. With this logic, the river passes and collects geological material from the region of Trentino before arriving in Verona, or as best described by Piovan, S., et al. (2010): “The Adige River is the second largest Italian river by length (410 km) and the third largest by catchment area (12,200 km²). It leaves the Alps near the city of Verona after running through a north–south alpine valley mainly cut in carbonate and felsic volcanic rocks”. It is precisely the material present in this river, due to its properties and its ease of access that it was being used in the construction, and more specifically in the production of mortars. In this sense, it is of the utmost importance to comprehend the geological context of the area of Trentino, even more than the one of Veneto, since it is from this where aggregates and sands were originally sourced from. This can be better explained by Schiavon, N., et , G.A. Mazzocchin. (2009) when mentioning: “Moreover, it is well known that when the source rocks whose erosion provides the detritus for the fluvial drainage

basins, are located in high-relief, temperate- cold mountain settings where chemical weathering is negligible and sediment transport is rapid and short, (as it is the case in the Southern Alps setting), the river sand composition can be held as representative of the mineralogy of the parent rocks”.

In a general characterization of the sediments transported by the Adige, it is possible to encounter gravel from different types of rocks such as tuffs, ignimbrites, sandstones, limestones, and dolostones, among others (Brondi, A., et al. 1976). The recurrent presence of rocks of volcanic origin is due to the presence of the Atesino volcanic complex, which according to Brondi, A., et al. (1976) “extends within the borders of the Trentino-Alto Adige region, for about 3500-4000 km². The outcropping part, mostly concentrated in what is called the Atesino volcanic slab, has an area of about 1500 km². The effusive complex consists of a succession of lavas, tuffs, and ignimbrites of various compositions, alternating with volcanic-sedimentary and sedimentary levels”. As for the mineralogy of the outcrops related to this volcanic context, it is possible to identify the presence of quartz, biotite, K-feldspar, sanidine, plagioclases, and pyroxenes (which have a lower presence). According to Brondi, A., et al. (1976) these values could range between 10-15% for quartz, 5-15% biotite, and K-feldspar, and 1-5% for sanidine as single minerals, while the values would vary when found as phenocrysts on the interior of ignimbrites. As for the sandstones, which have fluvial or lake origin (Brondi, A., et al. 1976) shown by the intercalation with clayey layers, calcite to dolomite ratio can be distinguished as “the latter prevails over the former, therefore influencing the trend of total carbonates” (P. Jobstraibizer et P. Malesani. 1973).







Furthermore, specific studies regarding the geological and mineralogical composition of the sand of the Adige River have been carried out. In this study, the results show that “quantities of calcite, quartz, chert, potassium feldspar, and phyllosilicates are positively correlated with grain size, while dolomite, total carbonates, and heavy minerals show opposite behavior” (P. Jobstraibizer et P. Malesani. 1973). This same study shows that calcite has a prevalent presence with values between 9.8 and 25%. The high presence of dolomite, free silica, and k-feldspar is also highlighted. The presence of calcite, dolomite, biotite, hornblende, chert, Ti-rich ilmenite, orthoclase, albite, quartz, chlorite, muscovite, and “relatively large amounts of fragments of acidic volcanic rocks” (Gandolfi, G., Mordenti, A., & Paganelli, L. 1982) has been observed after performing SEM-EDS and XRD analysis on river sand samples from the Adige (Schiavon, N., et al., G.A. Mazzocchin. 2009).





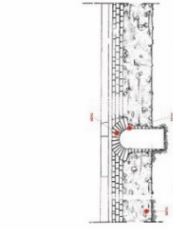

5. **Chapter V - Population: an introduction to the Samples**


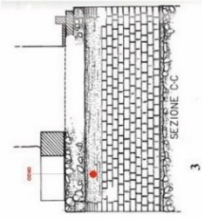


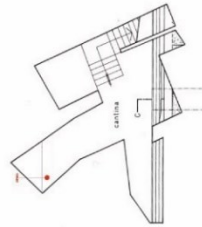


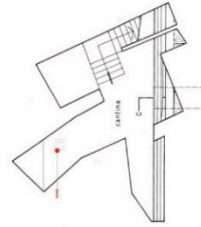


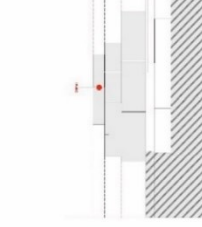

5.1. AN INTRODUCTION TO MORTAR SAMPLES



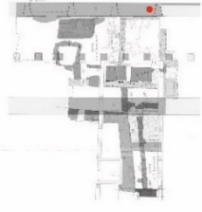

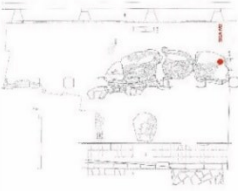

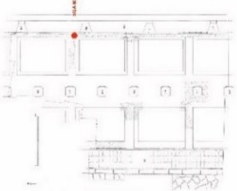

The acquisition of the mortar samples of the Roman buildings of Verona was performed beforehand as part of the Ph.D. research project of Eliana Bridi, on the study of Roman construction in Verona. The entire population is composed of 49 samples collected from 9 different sites. The sampled buildings were: Torre della Porta, the Odeum, the temple in Castello S. Pietro, the Capitolium and Archeological area of the Corte Sgarzerie, the Curia, Porta Leoni, the defense city walls in via S. Cosimo, the Amphitheatre (or Arena di Verona) and the roman theatre. These structures encompasses most of the known public Roman buildings present in Verona, therefore the samples dataset is highly representative of the construction techniques and technological advances in mortar production.


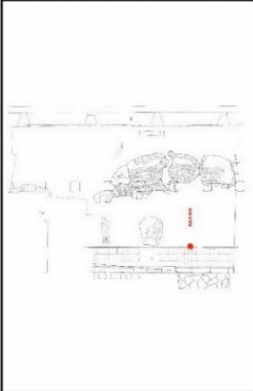
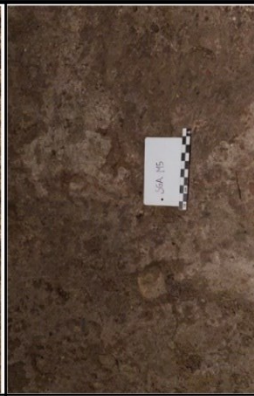
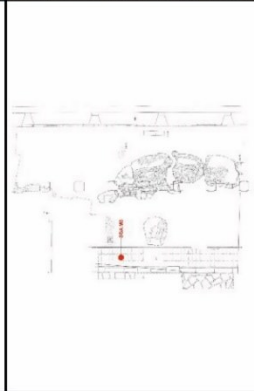

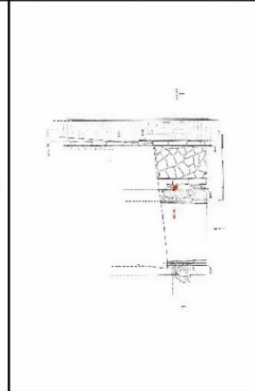

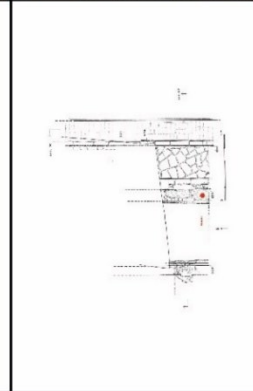
The following table (table 01) presents the population; their ID or code, the site where they were collected, and the chronological context for each construction. It should be mentioned that, since the sampling procedures were done by Eliana Bridi, the information presented here is based on the information provided by her.





Sample	Context / site	Construction phase (chronology group)	Structural function	Construction Technique	Sampling location	
RED M1	Torre della porta	First phase (End of first s. b.C.)	Foundation	Bricks + bedding mortar. Homogeneous structure.		
RED M2	Torre della porta	First phase (End of first s. b.C.)	Foundation	Bricks + bedding mortar. Homogeneous structure.		
RED M3	Torre della porta	First phase (End of first s. b.C.)	Foundation	Bricks + bedding mortar. Homogeneous structure.		

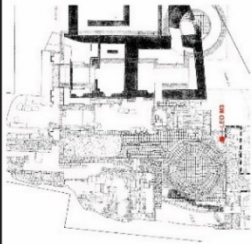

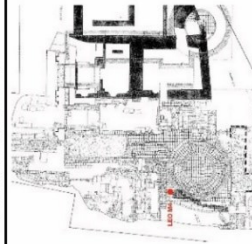

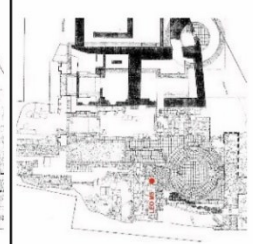

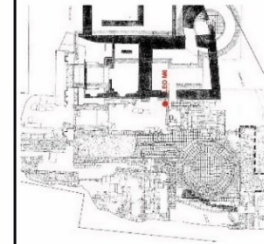

RED M4	Torre della porta	First phase (End of first s. b.C.)	Foundation	Bricks + bedding mortar. Homogeneous structure.		
RED M5	Torre della porta	First phase (End of first s. b.C.)	Foundation	Regular tuff blocks + mortar		
OD M1	Odeum	Second phase First half of first s. a.D.	Foundation	Concrete		
OD M2	Odeum	Second phase First half of first s. a.D.	Foundation	Concrete		









OD M3	Odeum	Second phase First half of first s. a.D.	Vault	Concrete			
OD M4	Odeum	Second phase First half of first s. a.D.	Foundation	Concrete			
OD M5	Odeum	Second phase First half of first s. a.D.	Structure holding the curtains of the stage system called aulleum	Bricks + bedding mortar. Homogeneous structure.			
CSP M1	Tempio (castello S. Pietro)	Phase 0 Beginning of first s. b.C.	Wall	Regular tuff blocks + mortar			









RM M1	Capitolium and Archeologic al area Corte	First phase Third quarter of the first s. b.C.	Foundation	Bricks + bedding mortar. Homogeneous structure.		
SGA M1	Capitolium and Archeologic al area Corte	First phase Third quarter of the first s. b.C.	Wall	Irregular tuff blocks + core in concrete		
SGA M2	Capitolium and Archeologic al area Corte	First phase Third quarter of the first s. b.C.	Vault	Concrete		
SGA M3	Capitolium and Archeologic al area Corte	First phase Third quarter of the first s. b.C.	Foundation	Regular tuff blocks + mortar		

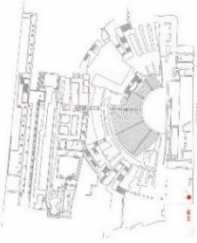

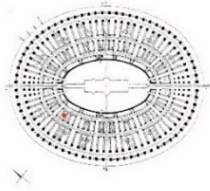

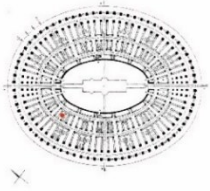

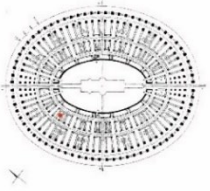

SGA M4	Capitolium and Archeologic al area Corte	First phase Third quarter of the first s. b.C.	Wall	Concrete + coating		
SGA M5	Capitolium and Archeologic al area Corte	First phase Third quarter of the first s. b.C.	Foundation	Bricks + bedding mortar. Homogeneous structure.		
SGA M6	Capitolium and Archeologic al area Corte	First phase Third quarter of the first s. b.C.	Foundation	Pebbles + mortar		
SGA M7	Capitolium and Archeologic al area Corte	First phase Third quarter of the first s. b.C.	Wall	Irregular tuff blocks + core in concrete + layer of brick		


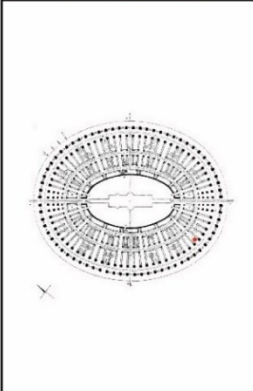

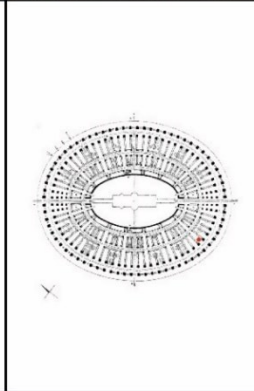

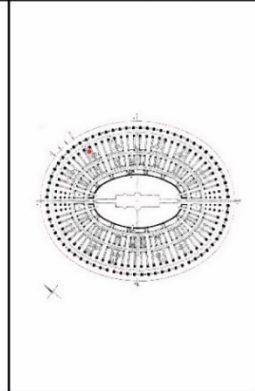

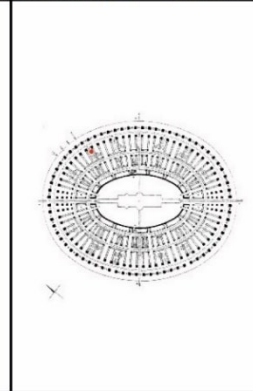
SGA M8	Capitolium and Archeological area Cortes	First phase Third quarter of the first s. b.C.	Wall	Bricks + bedding mortar. Homogeneous structure.	
AP M1	Curia	Second phase First half of the first s. a.D.	Wall	Irregular tuff blocks + core in concrete	
LEO M1	Porta Leoni	Second phase First half of the first s. a.D.	Foundation	Pebbles + mortar	
LEO M2	Porta Leoni	First phase Half of the first s. b.C.	Foundation	Pebbles + mortar	


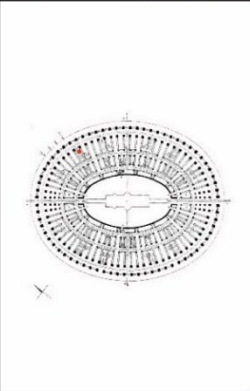


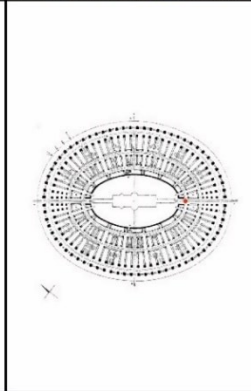
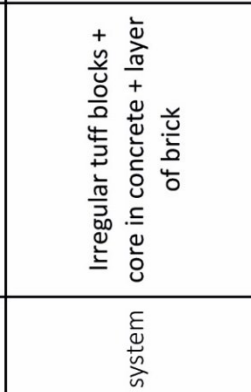

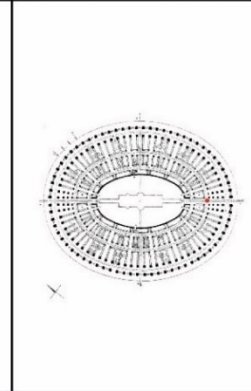
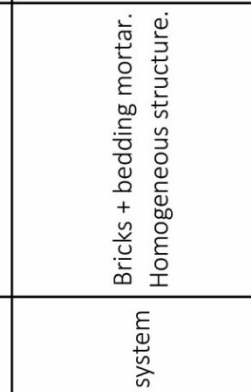

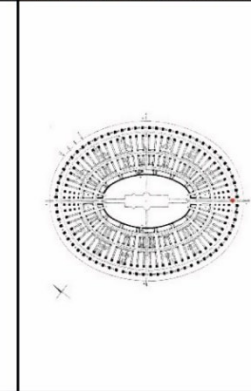
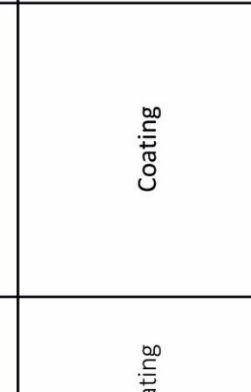
LEO M3	Porta Leoni	First phase Half of the first s. b.C.	Foundation	Pebbles + mortar		
LEO M4	Porta Leoni	First phase Half of the first s. b.C.	Coating	Bricks + bedding mortar. Homogeneous structure.		
LEO M5	Porta Leoni	First phase Half of the first s. b.C.	Coating	Bricks + bedding mortar. Homogeneous structure.		
LEO M6	Porta Leoni	First phase Half of the first s. b.C.	Sewer system	Bricks + bedding mortar. Homogeneous structure.		

COS M1	Defensive walls on San Cosimo	First phase Half of the first s. b.C.	Foundation	Pebbles + mortar		
COS M2	Defensive walls on San Cosimo	First phase Half of the first s. b.C.	Wall	Bricks + bedding mortar. Homogeneous structure.		
COS M3	Defensive walls on San Cosimo	Third phase Half of the third s. a.D.	Vault	Pebbles + mortar		
COS M4	Defensive walls on San Cosimo	Third phase Half of the third s. a.D.	Triangular "sperone"	Re-used stone blocks + bedding mortar + possible core in concrete		

COS M5	Defensive walls on San Cosimo	Third phase Half of the third s. a.D.	Wall	Pebbles + mortar		
COS M6	Defensive walls on San Cosimo	Third phase Half of the third s. a.D.	Wall	Re-used stone blocks + bedding mortar + possible core in concrete		
COS M7	Defensive walls on San Cosimo	Third phase Half of the third s. a.D.	Wall	Bricks + thick bedding mortar		
COS M8	Defensive walls on San Cosimo	Third phase Half of the third s. a.D.	Wall	Bricks + thick bedding mortar		

TR M1	Theatre	First phase End of first s. b.C.	Wall	Concrete core + Opus reticulatae (tuff, 45 degrees)		
AR M1	Arena (amphitheater)	Second phase 40-50 a.D.	Foundation	Pebbles + mortar		
AR M2	Arena (amphitheater)	Second phase 40-50 a.D.	Foundation. Lever over foundation	Pebbles + mortar		
AR M3	Arena (amphitheater)	Second phase 40-50 a.D.	Arcovolo	Irregular tuff blocks + core in concrete + layer of brick		

AR M4	Arena (amphitheater)	Second phase 40-50 a.D.	floor. Preparation level of floor	Brick layer over mortar		
AR M5	Arena (amphitheater)	Second phase 40-50 a.D.	Foundation	Pebbles + mortar		
AR M6	Arena (amphitheater)	Second phase 40-50 a.D.	Vault	Concrete		
AR M7	Arena (amphitheater)	Second phase 40-50 a.D.	Vault. Extradoso= exterior part of the vault	Concrete + gravel		

AR M8	Arena (amphitheater)	Second phase 40-50 a.D.	Vault. Extradoso= exterior part of the vault	Concrete + gravel			
AR M9	Arena (amphitheater)	Second phase 40-50 a.D.	Sewer system	Irregular tuff blocks + core in concrete + layer of brick			
AR M10	Arena (amphitheater)	Second phase 40-50 a.D.	Sewer system	Bricks + bedding mortar. Homogeneous structure.			
AR M11	Arena (amphitheater)	Second phase 40-50 a.D.	Coating	Coating			


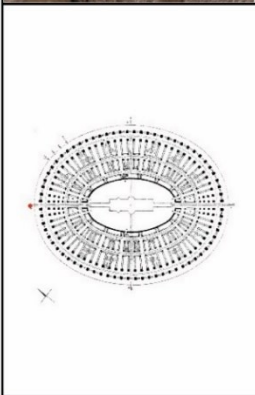

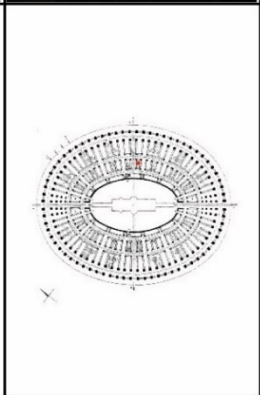
AR M12	Arena (amphitheater)	Second phase 40-50 a.D.	Foundation	Pebbles + earthen mortar	 
AR M13	Arena (amphitheater)	Second phase 40-50 a.D.	Vault	Concrete	 

Table 01. Population of mortar samples.

5.2. SAMPLE SELECTION

The need to reduce the number of samples to be analyzed by optical microscopy, due to the required procedures of thin section production, required a further sub-selection of the materials. This selection was based on the matrix properties, the abundance of inclusions (as well as their dimensions) and the abundance of the sample (in order to have more material for further studies). The process for samples' selection then followed these steps: 1. Overview of the general context and the information available (data, notes, plans of localization, and pictures) on the sampling process carried out by Eliana Bridi and professor Caterina Previato. 2. Grouping of all the samples that, coming from the same building, were collected from the same area (walls, foundation, vaults...). It is worth mentioning that the samples were previously grouped by building and properly labeled. 3. Some observation of the macro characteristics of the mortar matrix was performed in all the samples from the same group, having a special emphasis on the observation of the previously mentioned parameters of selection. 4. The final step, therefore, is the proper selection of the samples and their tagging, establishing the priority list of the samples to be analyzed based on the building where it comes from. This is done due to the high number of samples.

The previously mentioned process led to the selection of a total of 30 samples out of the 49. The final selection of these samples can be visualized in the table (Table 02).

Context	Tag / code	Sample group	Sample criteria	Notes by Eliana Briti	Notes on the observed macro characteristics during selection procedure
Torre della porta	RED M2	RED M2	Only sample in the group	"with fr. coal (harvested)"	<ul style="list-style-type: none"> • Fine, compact, homogeneous • Contains more limestone that samples RED M4 and M5

	RED M5	RED M4, RED M5	Most representative matrix	"very earthy; alloy pebbles, tuff blocks, fr. Bricks"	<ul style="list-style-type: none"> • Mixed matrix with soil • Contains chunks of lime • Concrete like context
Odeum	OD M2	OD M1, OD M2, OD M4	Presence of inclusion. Representative matrix	"S side"	<ul style="list-style-type: none"> • Concrete like context • Pebbles are abundant in the sample • It may have some superficial contamination but there is not a mixture with soil
	OD M3	OD M3, OD M5	Most representative matrix	"Bottom, left wall"	<ul style="list-style-type: none"> • Compact, lime based, small aggregates
Tempio (Castello S. Pietro)	CSP M1	CSP M1	Only sample in the group	"It is not present among all blocks"	<ul style="list-style-type: none"> • Lime base mortar with small aggregates
Capitolium and Archeological area Corte	RM M1	RM M1	Only sample in the group	"The drippings of mortar on the bricks are clearly visible"	<ul style="list-style-type: none"> • May be contaminated by soil due to the construction technique used, however there is no indication that soil added to the mixture.
	SGA M1	SGA M1, SGA M4	Most representative matrix	"Very crumbly"	-
	SGA M2	SGA M2	Only sample in the group	"White, with small, very tenacious gravel inclusions"	-
	SGA M3	SGA M3, SGA M5	Sample SGA M5 uses finer aggregates since it comes from a leveling context. Most representative matrix	"Very crumbly"	<ul style="list-style-type: none"> • Coarser aggregates than SGA M5

	SGA M6	SGA M6, SGA M7, SGA M8	Most representative matrix	-	<ul style="list-style-type: none"> • Coarse • Presence of coarse aggregates.
Curia	AP M1	AP M1	Only sample in the group	"Very friable, with inclusions of small pebbles and fine gravel; there is none among all blocks"	-
Porta Leoni	LEO M1	LEO M1, LEO M2, LEO M3	Presence of inclusion. Representative matrix	"White and compact"	<ul style="list-style-type: none"> • Presence of coarse aggregates.
	LEO M2		Presence of inclusion. Representative matrix	-	<ul style="list-style-type: none"> • Presence of gravels. • Presence of coarse aggregates.
	LEO M4	LEO M4, LEO M5, LEO M6	Location of extraction. Noticeable differences between the macro-characteristics of the samples	"Very crumbly"	<ul style="list-style-type: none"> • Matrix can be described as lumpy.
	LEO M5		Location of extraction. Noticeable differences between the macro-characteristics of the samples	-	<ul style="list-style-type: none"> • Extracted from the city walls
Defensive walls on San Cosimo	COS M1	COS M1, COS M2	Noticeable differences between the macro-characteristics of the samples	-	<ul style="list-style-type: none"> • Presence of coarse aggregates. • Possible addition of soil into the mixture.
	COS M2		Noticeable differences between the macro-characteristics of the samples	-	-

	COS M3		The sample comes from a different context within the same group (since it is taken from the vaults).	-	-
	COS M4	COS M3- COS M8	It is necessary to study the mortar from this structure due to the current uncertainty of its chronology	-	<ul style="list-style-type: none"> • Presence of lime clumps.
	COS M5		Less amount of soil in the sample. Most representative matrix	"External side"	<ul style="list-style-type: none"> • Presence of soil in the matrix (soil must have been added to the mixture)
	COS M7		Less chaotic than COS M8. Most representative matrix	"Inner side"	-
Theatre	TR M1		TR M1	Only sample in the group	-
Arena (amphitheater)	AR M1	AR M1, AR M2, AR M5	Extracted from the nucleolus of the foundation, therefore is more homogeneous than other wall samples	"With large pebbles"	-
	AR M3	AR M3	Only sample in the group	"With gravel"	<ul style="list-style-type: none"> • concrete like context • Lime based mortar • Porous, friable, chaotic and earthy
	AR M5	AR M5	Only sample in the group	-	-
	AR M7	AR M6, AR M7, AR M8	Both samples present very similar macro-characteristics, AR M7 is selected due to its abundance.	-	<ul style="list-style-type: none"> • Concrete like context

AR M9	AR M9, AR M10, AR M11	Noticeable differences between the macro-characteristics of the samples	-	• Due to it's function it is necessary for it to have an to have a hydraulic function
AR M11		Noticeable differences between the macro-characteristics of the samples	-	• Due to it's function it is necessary for it to have an to have a hydraulic function
AR M12	AR M12	Only sample in the group	"Earth mortar"	• Earthen based mortar (lime could have been added to stabilize the mortar).
AR M13	AR M13	Only sample in the group	-	-

Table 02. Sample selection for thin section production.

6. Chapter VI - Methodology

6.1. ACTION PLAN OVERVIEW

As previously established, the main objective of the thesis here presented is to provide a comprehensive characterization of the mortar samples extracted from the public structures of Roman buildings in Verona. For this purpose, a series of analytical procedures are proposed following the procedures thoroughly described in literature by authors such as Arizzi, A., et Cultrone, G. (2021), Elsen, J. (2006) or Ergenç, D., et al. (2021). In this sense, both the binder and the aggregate fraction were studied through procedures such as colorimetry, x-ray powder diffraction (XRPD), optical microscopy, and scanning electron microscopy coupled with energy dispersive spectroscopy (SEM-EDS). The characterization procedures proposed in this thesis are constituted by a general to specific path, in which samples are analyzed and described from the general physical properties to more detailed physical-chemical ones. The following procedures are selected and carried out according to the observations and results obtained through the characterization process. Furthermore, sample selection is carried out according to both the results obtained and the specific requirements for each analytical technique. In this sense, samples presenting similar characteristics will be grouped and a careful selection of one (or more) samples representing the characteristic properties of each group will be selected for further analysis. Therefore, general conclusions regarding the groups will be obtained from the individual analysis of the representative samples. The following diagram roughly demonstrates the procedures taking place in the mortars' characterization here presented.

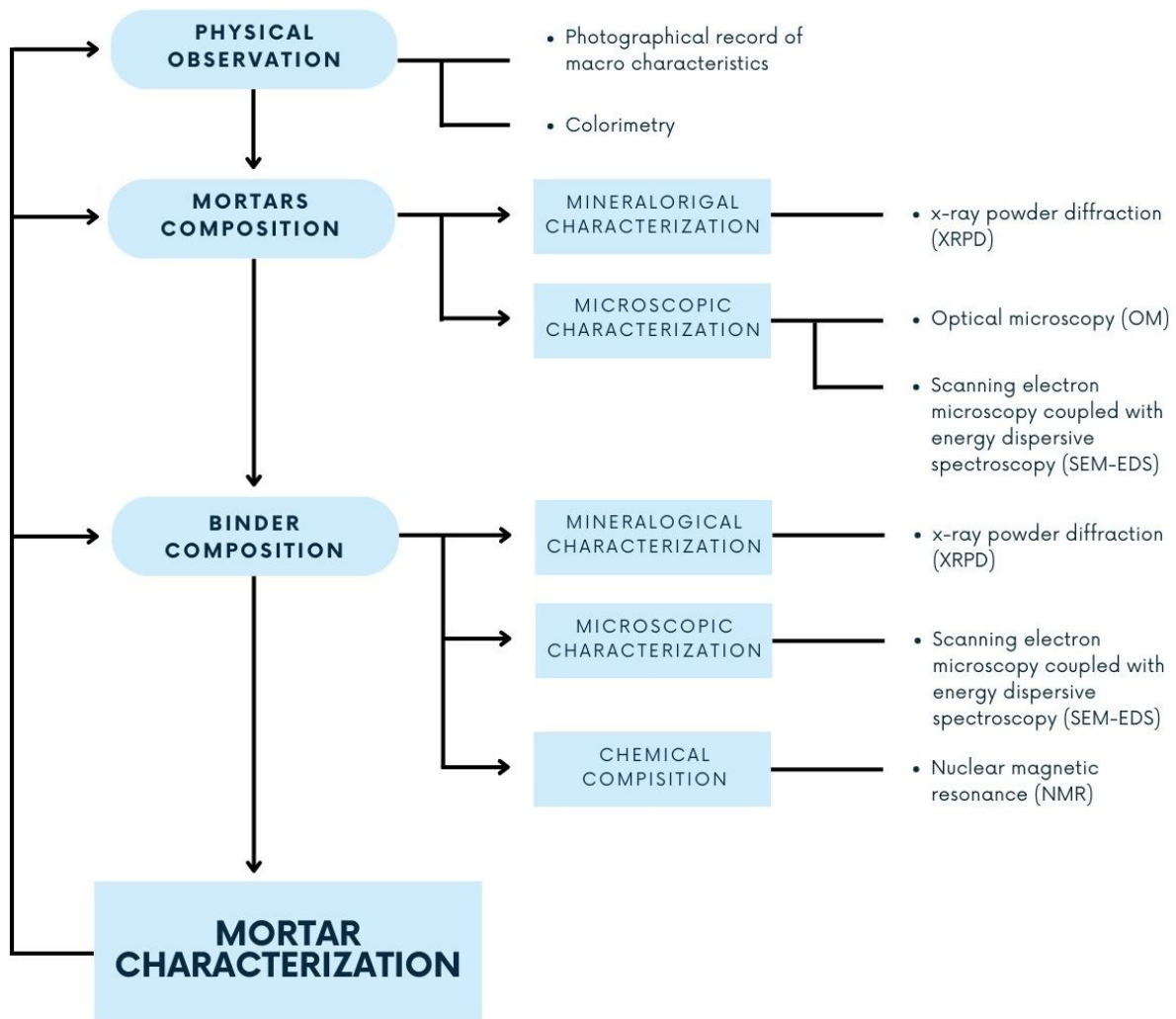
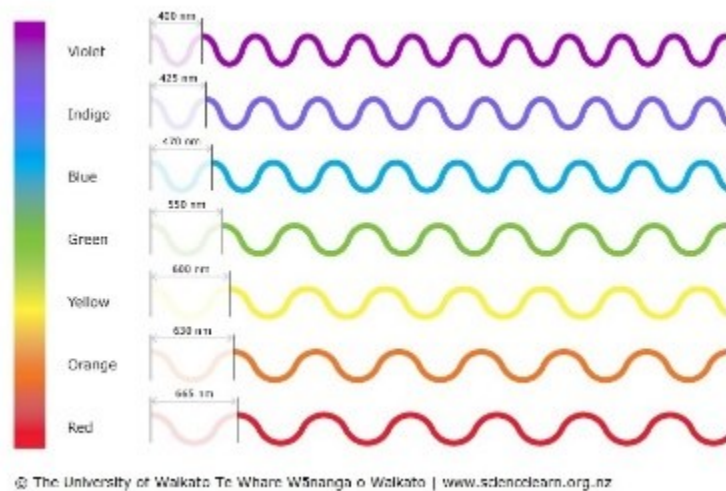


Figure 29. Methodological plan workflow diagram

6.1.1. COLORIMETRY

Colorimetry is a non-destructive analytical technique that, as its name suggests, is used for the identification and measurement of color by assigning mathematical values that represent it (Navarro-Mendoza, E. G., et al. 2023), or better described by Gilchrist, A., et Nobbs, J. (2017): “Colorimetry is the science of measurement of color. It involves the replacement of subjective responses, such as 'light blue', 'rich dark purple', 'bright gold',



© The University of Waikato Te Whare Wānanga o Waikato | www.sciencelearn.org.nz
Figure 30. Difference of wavelength and color perception. Image taken from: The University of Waikato Te Whare Wānanga o Waikato (2019) Colours of light, Science Learning Hub. Available at: <https://www.sciencelearn.org.nz/resources/47-colours-of-light>

with an objective numerical system”. Its goal is to provide a more precise and objective measurement for color identification than the one provided by human perception (Clydesdale, F. M., & Ahmed, E. M. 1978).

In order to have a better understanding of colorimetry it is necessary to first comprehend color and the perception of color. The perception of color by the human eye is caused by the reflection and absorption of electromagnetic waves of certain wavelengths within the visible area of the spectrum by an object's surface. In this sense, a light source emits electromagnetic waves of different wavelengths, these waves hit the object's surface, where some of them are absorbed and others are reflected. The reflected waves, with their distinctive wavelength, then hit the observer's eye, in which color is perceived (Kuehni, R. G. 2012). Then, color perception can be determined by three main parameters: “the nature of the illumination, the optical properties of the object itself, and the response of the human eye” (Gilchrist, A., & Nobbs, J. 2017). The nature of the illumination refers to the light source since it is the main source of electromagnetic waves that have a profound effect on color perception (e.g.: Daylight/moonlight, warm/cold light...). The optical properties are intrinsic to observed object, depending on its capacity to absorb or reflect light from certain wavelengths. Finally, the response of the human eye is affected not only by the subject itself but by the angle of observation and the distance from the object, allowing a higher

or lower intensity to be perceived (Gilchrist, A., & Nobbs, J. 2017). It is precisely because of this third factor, human perception, that color perception is often subjective since two different persons can see two different colors. It is in this exact frame where a system that can objectively determine the exact color is necessary. It must be highlighted as well the second factor of color perception, the observed object. This is of the utmost importance, since the color is a result of the composition of the object itself, providing not only aesthetical characterization but a chemical one as well. In this sense, as mentioned by Clydesdale, F. M., et Ahmed, E. M. (1978), “the application of color measuring techniques may be utilized in a predictive sense for not only an estimate of visual appearance but also as a tool for chemical analysis”. In other words, the variation of color refers to a variation in the chemical composition of an object, therefore, a mechanism that allows the mathematical measurement of color becomes an important tool for the initial characterization of a material. But then, the controversial question arises: how is it possible to measure color? What code system should be assigned for its identification?

Different color code systems have been established, such as RGB, CMYK, XYZ, and $L^*a^*b^*$, among others. Each one of these has its parameters, providing a numerical value for every existing color. The first system to be developed was the RGB color system, which was based on a color-matching methodology of an additive system whose working principle is based on the trichromatic theory of color vision (Gilchrist, A., & Nobbs, J. 2017). This means that based on the admixture of red, green, and blue it is possible to obtain any existing color, as proven by the experiment proposed by Guild and Wright (Gilchrist, A., & Nobbs, J. 2017). In this experiment, observers were asked to match different colors by controlling the intensities of red (R), green (G), and blue (B) lights on a screen. Then, “the coefficients or tristimulus values of the primaries could be plotted at various wavelengths to obtain standard-observer curves for the visible spectrum” (Clydesdale, F. M., & Ahmed, E. M. 1978). However, one of the most essential characteristics of color, luminosity (or lightness), could not be properly matched, since the system only allowed for positive values. It is for this reason, that the XYZ system was proposed. According to Clydesdale, F. M., et Ahmed, E. M. (1978) this new system differentiated from the previous one by proposing negative values of the RGB parameters, since:

“1. All possible real colors could be "matched" by positive amounts of the primaries;

2. A relatively large range of colors in the yellow-red region could be "matched" with only two primaries (note in Figure 30) that the z curve ends in the yellow region, and colors beyond this may be matched by x and y only); and

3. The intensity (luminosity or lightness) of the light needed to make the "match" is specified by the Y primary alone.” (Clydesdale, F. M., & Ahmed, E. M. 1978).

Later, the $L^*a^*b^*$ color system was created, which had a similar working system of additive admixture. Nonetheless, it differentiates from the previously mentioned systems by the implementation of the principle of exclusion, which dictates that color cannot be both red and

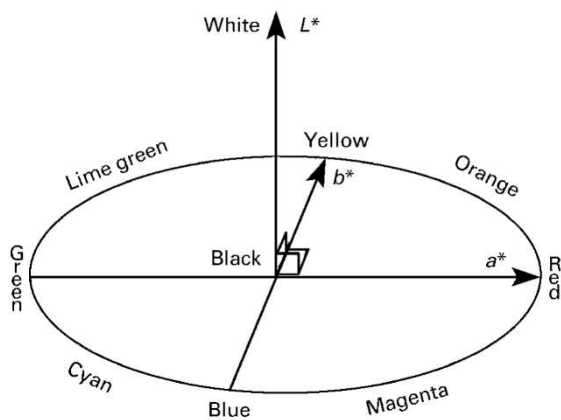


Figure 31. $L^*a^*b^*$ coordinate system. Image taken from: Gilchrist, A. and Nobbs, J. (2017) 'Colorimetry, theory'. Fig. 5. *Encyclopedia of Spectroscopy and Spectrometry*, pp. 328–333. doi:10.1016/b978-0-12-803224-4.00124-2.

green at the same time, or yellow and blue. The same principle was applied to lightness and darkness, therefore these colors “form a group of six basic color properties that can be grouped into three opponent pairs, white/black, red/green and yellow/blue” (Gilchrist, A., & Nobbs, J. 2017). A specific color could be placed in the area comprehended by these parameters, where L^* represents the light intensity of the color, a^* the red/green axis, and b^* the blue/yellow one (Wyszecki and Stiles, 2000).

In this way, colors were assigned to numerical values according to the specific parameters established by the different color systems. It is therefore necessary to create a system in which the problem of subjectivity is solved: in this way, colorimetry appears as a solution for color measurement. This analytical technique makes use of the relation between the initial three parameters (light source, the optical properties of the object, and the observer) as a base of interaction to obtain the final measurements. Nevertheless, the factors of variability in the resulting color, light source, and observer are replaced to obtain the desired results. In this sense, the light source is a controlled parameter within the machine, and the observer is replaced by a detector which can vary according to the type of machine used for the acquisition (Hiller, G. 2019). Since the position of the observer from the object affects to a great extent the final color perception, the geometry of acquisition is also defined by the individual machine used. In this, “the measurement

geometry defines the angle of illumination and the angle of viewing simulated by the instrument” (Hiller, G. 2019). The sensor, which can vary significantly, represents the main difference between the two systems of acquisition, which are spectrophotometry and tristimulus colorimetry. In spectrophotometry, the sensor system is mainly composed of a prism that diffracts the path of the different wavelengths of the acquired signal (Ohta, N., et Robertson, A. A. 2006). On the other hand, the tristimulus colorimetry sensor is based on the use of “filters to record the amount of light reflected in 3 wavelength ranges across the visible spectrum” (Hiller, G. 2019). The selection of the technique is done according to the desired results and the purpose of the investigation. The use of this technique for the characterization of historical mortars is commonly used for aesthetical purposes, in order to obtain the desirable characteristics for restoration purposes, as is the case of (Arizzi, A., & Cultrone, G. 2021; Navarro-Mendoza, E. G., et al. 2023). Nevertheless, this system can also be used for an initial characterization of the mortars or as a method of comparison or grouping for further characterization, due to the response of color to the chemical properties of the material, as can be seen in studies such as (Villa, C. F. R., et Blanco-Várela, M. T. 2000).

6.1.2. X-RAY DIFFRACTION (X.R.D.)

X-ray diffraction (XRD) is a destructive analytical technique commonly applied for archeometric studies, based on the measurement of the incident signal resulting from the diffracted X-ray in crystals. This technique according to Artioli, G. 2010: “easily represents the cheapest and most reliable technique for identifying crystalline phases both in natural and man-made materials”. It provides not only the type of mineralogical composition of the analyzed sample but also the relative concentration of these minerals (Stanjek, H. et Häusler, W. 2004). In this sense, a broad range of applications are offered by XRD when analyzing different materials in their solid state. It can provide information regarding “(1) the identification of unknown crystalline phases, (2) the quantification of phase abundance in polycrystalline mixtures, (3) crystal structure determination and refinement, (4) physical analysis of the sample in terms of crystallite size, lattice micro-strain, or orientation texture of the crystal domains.” (Artioli, G. 2010), giving essential data for the understanding of production techniques, firing temperatures, and the origin of materials. According to Artioli, G. 2010, when applied in a non-destructive way the technique can also provide key insights for the textural analysis of a material.

The technique is based on the interaction between X-ray and the systematic organization of atoms in a crystal. The atoms in a crystal are organized in systematic, periodic three-dimensional arrangements. This means that “crystals are composed of regularly spaced atoms, each crystal contains planes of atoms which are separated by a constant distance. The distances between planes are characteristic of the crystalline species” (Whittig, L. D. et Allardice, W. R. 1986). This organization of atoms in space is an intrinsic characteristic of each crystalline material, defining and distinguishing it (Stanjek, H. et Häusler, W. 2004).

X-rays, as defined by Encyclopædia Britannica 2023, are “electromagnetic radiation of extremely short wavelength and high frequency, with wavelengths ranging from about 10^{-8} to 10^{-12} meters and corresponding frequencies from about 1016 to 1020 hertz (Hz)”.

The interaction is, therefore, produced when an X-ray is emitted and directed to an analyzed material in its solid state, hitting it and interacting with the single atoms present in the crystalline structure. When the X-ray encounters an atom, the energy it contains is absorbed by the atom by transferring the electrons within it to higher energy levels (outermost shells) and creating in this way electron vacancies within the orbital. However, it is not a stable state for the atom, therefore the electrons are obliged to return to their initial state, releasing in this way the absorbed energy in a process called elastic scattering (Whittig, L. D. et Allardice, W. R. 1986; Bruker corporation 2019).

These incident rays, scattered through all directions, will either be amplified by constructive interference or erased by destructive interference (Stanjek, H. et Häusler, W. 2004). The constructive interference of the scattered rays “is obtained when the path of the wavelet scattered on the lower of the two planes is longer by an integer number of wavelengths λ than that of the wavelet scattered off the upper plane” (Stanjek, H. et Häusler, W. 2004), as described by the Bragg equation. According to this and due to the organized and rhythmic atomic structure of crystals, the incident rays can only be observed at specific angles, in the process called diffraction (Whittig, L. D. et Allardice, W. R. 1986). Therefore, the detection of an energy peak at a specific angle will rely on the distance of separation of atomic planes, and therefore of the crystal itself (Stanjek, H. et Häusler, W. 2004). Or as defined by Artioli, G. 2010: “The data collected are generally intensity profiles of the diffracted X-rays as a function of the scattering angle, which show the Bragg diffracted peaks characteristic of each crystalline phase. The angular position, the

integrated intensity, and the peak profile shape of the diffracted signal are important for the subsequent analysis based on Bragg's Law". In this sense, the identification of a crystal is possible thanks to the unique atomic arrangement within it. When subjected to the analysis, it will result in an X-ray diffraction pattern, showing the position (or angle) and the intensities of the diffraction peaks (Stanjek, H. et Häusler, W. 2004).

The equipment or machine used for these analytical techniques consists of a rotatory X-ray source, a rotatory detector, and sample holders (Artioli, G. 2010). The X-ray beam will be emitted by the X-ray generator and collimated by various slits (to control the length of the beam and therefore the analyzed area of the sample), while the the diffracted beam will pass through anti-scattered slits (to reduce noise), diffraction slits (to control the resolution), finally reaching the detector and the system to transmit the collected information. Sample holders and sample preparation procedures may vary according to the type of analysis performed (Whittig, L. D. et Allardice, W. R. 1986; Artioli, G. 2010).

6.1.3. OPTICAL MICROSCOPY

Polarizing transmitted light microscopy is an analytical technique commonly used for the observation and identification of mortars' physical properties and characteristics. The microscope used for this purpose consists of an illuminator or light source, a polarizer, a condenser, a diaphragm, an aperture, a stage, objectives with different magnifications, a compensator, an analyzer, and an eyepiece. Each of the aforementioned parts serve a specific function for the acquisition of high-quality and in-detail images. Some microscopes count as well with cameras, to digitally store the desired image.



Figure 32. Typical aspect of a polarizing optical microscope.

In the microscope, light is emitted from the illuminator, then passes through the condenser, the polarizer, and the diaphragm where it is filtered and focused into the aperture, and later into the specimen or sample. As mentioned by Frandsen, A. F. (2016), “polarizer restricts the exiting light to one plane of vibration”, being this an essential role in the polarizing microscope. Then, light is spread throughout the specimen, interacting with it. This interaction relies on the physical properties which then results in a clear image of the sample. According to Davidson, M. W. et Abramowitz, M. (2002) “Some of the light passing through the specimen is deviated when it encounters parts of the specimen” This resulting light is then called diffracted light.

In this sense, and as mentioned by the aforementioned author, “Many transparent solids are optically isotropic, meaning that the index of refraction is equal in all directions throughout the crystalline lattice”. This phenomenon is due to the bi-refraction of crystals. This can be explained as the fact that when light interacts with a non-equivalent axis present in a crystal (due to the specific structure and axes of the crystal) it gets split or refracted into two different rays, each one with its vibration direction and velocities (Davidson, M. W. et Abramowitz, M. 2002). The light resulting from this interaction is captured by the objectives and further focused into the eyepiece. In polarizing microscopes, this resulting light can be filtered once again into one specific plane by the analyzer.

Crystals can be identified according to their isotropy or anisotropy. This is precisely what allows the observation of the properties and characteristics of the mortars. It should be mentioned however that this analytical method is highly dependable on the observer since it relies on his or her particular knowledge and expertise when performing the observation and identification. Another difficulty

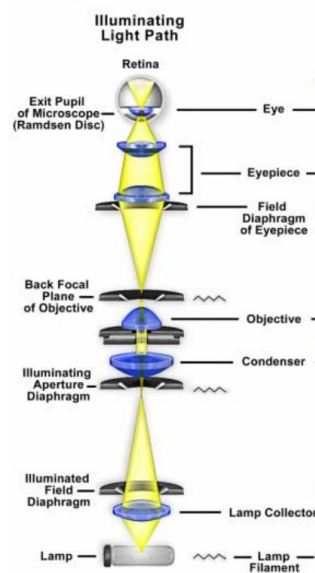


Figure 33 Davidson, M.W. and Abramowitz, M. (2002) 'Optical microscopy', Encyclopedia of Imaging Science and Technology [Preprint]. doi:10.1002/0471443395.img074.

presented by this technique of analysis is the requirement of the destruction of the sample to create thin sections. This procedure (thoroughly discussed in Chapter 6.2) will result in sections of mortar of 30 mm in thickness (Alfieri, P. V. et al. 2020). This thin section will provide the ideal conditions for the desired observation.

These observations have been applied to cultural heritage materials for numerous reasons and in a great variety of materials such as wood (Alfieri, P. V. et al. 2020), or ceramics (Riederer, J. 2004). In the case of historical mortar analysis, as mentioned by Arizzi, A., et Cultrone, G. (2021) “is an essential step in their characterization, as it enables us to observe the main textural and compositional features of these materials, from which important information can be gleaned about the mortar manufacturing and application conditions”. It has been used on several occasions for the identification of minerals resulting from hydraulic phases (Elsen, J. 2006), manufacturing technologies, and provenance studies (Ergenç, D., et al. 2021). It allows for the observation of the binder’s fabric and the voids present in it, identification of inclusions, aggregates, and additives, and deterioration processes according to the sampled material (Quinn, P. S. Composition of Archaeological Ceramics in Thin Section. 2003; Stoops, G. 2003; Arizzi, A., et Cultrone, G. 2021). However, as previously mentioned, this is a qualitative characterization that depends on the observers’ knowledge and experience. Nonetheless, some quantification analysis can be performed throughout the digital analysis of the acquired photographs (Riederer, J. 2004). According to Elsen, J. (2006), “Quantitative optical microscopy methods can be used to determine the aggregate size distribution of historic mortars and are very useful when only a limited amount of sample is present”.

6.1.4. SCANNING ELECTRON MICROSCOPY (S.E.M.)

Scanning electron microscopy (SEM), like other microscopy techniques, serves to visualize small features of objects. Nonetheless, as it is based on the acquisition of images using the electron beam rather than light, it is possible to obtain a higher magnification, resolving in this way finer details of the analyzed material (Ul-Hamid, A. 2018). According to Artioli, G. (2010): “Typically, scanning electron microscopes (SEM) employ electron beams accelerated in the range 102–104 eV, corresponding to wavelengths of the order of 0.123–0.012 nm, and therefore may reach magnifications over 100 000 times, compared with magnification factors for the best optical

microscopes of about 1000". The use of this microscope allows for both the observation of the sample's topography and elemental composition, according to the method used (which consists of secondary electrons or backscattered electrons) (Artioli, G. 2010).

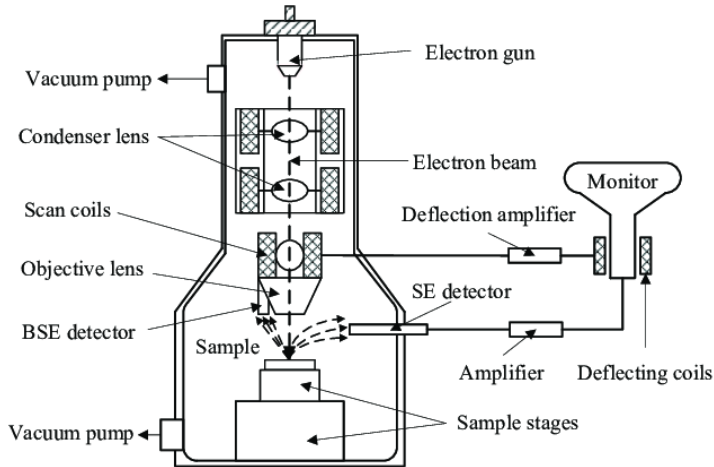


Figure 34. Sheng, Y. et al. (no date) Schematic diagram of SEM setup with various components. A review of computer micro-vision-based precision motion measurement: principles, characteristics and applications. Available at: <https://www.research>

The SEM consists of three major components: the electron column, the specimen chamber, and the computer (Ul-Hamid, A. 2018). Each of these has its specific function in order to acquire the images and analysis. As mentioned by Ul-Hamid, A. (2018), in the electron column, the electron beam is generated and focused through electromagnetic lenses, also referred to as the electron beam

manipulation system. The specimen chamber, on the other hand, consists, as its name suggests, of the chamber where the sample is placed. It is in this section of the SEM where the interaction between the beam and the sample takes place, and where the detection of the resulting electrons is performed. It should be highlighted that both the electron column and the specimen chamber are kept under vacuum to guarantee the proper mobility of the electrons. Finally, the computer or display system refers to the section in which the visualization of the acquired electron signal takes place. In this, it is possible to manipulate the parameters of the image acquisition to obtain better results (Dunlap, M. et Adaskaveg, J. E. 1997).

As previously mentioned, this analytical technique allows for the observation of the sample's topography and elemental information. This aspect is better explained by Ul-Hamid, A. (2018), who mentions: "Imaging can be performed using both secondary electrons (for topographic contrast) and backscattered electrons (for topographic and/or compositional contrast). Microchemical information is generally obtained using an energy dispersive x-ray spectrometer (EDS) detector attached to the SEM." In this sense, the acquisition of the signal emitted by a specific group of electrons will determine the observed properties of the material. Furthermore,

the coupling of SEM with the use of energy dispersive spectroscopy (EDS) will result in the acquisition of semi-quantitative elemental composition of the sample.

The acquisition process of the magnified images starts in the electron column. In this, as previously commented, the electron beam is generated and focused into the sample, which is located in the chamber. Then, it penetrates the sample (just a few microns), where it interacts with its atoms (Ul-Hamid, A. 2018). This interaction, as described by Ul-Hamid, A. (2018), causes the elastic scattering of electrons. These scattered electrons can be scattered off the surface of the sample without further interaction with the atoms. The resulting electrons from this interaction are called secondary electrons, showing in this way the topography of the material's surface (Ul-Hamid, A. 2018). On the other hand, some of the primary electrons from the beam may interact with the atoms of the samples, producing backscattered electrons. These electrons, due to this interaction, will reflect on the atomic composition of the sample. This interaction occurs, as explained by Ul-Hamid, A. (2018) in the following manner: “Primary electron beam penetrates the specimen material and interacts with the inner shells of atoms. As a result, inner-shell electrons of target atoms are ejected from their orbits and leave the bounds of the atom. The process of electron ejection results in a vacancy in the orbital and turns the atom into an ion of an excited or energized state. This vacancy is immediately filled when an outer shell electron is transferred to the inner shell, which brings the atom to its ground (lowest energy) state with an accompanying release of energy equal to the difference in the binding energy of the two shells. This excessive energy is released in the form of an x-ray photon which has energy equal to the binding energy between the two shells”. In addition, it is because of this emitted signal that it is possible to acquire the semi-quantitative composition of the sample by the use of the EDS. Finally, the emitted signal of the electrons (either the secondary or the backscattered) is detected, providing information on both the intensity and the

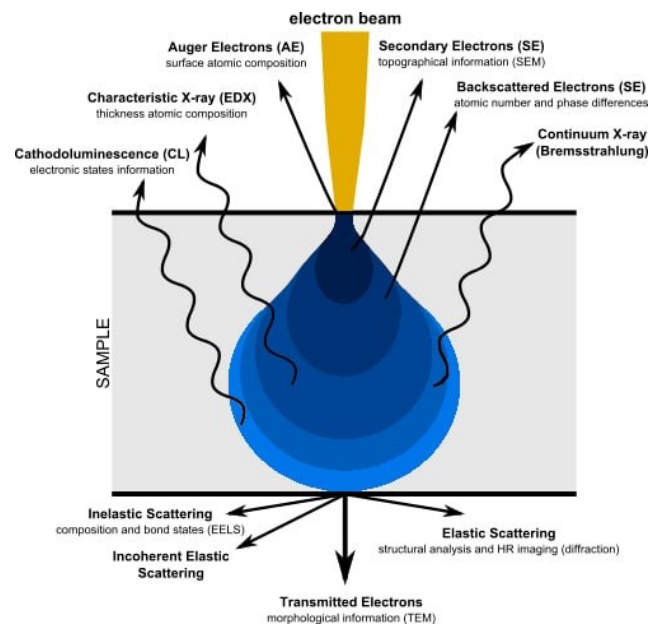


Figure 35. Interaction between the electron beam and the atom. Atria Innovation (2022) *Soluciones Tecnológicas para la industria 4.0*, ATRIA Innovation. Available at: <https://www.atriainnovation.com/> (Accessed: 30 July 2023).

location of the signal (Ul-Hamid, A. 2018). This signal is later displayed and recorded on the screen (Ul-Hamid, A. 2018). It should be mentioned that the primary beam is deflected along the sample's surface, which leads to the acquisition of the signal in a scanning way.

Once the image is displayed on the screen it is possible to adjust the parameters to ensure the recording of a high-quality image (Dunlap, M. et Adaskaveg, J. E. 1997). The adjustable parameters consist of brightness and contrast, resolution, magnification, depth of field, noise (or signal-to-noise ratio), composition, and the used voltage. All of these parameters will result in significant differences in the images, making them more or less clear and understandable (Dunlap, M. et Adaskaveg, J. E. 1997). The parameters should be adjusted for each individual sample, regardless of the acquired information (either topographical or elementary) to ensure a high-quality image (Dunlap, M. et Adaskaveg, J. E. 1997).

The sample preparation, on the other hand, may change according to the desired results. According to Ul-Hamid, A. (2018), “any sample preparation method should take into account the manufacturing method and usage history of the product under examination. The aim of sample preparation should be clear at the outset”. The author mentions as well that the material of the sample to be examined should be taken into account, since they may require further treatment. Nevertheless, the general sample preparation consists of the coating, either with metal or graphite, of non-conductive samples (Artioli, G. 2010). Other sample preparations may include the cleaning of the sample, polishing, coating, embedding, or grinding (Ul-Hamid, A. 2018). However, it should be highlighted that due to the properties of the SEM, it is possible to analyze solid and powdered samples, either wet or dry with different dimensions (according to the specifications of the individual SEM) from both organic or inorganic origin (Ul-Hamid, A. 2018).

6.1.5. WET GRAVIMETRIC SEPARATION AND BINDER ANALYSIS

Wet gravimetric separation is, as its name indicates, a technique used for the separation of binder and aggregate present in the mortar. This is done in order to determine the nature of the binder, which provides unique and decisive information concerning the manufacturing technique of mortar and the interaction between the aggregates and the binder (Maravelaki-Kalaitzaki, P., et al. 2003). This separation of both components is suggested by several authors and discussed in

articles such as Arizzi, A., et Cultrone, G. (2021) and Ergenç, D., et al. (2021), who also propose techniques such as mechanical disaggregation, chemical etching with hydrochloric acid (8–10% HCl) (which according to Ergenç, D., et all. (2021) is only suitable for air-lime mortars with silica aggregates), or wet chemical methods.

6.2. ANALYTICAL PROCEDURES

6.2.1. COLORIMETRY

The process of acquisition of color values for each of the 49 samples was performed with the use of the colorimeter PCE-XXM 30 of PCE-instruments with an angle measurement of D/8-SCI, an aperture of 8Ø, and a range of wavelength of 400-700 nm. The time of acquisition per sample was of less than a minute and the color code was given on the L*a*b* color space. The color measurements were done on the powdered form of the mortar due to the homogenization it provides of both binder and aggregates. There was no need for further preparation of the samples since the powdered form of the mortars was recovered from the preparation treatments for XRPD analyses. It should be highlighted that the color acquisition was performed on the mortar powder without the addition of zinc oxide, since this could result in a variation of the true color values of the sample.

6.2.2. X-RAY DIFFRACTION (X.R.D.)

The entire procedure, for both sample preparation and analysis, took place in the



Figure 37. Sample after initial grinding

laboratories of the University of Padova. The selected procedure for the XRD analysis on the mortar samples of the Roman buildings of Verona was X-ray powder diffraction (XRPD). For this reason, the first step in



Figure 36 FIG. XRD1. Instrumentation used for initial grinding

the sample preparation procedure was the selection of the fraction of

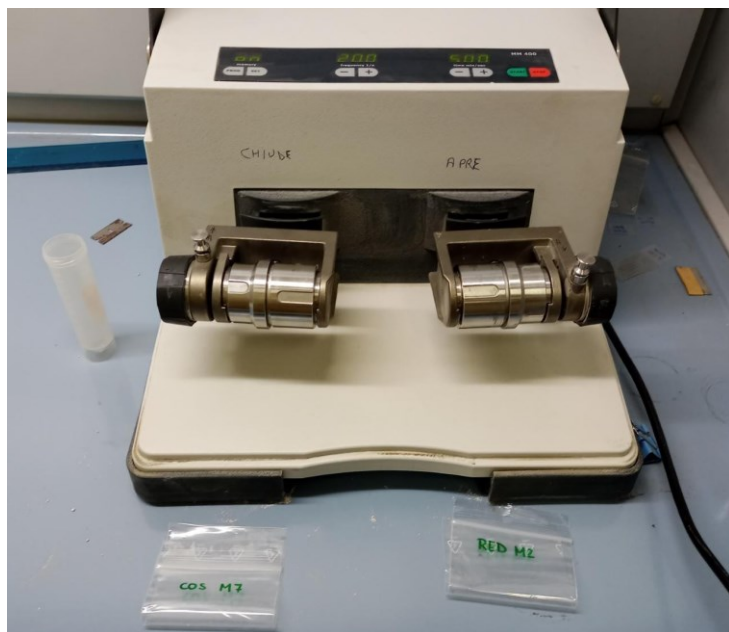


Figure 38. second step of grinding

the sample to be prepared and further analyzed. The selection criteria were based on the representativeness of the sample. In this sense, the fraction should represent the entire sample, containing both the matrix and the aggregates present in it. The quantity of the fraction was variable since it depended on the total amount of sample and its homogeneity (since a more homogenous mortar could be represented by a lower quantity than a heterogeneous one). It should be

mentioned as well that for most of the samples (28 out of 30) a fraction of similar properties was left as a testimony. The following step was the initial grinding. In this step, the selected fraction was coarsely ground by crushing it with a hammer on a closed container (fig. 35 XRD1). The remaining powder, comprised of particles with a millimetre-sized granulometry, was kept aside in a different container than the testimony for further grinding. Due to the requirements of the technique, the samples were then subjected to a second round of grinding. In this case, the pulverization was performed with the Retsch mixer mill MM 400, obtaining a powder of around 50 microns of granulometry. The procedure was done by pulverizing 15 mL of the ground sample for 5 minutes (fig. 36 XRD2 and fig. 37 XRD3).

Finally, the third and last grinding procedure, called micronization, took place, obtaining a fine powder with a granulometry of approximately 5 microns. The grinding procedure was performed with a McCrone XRD-mill. A homogeneous portion of the ground sample was mixed with 15 ml of ethanol (to avoid the agglomeration of particles) for 5 minutes at a working speed of 75% (fig. 38 XRD4). The resulting mixture of ethanol and powder is then left to dry for 1 day on a watch glass (fig. 38 XRD5).

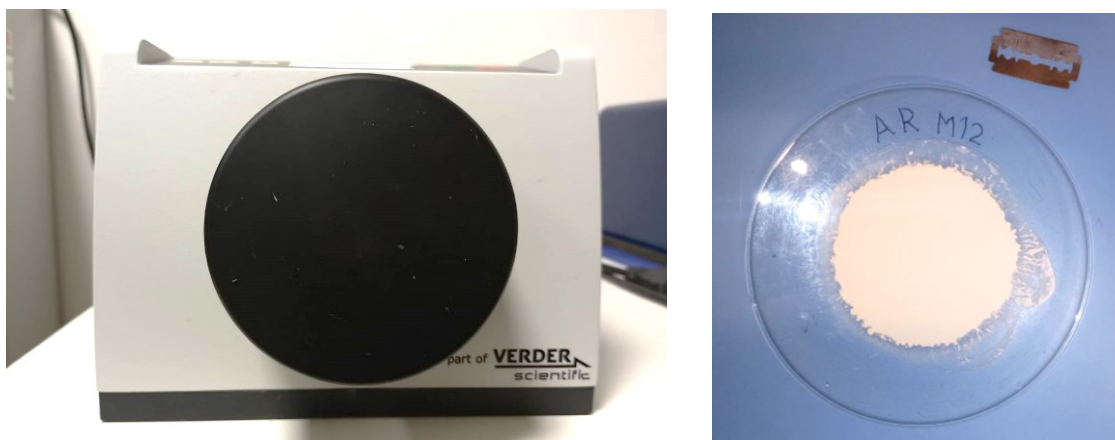


Figure 39. XRD 3 and 4. Final grinding procedure

The dry powder is then recovered for the glass watch by scraping it off the container with a metal blade. Then, with the help of the analytical scale PR series of Ohaus, 0.8 g of powder is placed in a different glass watch together with 0.2 g of zinc oxide, having a total of 1 g of prepared powder mixture for the analysis. It should be mentioned that the addition of the standard to the sample is done to



Figure 40 XRD 5. Sample mounting instrumentation.

achieve a better comprehension of the sample's composition and a better reading of the presence of amorphous content in it. The two powders are later manually mixed in a mortar and placed on the sample holder. This action is performed by applying the back-loading technique in order to avoid the preferred orientation of the crystals in the sample (fig 39 XRD5).

XRPD measurements were then acquired with a PANalytical X'Pert PRO diffractometer in Bragg-Brentano geometry equipped with a cobalt X-ray tube and a X'Celerator detector. The working conditions were: CoK α radiation, 40 kV voltage, 40 mA current, 3-85° 2 θ range, step size 0.02° and 100 s counts per step. Mineral phases were identified using the X'Pert HighScore Plus software and further quantitative analysis by Rietveld refinement was performed using Topas software.

6.2.3. THIN SECTION PRODUCTION

The production of the thin sections of Roman mortars was performed in the laboratory of Université Bordeaux Montaigne, where a photographic record of the samples was performed before the production of the thin sections took place, in order to obtain a detailed register of the samples before subjecting them to irreversible changes. The process carried out followed the guidelines proposed by Spiteri in her manual “Thin section preparation manual adapted for archeological materials”. It consisted of 16 main steps as follows: 1) Mortar samples are placed (with a flat bottom down preferable to avoid the movement of the sample when pouring the resin) in rectangular aluminum containers. Samples will be placed following the order from the list mentioned above and, according to their size, will be paired or placed individually on the container (fig 40). 2) After the placement of each pair or individual sample, careful labeling of the sample is done by drawing a sketch and labeling the sketch with the sample code and photographing the tray and the label (for future reference). 3.) The samples are then placed inside an oven at 45 degrees Celsius for some hours to extract any possible remaining humidity. It is worth mentioning that due to the number of samples and practical reasons the production of the thin sections was divided into two batches. 4) The epoxy resin is later prepared and poured into the containers with the samples. It should be noted that the resin used in this case is Araldite 2020 and due to the dimensions of some of the samples it was not possible to completely cover them on resin, only partial coverage was possible in this case. 5) once the resin is poured, the containers are placed inside a vacuum chamber (in groups of 4 or 5 due to the dimensions of the chamber) and subjected to three vacuum

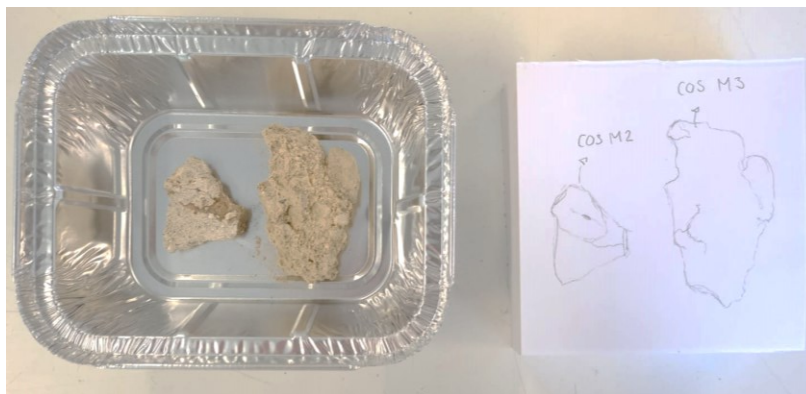


Figure 41. Samples COS M2 and COS M3 embedded in resin on an aluminum container

cycles. These cycles consist of the placement of samples under vacuum (at 0.8 bar) for a variable period, normally some minutes depending on the response of the sample. This process is done in order to extract all possible air inside the sample and its replacement with

the resin (to ensure the proper penetration of the resin and the correspondent stabilization of the sample). 5) Samples then should be reoriented if needed. 6) Although resin normally takes 24 hours to harden, in this case, it was left for a period of 36 hours approximately due to the thickness of the samples. 7) After the curing process is over samples are then cut into blocks of 30 x 45 mm with a saw. 8) the surface of the block was prepared by gritting it with diamond grit first and then with 400 and 600 abrasive papers.

9) Samples are then left to dry on a hot plate. 10) Samples are glued to a glass holder (which was dried over the hot plate) by placing approximately 2 g of resin per sample. It is important to place the glass gradually to avoid bubbles. The samples should be left to dry on a gluing bench overnight (fig.41). 11) Once dry, the samples were cut once again by using a diamond saw leaving approximately 600 microns



Figure 42. Cut samples with glued glass on the hot plate.

of thickness. 12) The thickness of the sample blocks was reduced by using a grinding machine until a thickness of 30 microns is obtained. 13) The final thickness of the thin sections needs to be evaluated by measuring different points with a comparator (measuring first the glass and then different areas of the section). 14) If some of the areas of the thin section have a different thickness than 30 microns, further steps should be taken by manually grinding it with powdered silicon carbide and water. To check the effectiveness of the grinding, thin sections should be observed under the optical microscope (by observing the interference colors of quartz). 16) Final steps consist of polishing the surface with an automatic polisher.

6.2.4. OPTICAL MICROSCOPY OBSERVATION

After the production of this section is finalized, samples are ready to be analyzed under the Leica DM750 P Polarized Light Microscopy (PLM) in transmitted light (TL) operating with the

integrated digital camera FLEXACAM C1 with objectives 1.6X, 4X, and 10X. For this purpose, thin sections are observed under different magnifications in order to analyze them under diverse levels of detail. The general approach for the observation proposed a general to specific structure. In this, observations in lower magnification were first performed to obtain a general idea of the composition and characteristics of each specific sample and then further information and in detail knowledge was obtained with higher magnifications. Sample description was done by monitoring and recording the following criteria: general observation of characteristic macro aspects, binder type, presence and type of lumps, presence and type of voids, and finally, the presence and type of aggregates identified.

6.2.5. SCANNING ELECTRON MICROSCOPY (S.E.M.)

After analyses were done under optical microscope and XRPD, samples to be analyzed under the SEM were chosen based on the results obtained from the previous analysis. Since the parameters chosen for this selection concern the results of the previously mentioned procedures, this selection will be later discussed in chapters seven (7) and eight (8). Sample preparation for SEM-EDS analysis for each of the 20 samples consisted of the coating of thin sections (previously observed in optical microscopy) with a thin layer of gold on the rotatory pumped coater Quorum Q150R, through a sputter procedure. This coating procedure is done in order to improve the spatial resolution of the acquired images thanks to the conductive properties of gold.

The prepared samples were then analyzed individually in the tabletop SEM EM-30 plus of Coxem with an acceleration voltage of 20 kV. Samples were observed at variable magnifications using the secondary electrons to obtain chemical information of the sample. Further semi-quantitate elemental composition of the samples was obtained by EDS analysis.

6.2.6. WET GRAVIMETRIC SEPARATION AND BINDER ANALYSIS

The wet gravimetric separation of the binder and the further analysis carried out through XRPD and SEM-EDS is divided into three different procedures; the binder separation process, the XRPD analysis, and the SEM-EDS analysis.

WET GRAVIMETRIC SEPARATION

The first procedure carried out was the separation of the binder portion of the mortar samples through the implementation of a wet gravimetric separation. This process was carried out in the laboratories of the Department of Geoscience of the University of Padova under the guidance of dr. Giulia Ricci. The procedure encompassed the following steps: 1) The selected samples of mortar were disaggregated by mechanical means in order to obtain a grain size ranging from powder to fine gravel. At least 30 grams of mortar should be obtained to obtain sufficient material for further analysis. 2) To ensure the precise amount of material, the disintegrated mortar is then weighted and placed into a beaker. It should be mentioned that before any container is used it is carefully cleaned with hydrochloric acid (HCl 10%) and Milli-Q water to avoid any possible contamination. 3) Milli-Q water is added to the beaker with the mortar until the water level reaches 200 ml. The beaker is then closed and sealed with parafilm and left for an ultrasonic bath in a Elmasonic 5 apparatus for 30 minutes. 4) After the 30 minutes are over, the resulting water is then poured into a glass graduated cylinder. It should be highlighted that only the water portion should be poured, no solid parts should be present in the cylinder. 5) Steps 3 and 4 are repeated, adding Milli-Q water into the beaker with the solid portion of the mortar and placed into the ultrasonic bath. Once again, the water from the beaker is placed inside the cylinder. 6) 0.5 grams of sodium hexametaphosphate are weighted and placed into an Erlenmeyer Flask, where it is diluted into 1 L of Milli-Q water. The addition of hexametaphosphate is done in order to avoid the flocculation of binder particles into the cylinder. 7) The previously mentioned solution is then placed in the graduated cylinder containing the water obtained from the ultrasonic bath of the mortar. To this, Milli-Q water is added, if needed, until a level of 500 ml is reached. 8) the cylinder is then sealed, once again with parafilm, and left to settle for approximately 24 hours. 9) After the 24 hours have passed, the sample is placed inside a Falcon tube with the help of a pipette. For this procedure, the upper layer is extracted from the cylinder, since it is precisely in this part where the binder fraction can be found. During the extraction with the pipette, it was necessary to proceed with special attention, since the upmost layer of mixture may only contain water, therefore the extraction of this layer should be avoided. Two Falcon tubes should be extracted from each sample, providing in this way two different aliquots for each mortar. 10) The already filled Falcon tubes are weighted

and placed inside the centrifuge Rotina 380 with a fixed angle of 45 degrees. The centrifuge is set with a three-step circuit (1. gradual increasing 2. Stable high velocity and 3. decreasing velocity) for a 20-minute round that reached 10000 RPM. 11) After the centrifuge cycle is over, and the Falcon tubes are extracted from the machine, the residue water is poured out of the Falcon tubes, leaving only the solid fraction. 12) A small amount of ethanol (not measured) is then added to the Falcon tubes containing the binder fractions and placed in an ultrasonic bath until the binder dilutes into the ethanol. 13) The resulting mixture of ethanol and powder is then left to dry for 1 day on an already labeled watch glass. 14) The dried binder is then recovered with the help of a blade and placed inside a plastic tube for further analysis.

It should be mentioned however that samples AP-M1, AR-M12, and LEO-M5 presented some difficulties and required extra steps due to the flocculation of the binder. For this reason, Sample AP-M1 passed through a series of extra washes in order to eliminate the presence of possible salts causing the agglomeration of particles. On the other hand, samples AR-M12 and LEO-M5 were directly extracted and processed without the extra washes.



Figure 43 Sample before and after 24 hour with a clear differentiation of the binder fraction



Figure 44 Centrifuge Rotina 380

XRPD

Due to the fact that the analysis procedures were carried out once again in the laboratories of Geosciences of the University of Padova, the process for sample preparation follows the same working principles. However, as a consequence of the total amount of material available for the analysis (around 0.06 grams per aliquote), the procedure had to be adapted, using this time a zero-background sample holder. Another important variation that should be mentioned is that, since the sample obtained by gravimetric separation already has the desirable granulometry, there is no need for grinding or milling. Therefore, the sample preparation was carried out through the following steps: 1) 0.02 grams of sample and 0.005 grams of zinc oxide standard are weighted with the help of the analytical scale, maintaining once again an 80% sample to 20% standard proportion. 2) Both the standard and sample are then homogenized in a mortar, making sure the two powders are properly mixed. 3) The resulting powder is then placed on the central part of the zero-background sample holder. In this, the powder is ideally distributed homogeneously without leaving any empty spots. 4) The zero-background sample holder is then carefully placed and leveled in a steel sample holder corresponding to the machine's requirements, leaving the sample ready at this point for the analysis to be carried out.

SEM-EDS

Sample preparation for SEM-EDS analysis of the binder fractions consists of a rather simple procedure. For this, the recovered binder samples used for the XRPD analysis (containing 20% zinc oxide) were used and treated in order to obtain optimal working conditions to extrapolate the chemical composition of the binder under by SEM-EDS. Each sample was compressed manually by mechanical means, in a similar way in which FT-IR sample preparation is performed, to obtain as a final result a compact tablet. The tablets were then placed over a strip of carbon tape on a sample holder for observation to take place. It should be mentioned that no gold coating was performed due to the fragility of the samples analyzed.

The chemical composition of the samples was then obtained using the FEI Quanta 200 scanning electron microscope with an acceleration voltage of 20 kV located in the CEASC laboratory of the University of Padova. The software used for image analysis and elemental quantification was Aztec 5.0 SP1 from Oxford Instruments. In it, both areal analyses and chemical maps were acquired to comprehend the general chemical composition of the samples and the correlation of certain elements that could be found within it. The acquisition procedure retrieved elemental data from three different randomly selected points from the sample since no special elemental distribution of the sample could have been found due to its powder nature. The quantification of the elements was later treated through statistical analysis to obtain both the means and the standard deviation of its chemical composition. It should be highlighted as well that the quantification of zinc oxide previously added to the sample was used as a guide to corroborate the accuracy of the results but was no longer considered in the general analysis since it does not belong to the sample itself.

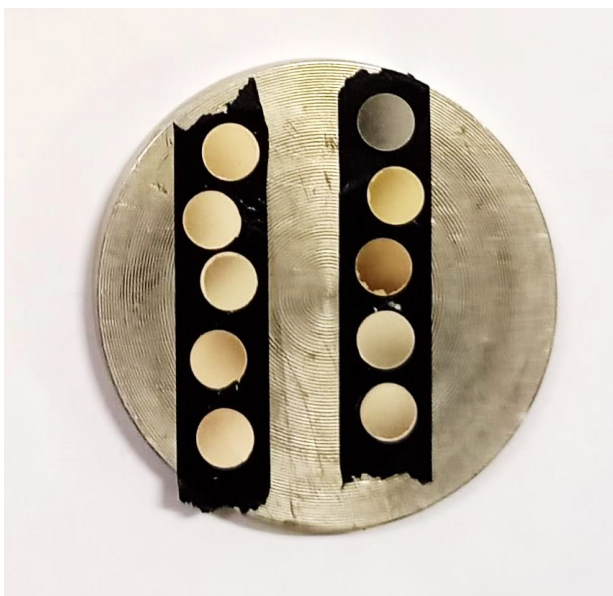


Figure 45 Prepared compressed samples over sample holder for SEM-EDS analysis

7. Chapter VII - Results:

7.1. COLORIMETRY

The results obtained from the the color measurements on the 49 mortar samples are presented in the following table (table 03), where it is possible to observe the original obtained values in the L*a*b* color space, as well as their correspondence in the RGB color space and a visual representation of the mentioned color. It is possible to observe that the values of the mortars do not show great variability, with some exceptions, such as AP-M1 or AR-M8.

SAMPLE	L A B Values			R G B values			Color
	ID	L*	a*	b*	R	G	B
RED M1	82,3	3,0	8,7	216	202	189	
RED M2	81,9	2,6	8,0	213	202	189	
RED M3	80,2	2,8	10,1	210	197	180	
RED M4	78,8	3,2	11,3	207	193	174	
RED M5	79,1	3,2	10,3	208	193	177	
OD M1	84,8	2,3	9,0	221	210	195	
OD M2	82,5	2,3	8,1	214	204	190	
OD M3	83,5	1,9	7,3	216	207	194	
OD M4	82,3	2,3	8,2	214	203	189	
OD M5	82,8	2,1	8,5	215	204	190	
CSP M1	85,9	2,3	8,4	224	213	199	
RM M1	83,4	2,5	7,4	217	206	194	
SGA M1	84,8	2,2	8,5	221	210	196	
SGA M2	86,8	2,2	7,1	226	216	204	
SGA M3	83,9	2,5	8,4	219	207	193	
SGA M4	85,0	2,2	7,1	221	211	199	
SGA M5	83,1	3,5	9,5	219	204	189	
SGA M6	82,0	2,4	8,2	213	202	189	
SGA M7	83,1	2,3	8,9	217	205	190	
SGA M8	82,9	1,6	10,3	215	205	187	
AP M1	81,5	4,8	10,5	218	199	183	
LEO M1	78,2	2,9	6,2	203	191	182	
LEO M2	90,8	1,2	4,4	234	228	220	
LEO M3	86,1	1,9	6,3	223	214	204	
LEO M4	81,6	2,3	6,9	211	201	190	
LEO M5	82,1	2,1	7,7	213	203	190	

LEO M6	80,4	2,7	10,5	211	197	180	
COS M1	85,3	2,0	7,4	221	212	199	
COS M2	83,1	2,4	7,4	216	205	193	
COS M3	83,1	2,2	8,2	216	205	192	
COS M4	89,4	1,4	3,9	230	224	217	
COS M5	84,8	1,3	9,3	220	210	194	
COS M6	73,0	3,1	10,4	191	177	160	
COS M7	84,4	2,3	8,2	220	209	195	
COS M8	85,0	2,0	6,1	220	211	201	
TR M1	85,0	2,0	6,8	220	211	200	
AR M1	84,5	2,0	8,0	219	209	196	
AR M2	80,9	2,4	9,1	211	199	184	
AR M3	79,7	2,9	9,9	209	195	179	
AR M4	83,2	3,3	9,1	219	205	190	
AR M5	84,4	2,9	9,1	221	208	194	
AR M6	82,1	2,6	8,3	214	202	189	
AR M7	86,8	2,3	7,1	226	216	204	
AR M8	67,1	4,5	12,2	178	160	142	
AR M9	83,7	2,1	8,0	217	207	194	
AR M10	82,1	2,1	7,7	213	203	190	
AR M11	83,0	2,4	7,8	216	205	192	
AR M12	74,9	3,0	13,0	197	182	161	
AR M13	87,6	2,7	6,8	229	218	207	

Table 03. Colorimetry results on powder form of mortar samples.

7.2. X-RAY DIFFRACTION (X.R.D.)

The resulting XRPD patterns of the total population of samples (49 mortar samples) were analyzed both qualitatively and quantitatively. Mineral phases were identified with the utilization of X'Pert HighScore Plus software, and quantitative analyses according to the Rietveld method were performed with the Diffrac.Topas software from Bruker. The quantitative values obtained from the analysis are reported in the following table.

	Quartz	Calcite	Dolomite	Ilmenite	Gypsum	Hornblend	Talc	Albite	K feldspar	Mica	Chlorite	AFM	Hematite	Dipside	Amorph.
RED M1	16.73	27.93	0.00	0.29	1.71	0.95	0.00	6.34	2.93	5.98	2.33	1.36	0.00	0.00	33.46
RED M2	14.12	22.76	0.00	0.57	0.59	0.83	0.00	4.39	2.87	5.48	1.69	1.69	0.00	0.00	45.01
RED M3	16.89	19.01	0.41	0.46	2.93	1.13	1.43	6.36	1.51	5.95	2.60	0.61	0.00	0.00	40.71
RED M4	23.85	28.63	13.74	0.38	0.05	0.00	0.00	7.07	3.94	2.22	1.05	0.00	0.00	0.00	19.08
RED M5	14.64	19.71	36.03	0.25	0.54	0.00	0.00	6.74	3.39	1.62	1.52	0.00	0.00	0.00	15.55
OD M1	21.71	29.80	19.10	0.32	0.00	1.03	0.00	3.90	2.09	0.51	1.12	1.04	0.00	0.00	19.37
OD M2	11.12	36.05	17.93	0.42	1.28	0.00	0.00	4.88	2.49	0.54	1.29	0.85	0.00	0.00	23.15
OD M3	9.09	36.90	23.61	0.35	0.00	0.00	0.00	3.32	2.88	0.71	1.13	0.96	0.00	0.00	21.06
OD M4	18.48	42.22	18.94	0.39	0.48	0.00	0.00	2.58	2.06	0.93	1.14	1.39	0.00	0.00	11.39
OD M5	17.00	31.01	20.37	0.00	0.60	0.00	0.00	6.33	1.78	2.03	1.24	2.01	0.00	0.00	17.64
CSP M1	10.53	50.80	22.85	0.39	0.00	0.00	0.00	3.97	2.87	1.09	0.80	0.93	0.00	0.00	5.77
RM M1	14.06	24.06	0.05	0.13	0.92	0.44	0.00	3.61	1.44	4.42	1.65	0.00	0.00	0.00	49.22
SGA M1	16.26	35.85	22.09	0.40	1.37	0.00	0.00	5.70	4.00	2.12	1.95	0.00	0.00	0.00	10.25
SGA M2	13.17	43.42	17.34	0.00	0.00	0.00	0.00	5.52	2.54	1.27	2.05	0.00	0.00	0.00	14.69
SGA M3	14.53	28.02	32.36	0.00	0.00	0.00	0.00	5.81	5.57	2.07	1.09	0.00	0.00	0.00	10.56
SGA M4	12.36	37.61	18.92	0.37	0.26	0.93	0.00	4.57	2.87	0.91	1.98	2.07	0.00	0.00	17.16
SGA M5	12.17	44.76	12.16	0.52	0.00	0.86	0.00	4.27	2.95	3.24	1.15	0.93	0.00	0.00	17.01
SGA M6	11.98	25.77	44.61	0.35	0.00	0.00	0.74	5.41	3.06	1.48	1.11	0.73	0.00	0.00	4.75
SGA M7	17.28	34.56	26.47	0.48	0.00	0.85	0.00	7.23	3.41	1.53	1.62	0.00	0.00	0.00	6.57
SGA M8	20.19	27.95	18.63	0.30	0.00	0.00	0.00	9.47	3.64	2.74	1.58	0.82	0.00	0.00	14.69
AP M1	12.06	28.69	24.49	0.39	0.00	0.00	0.00	7.58	5.35	0.94	2.04	0.00	0.92	1.47	16.07
LEO M1	15.11	34.41	21.85	0.44	0.00	0.27	0.00	9.92	5.04	2.68	1.92	0.00	0.98	0.00	7.39
LEO M2	16.68	39.07	15.99	0.39	0.00	0.00	0.00	5.41	3.08	1.27	1.05	0.00	0.00	0.00	17.06
LEO M3	13.45	34.88	19.13	0.46	0.73	0.00	0.00	4.21	3.29	2.11	2.14	0.00	0.00	0.00	19.62
LEO M4	25.74	25.13	1.19	0.28	0.00	0.93	0.69	9.68	3.89	7.07	2.67	0.00	0.00	0.00	22.73
LEO M5	21.41	23.22	18.66	0.27	0.00	0.17	0.00	8.97	4.86	3.09	2.67	0.43	0.55	0.00	15.71
LEO M6	11.00	25.09	33.13	0.34	0.78	0.00	0.00	4.61	2.39	0.66	1.15	0.00	0.00	0.00	20.85
COS M1	12.74	38.92	27.09	0.24	1.24	0.00	0.00	4.39	2.66	1.03	1.56	0.00	0.00	0.00	10.13
COS M2	21.13	19.03	1.82	0.34	5.33	0.94	0.00	6.92	3.29	4.29	2.09	1.20	0.00	0.00	33.64
COS M3	15.87	35.18	22.17	0.42	0.00	1.21	0.00	6.67	3.94	1.93	2.14	0.00	0.00	0.00	10.48
COS M4	13.90	35.27	13.78	0.70	0.00	0.00	0.00	4.89	3.93	1.6	0.52	0.00	0.00	0.00	25.41
COS M5	24.12	35.14	5.91	0.55	0.00	0.00	0.00	11.62	4.39	4.79	3.02	0.00	0.67	0.00	9.80
COS M6	24.12	35.14	5.91	0.55	0.00	0.00	0.00	11.62	4.39	4.79	3.02	0.00	0.67	0.00	9.80
COS M7	19.71	14.44	7.51	0.45	0.00	0.23	0.00	8.57	3.93	4.61	2.27	0.00	0.79	0.00	37.50
COS M8	23.02	44.70	3.73	0.00	0.00	0.00	0.00	8.18	4.00	2.97	2.72	1.35	0.55	0.00	8.79
TR M1	6.97	47.43	29.16	0.18	0.00	0.00	0.21	1.95	1.69	1.41	1.37	1.14	0.00	0.00	8.50
AR M1	12.53	37.82	25.49	0.34	0.00	1.35	0.00	4.07	2.22	1.62	2.30	0.74	0.00	0.00	11.51
AR M2	12.05	36.53	32.95	0.44	0.00	0.00	0.00	4.67	3.40	0.87	1.06	0.00	0.00	0.00	8.03

AR M3	13.78	53.44	13.62	0.17	0.00	0.74	0.45	3.74	1.43	1.88	0.55	0.00	0.00	0.00	10.21
AR M4	2.49	65.43	3.96	0.33	0.00	0.00	0.00	1.40	1.62	0	0.00	0.00	0.00	0.00	24.77
AR M5	9.45	35.08	35.84	0.48	0.00	0.00	0.61	3.80	2.88	2.41	0.98	1.64	0.00	0.00	6.84
AR M6	4.75	23.24	43.08	0.28	1.94	0.00	0.00	2.78	1.67	0.4	0.47	0.97	0.00	0.00	20.43
AR M7	6.23	51.82	17.43	0.18	1.95	0.00	0.71	1.10	1.01	0.96	1.30	3.19	0.00	0.00	14.14
AR M8	6.61	40.43	13.89	0.18	0.77	0.00	0.00	2.12	1.60	0.53	1.75	1.62	0.00	0.00	30.49
AR M9	9.85	22.45	46.89	0.33	0.00	0.00	0.00	4.27	1.72	1.04	1.84	1.59	0.00	0.00	10.02
AR M10	12.79	40.59	21.65	0.35	0.00	0.00	0.00	3.91	2.72	1.15	2.30	0.67	0.00	0.00	13.88
AR M11	9.51	25.70	36.37	0.13	0.00	0.00	0.00	5.45	1.94	2.04	1.82	1.41	0.00	0.00	15.65
AR M12	19.26	20.95	19.60	0.45	0.00	0.00	0.00	13.41	5.11	5.92	4.19	0.00	0.00	0.00	11.11
AR M13	9.55	36.55	23.56	0.39	0.00	0.00	0.00	3.92	2.89	1.01	0.86	2.33	0.00	0.00	18.94

Table 04. XRPD results on powder form of mortar samples.

7.3. OPTICAL MICROSCOPY

The observation of the thin sections under the polarized light microscope was done on 30 representative mortar samples selected from the total sample population. According to these individual observations of the thin sections, it was possible to create coherent sample groups that demonstrated similar characteristics such as binder type, or an akin composition of the aggregate fraction. The following description provides an overview of the properties and characteristics of each individual group.

Group N. 1:

The first group consists of the following samples: RED-M5, OD-M2, OD-M3, CSP-M1, SGA-M2, SGA-M3, SGA-M6, LEO-M1, LEO-M2, COS-M1, TR-M1, AR-M1, AR-M3, AR-M5, AR-M7, AR-M9, AR-M11 and AR-M13. This group consists of gravel-rich mortars (fig. 45) with a bimodal distribution of medium to coarse gravels and fine sands when compared to the reference proposed by the Wentworth grain-size scale. The binder of the samples has a heterogeneous-zoned aspect, where birefringence colors may vary from high birefringence, indicative of carbonation of the lime paste, to dark birefringence, possibly imputable to the diffusion of hydrated phases. Some exceptions are represented by the binder in sample RED-M5 and CSP-M1, presenting a homogenous binder. Due to its heterogeneity, its structure varies from sparitic to micro-crystalline (micritic). The presence of lime lumps in the samples of group N.1 is also variable, being present in limited amounts in some of the samples, such as SGA-M2 or AR-M5, to occasional or few, as can be seen for the case of LEO-M1 and AR-M7, or simply not present at all. Furthermore, the presence of voids in this group of samples mainly consists of vughs, vesicles, some channels, and planar voids.

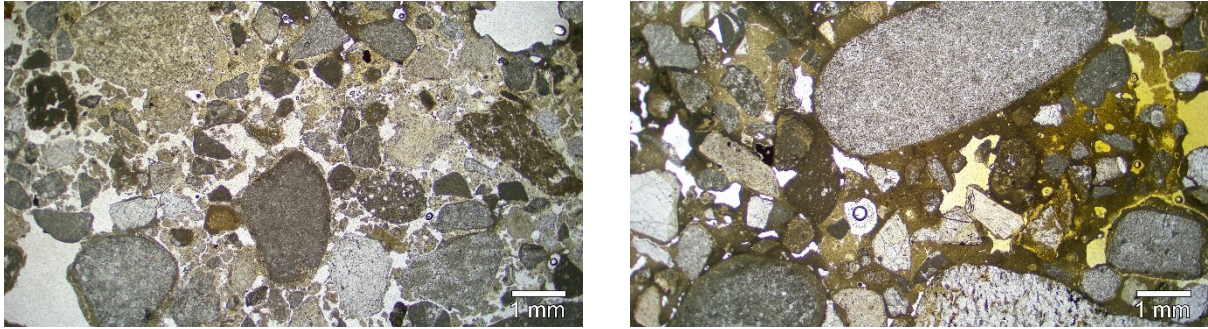


Figure 46 Samples AR-M7 and SG-M2, indicative of the general aspect of group N. 1 mortars

Nevertheless, the properties of the mortars are highly variable within the groups. As already mentioned, the indicative feature is the bimodal distribution and grain size of the aggregate fraction of the mortars. Petrographically, these aggregates primarily consist of carbonate clasts (both calcitic and dolomitic), volcanic clasts with feldspar microlites in the groundmass, occasional chert, clinopyroxene, quartz, quartzite, and granites/granitoids aggregates. Most of the carbonate clasts present reaction rims, clearly detected around dolostone clasts (fig. 46), indicative of dedolomitization phenomena (Katayama 2010).

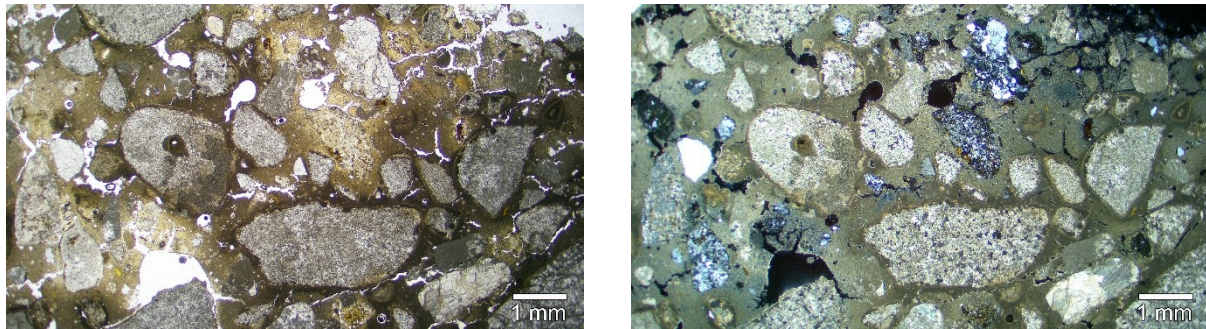


Figure 47 Sample TR-M1 demonstrating the presence of previously described aggregates and the characteristic dedolomitization.

The presence of shell fragments, micas, or under-burnt limestone fragments has also been observed in a limited amount of samples such as CSP-M1, TR-M1, and AR-M5. The majority of the aggregates are highly spherical and highly rounded, indicative of their provenance from riverbeds, identifiable with the River Adige, on the basis of their petro-mineralogical features (P. Jobstraibizer et P. Malesani. 1973). The aggregate is poorly sorted, as can be seen in samples AR-M3, OD-M2, and AR-M9.

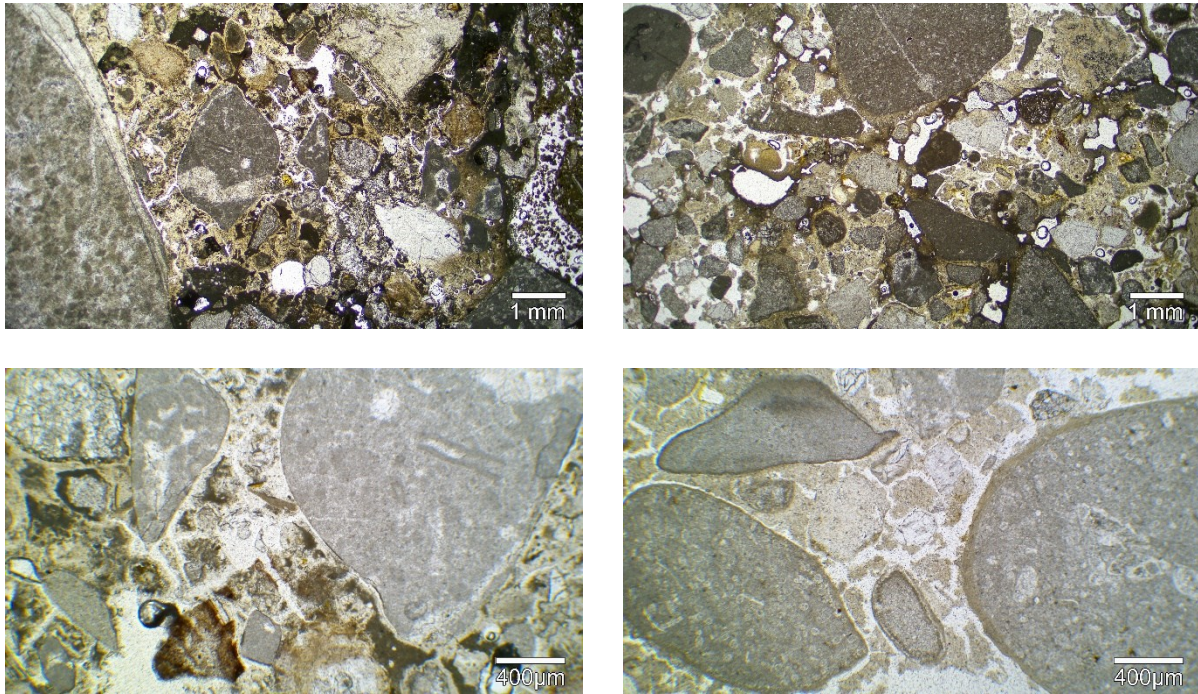


Figure 48 Samples OD-M2 and SGA-M3. showing the representative aggregate fraction composition of group N.1. Transmitted-light plane polars micrographs

Moreover, because of the high variability of the samples' characteristics, mainly due to the fact that they come from different structures and contexts, this main group can be subdivided into three sub-groups, namely 1A, 1B and 1C.

Sub-group 1A, containing samples RED-M5, OD-M3, CSP-M1, SGA-M6, LEO-M1, LEO-M2, COS-M1, AR-M7, AR-M11, and AR-M13, shows the higher concentration of quartz and volcanic rocks, mainly present as a finer fraction. This sub-group is also represented by its micritic, lime binder (fig. 48).

Sub-group 1B, with samples OD-M2, AR-M3, and AR-M5, is characterized by both a higher porosity and the presence of highly angular limestone chips.

Finally, sub-group 1C, consisting of samples SGA-M2, SGA-M3, TR-M1, AR-M1, and AR-M9, shows a higher concentration of medium to fine gravel with coarse sand.

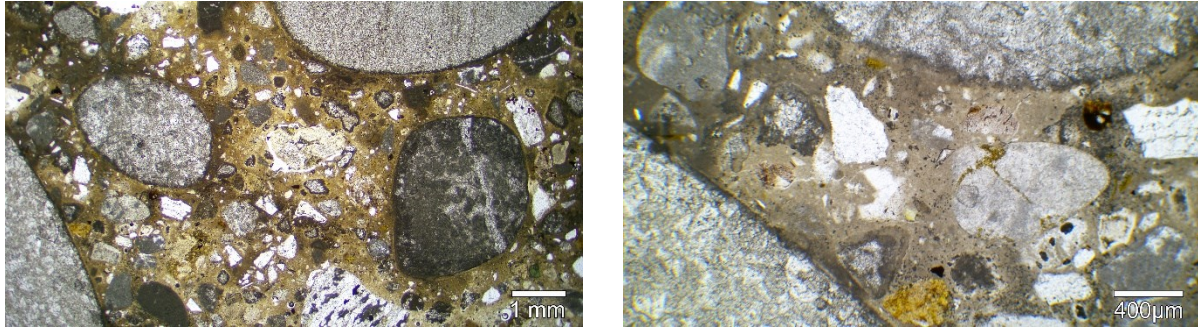


Figure 49 sample LEO-M1 showing the principal characteristics of sub-group 1A. Transmitted-light plane polars micrographs

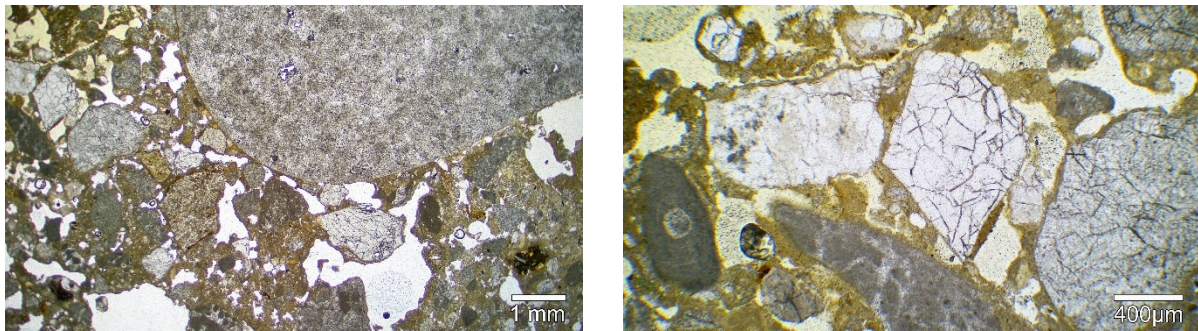


Figure 50 sample AR-M3 showing the principal characteristics of sub-group 1B

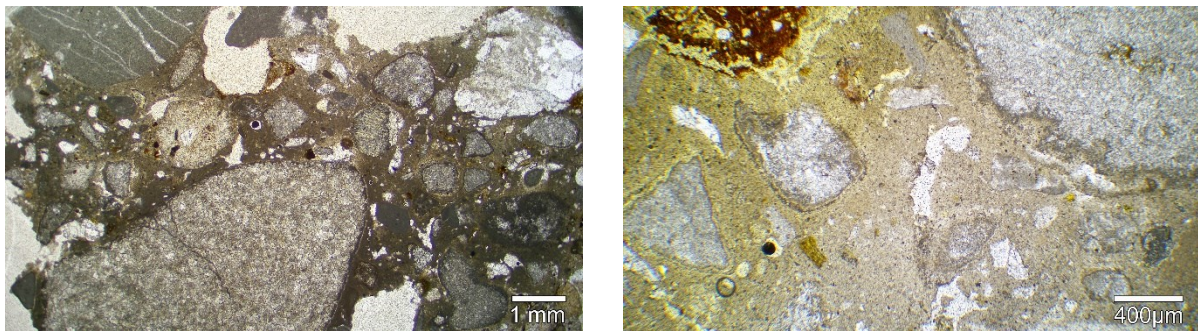


Figure 51 sample AR-M9 showing the principal characteristics of sub-group 1C

Group N. 2:

Samples SGA-M1, LEO-M4, COS-M2, COS-M3, COS-M4, and COS-M7, have been grouped together in group N.2 due to the high amount of mica occurring in all the samples. They present a fairly homogeneous lime-based binder having a micro-crystalline (micritic) structure, with prevalent low-birefringence colors, imputable to the uncomplete carbonation of lime. The presence of a high amount of lime lumps is constant in all of the group's samples. Furthermore, it is possible to identify the presence of channels, vughs, vesicles, and planar voids.

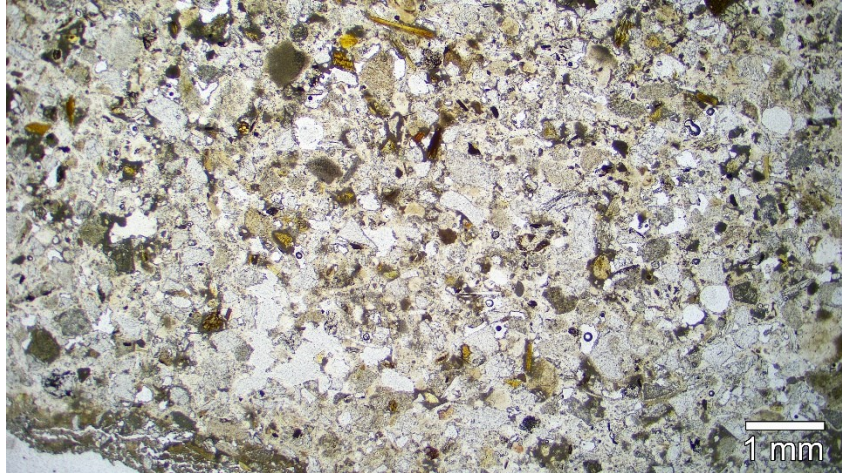


Figure 52 Sample LEO-M4 showing the distinctive properties of group N.2

In the aggregate fraction, as previously mentioned, the high amount of mica is highlighted as a distinctive characteristic of the group. In addition, it is possible as well to observe the presence of carbonate clasts, chlorite, chert, volcanic rocks, quarts, and quartzite. In contrast with the aggregates present in group N.1, in group N. 2 samples', the grain-size distribution varies in the field of fairly well-sorted medium to fine sands (fig. 52). Sample COS-M7 represents an exception for the presence of some the carbonate clasts ranging from coarse gravels to coarse sands. Moreover, the fine aggregate fraction of this sample present a reduced roundness and a relevant angularity, that is indicative of a limited erosion of sedimentary debris by river action, although the presence of rounded aggregates is also attested.

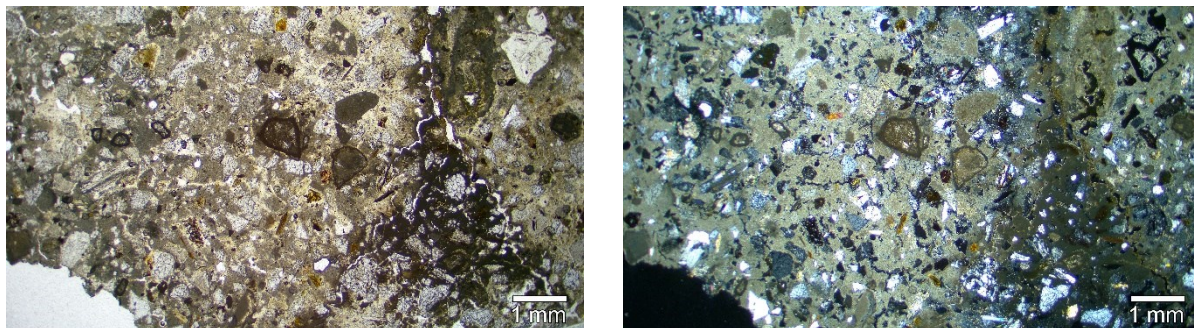


Figure 53 Sample COS-M2 demonstrating the characteristic aggregate fraction

This group, as the previous one, can be divided into three sub-groups, with samples LEO-M4, COS-M4, and COS-M7 in group N.2A, SGA-M1, and COS-M3 in 2B and finally, COS-M2 in the third subgroup, 2C.

Sub-group 2A shows a lower porosity with respect to the samples of sub-group 2B and 2C. It also shows a higher presence of lime lumps and sub-angular quartz and muscovite. Samples in sub-group 2B, in comparison, show a higher porosity and a lower concentration of mica. Finally, sub-group 2C can be defined as a “a fat” mortar, for the abundance of lime binder. The porosity is moderate and the concentration of quartz aggregates is higher in respect to sub-groups 2A and 2B.

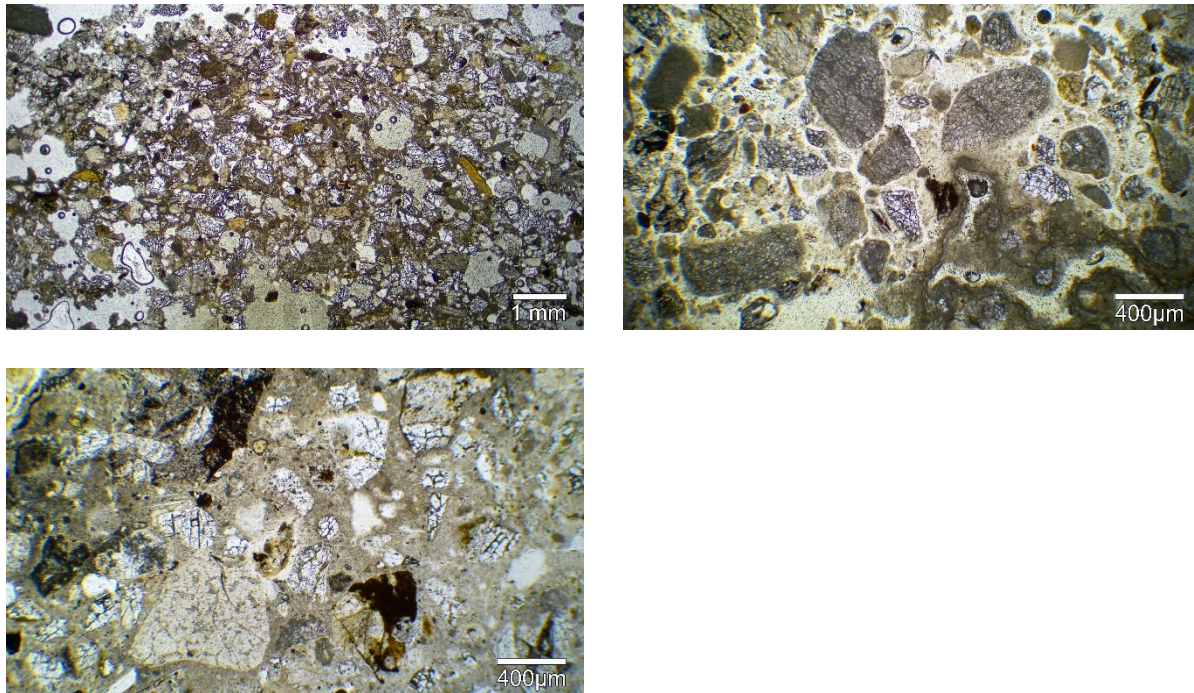


Figure 54 S samples COS-M4, COS-M3 AND COS-M2 showing the properties and characteristics of sub-groups 2A, 2B and 2C respectively.

Group N. 3:

Group N.3 consists of samples RED-M2, RM-M1 et AR-M12, which are distinguished in general terms by being lime and earthen mortars (fig. 54). Therefore, the binder of these mortars can be described as heterogeneous, with areas where the lime component is prevailing, and other ones where earthen clay-based fraction is more abundant. In general terms, these mortars present a low porosity. Regarding the aggregate fraction, samples of group N.3 contain quartz, micas, phyllosilicates, and chlorite with a size or dimension ranging from fine sand to silt. All three samples may be described as fairly well sorted (fig. 55).

Even within this group, two sub-groups can be distinguished: sub-group 3A, containing samples RED-M2 and RM-M1, connoted for the higher occurrence of lime binder, that sometimes is condensed in easily-detectable lime lumps, sub-group 3B, with the sample AR-M12, where, on the other hand, the clay-based fraction absolutely prevails. Moreover, differently from the other samples of group 3, AR-M12 contains also carbonate clasts with a grain size-distribution ranging from medium gravel to medium sand (fig. 56).

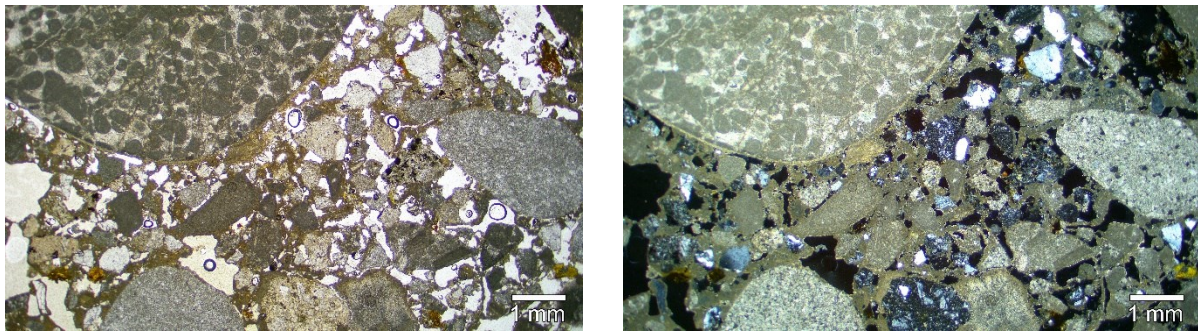


Figure 55 Samples RED-M2

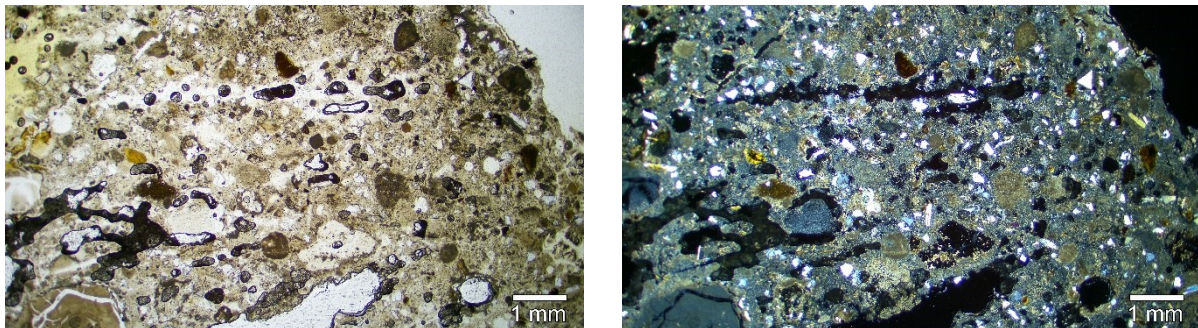


Figure 56 Sample RM-M1

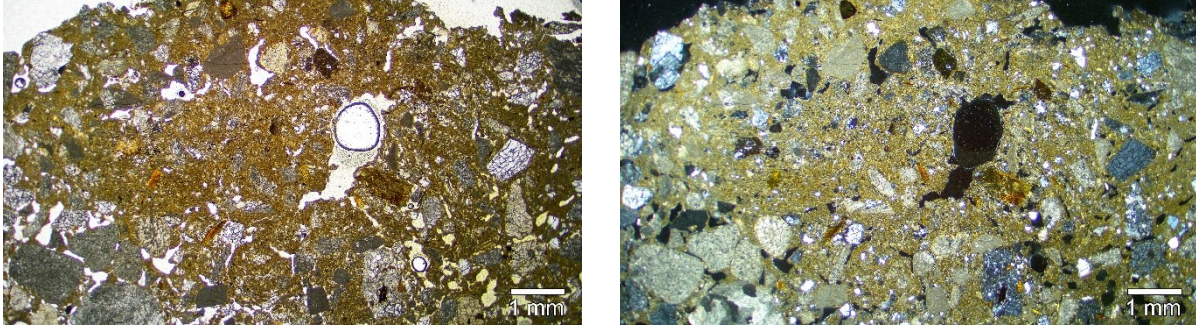


Figure 57 Sample AR-M12

Outliers:

Sample AP-M1:

This sample is distinguished from the others being a *cocciopesto* mortar, rich in terracotta fragments. The sample matrix can be defined as a homogeneous lime-binder with low birefringence colors, generally showing a sparitic structure. It has a high amount of lime lumps, as well as a high abundance of voids. These are mainly planar voids, channels, vughs, and vesicles. As already mentioned, the most important characteristic of this sample is the presence of terracotta elements, in the form of pluri-millimetric fragments and micrometric dust. The subordinate lithic fraction is composed of poorly sorted carbonate clasts, chert, volcanic rocks, clinopyroxene, quartz, and quartzite, granitoids with dimensions ranging from very coarse gravel to fine sand. It should be mentioned that even though terracotta fragments are commonly added to lime-based binders in order to obtain a hydraulic mortar, the lack of reaction rims around the ceramic fragments may indicate low reactivity of this fraction of the aggregate.

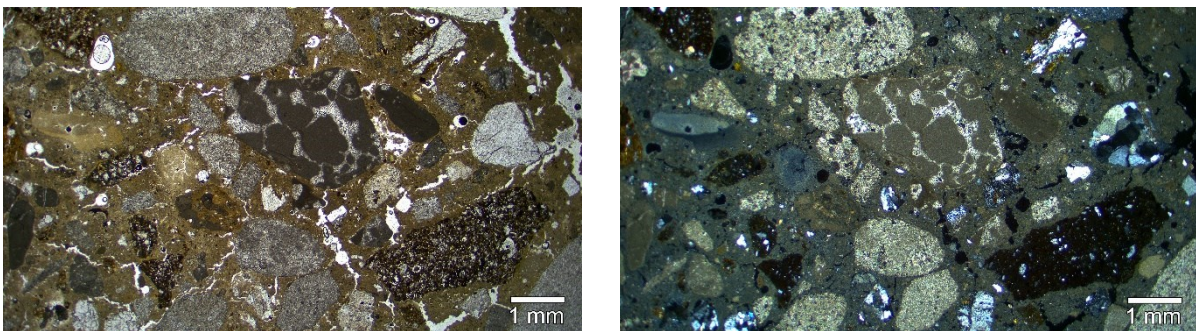


Figure 58 Sample AP-M1

Sample LEO-M5:

This sample is characterized by the low content of binder and it can be defined as a very lean mortar. Therefore, the sample presents a high porosity, with a noticeable abundance of vugh-like pores.

The aggregate fraction consists of carbonate clasts (both limestone and dolostone), chert, volcanic rocks, quartz and quartzite, granitoids with dimensions ranging from very coarse gravel to coarse sand. The aggregate fraction is poorly sorted.

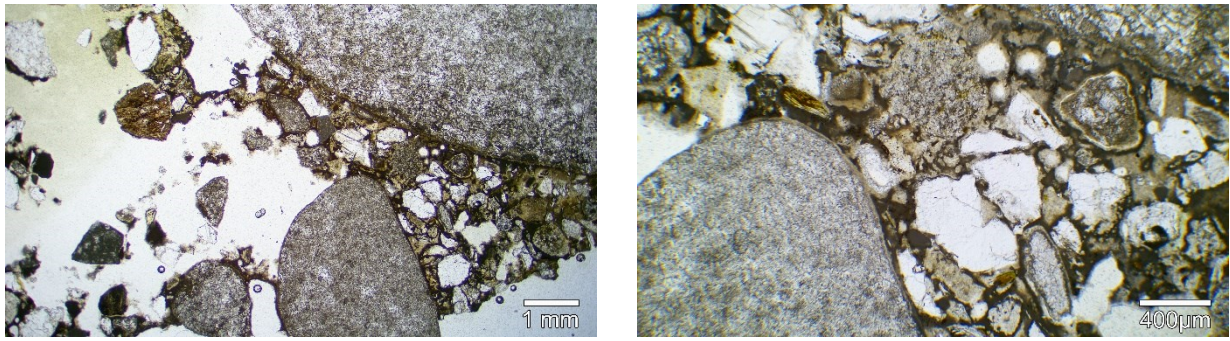


Figure 59 Sample LEO-M5

Sample COS-M5:

This sample has a fat homogeneous lime binder with a sparitic structure. This sample contains a high number of planar voids, as well as a presence of suspected hydromagnesite in the binder, recognizable by rounded aggregates of nanoparticles (Tapete, D. et al. 2014; Lanás, J. et al. 2006; Veiga, R. 2017). Differently from the other samples of the dataset, COS-M5 has probably a dolomitic binder, since no other sample contains hydromagnesite. The presence of some lime lumps can also be observed in the sample, nonetheless, they are present in a low amount.

Furthermore, the aggregate fraction of this sample consists mainly of well sorted carbonate clasts, chlorite, micas, quartz, and quartzite, with dimensions ranging from coarse to fine sand. These aggregates are characteristically spherical and well-rounded.

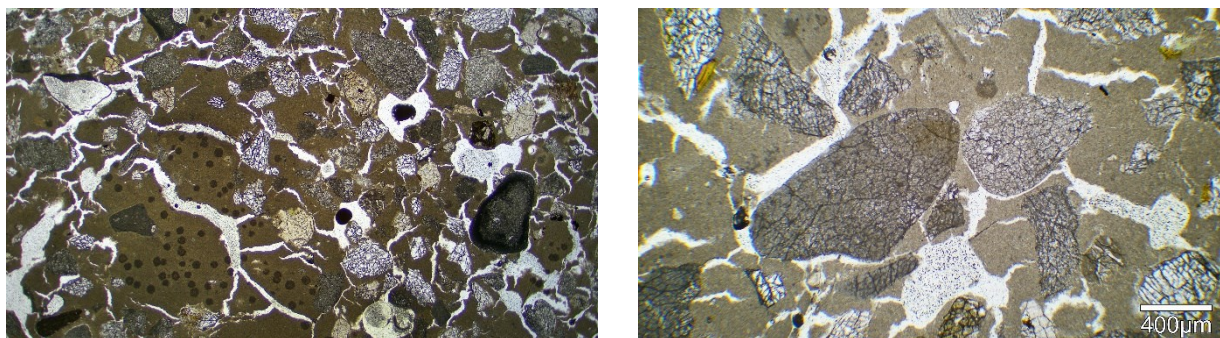


Figure 60 Sample COS-M5

Group	Sub-group	Sample	Description	
1	1A	RED-M5	<ul style="list-style-type: none"> • Gravel-rich mortar • Bimodal distribution (medium to coarse gravel and fine sand) • Heterogeneous-zoned binder • Sparitic to micritic binder structure • Presence of carbonate clasts, volcanic clasts with feldspar microlites in the groundmass, occasional chert, clinopyroxene, quartz, quartzite, and granites/granitoids • Higher concentration of quartz and volcanic clasts 	
		OD-M3		
		CSP-M1		
		SGA-M6		
		LEO-M1		
		LEO-M2		
		COS-M1		
		AR-M7		
		AR-M11		
	AR-M13			
	1B	1B	OD-M2	<ul style="list-style-type: none"> • Gravel-rich mortar • Bimodal distribution (medium to coarse gravel and fine sand) • Heterogeneous-zoned binder • Sparitic to micritic binder structure • Presence of carbonate clasts, volcanic clasts with feldspar microlites in the groundmass, occasional chert, clinopyroxene, quartz, quartzite, and granites/granitoids • Higher porosity • Higher concentration of medium to fine gravel
			AR-M3	
AR-M5				
1C	1C	SGA-M2	<ul style="list-style-type: none"> • Gravel-rich mortar • Bimodal distribution (medium to coarse gravel and fine sand) • Heterogeneous-zoned binder • Sparitic to micritic binder structure • Presence of carbonate clasts, volcanic clasts with feldspar microlites in the groundmass, 	
		SGA-M3		
		TR-M1		

		AR-M1	occasional chert, clinopyroxene, quartz, quartzite, and granites/granitoids
		AR-M9	<ul style="list-style-type: none"> • Higher concentration of medium to fine gravel with coarse sand
2	2A	LEO-M4	<ul style="list-style-type: none"> • High amount of mica • Fairly homogeneous lime-based binder • Micritic binder structure
		COS-M4	<ul style="list-style-type: none"> • High amount of lime lumps • Fairly well-sorted medium to fine sands
		COS-M7	<ul style="list-style-type: none"> • Carbonate clasts, chlorite, chert, volcanic rocks, quarts, and quartzite • Lower porosity
	2B	SGA-M1	<ul style="list-style-type: none"> • High amount of mica • Fairly homogeneous lime-based binder • Micritic binder structure • High amount of lime lumps
		COS-M3	<ul style="list-style-type: none"> • Fairly well-sorted medium to fine sands • Carbonateic clasts, chlorite, chert, volcanic rocks, quarts, and quartzite • Higher porosity • Lower concentration of mica
	2C	COS-M2	<ul style="list-style-type: none"> • High amount of mica • Fairly homogeneous lime-based binder • Micritic binder structure • High amount of lime lumps • Fairly well-sorted medium to fine sands • Carbonate clasts, chlorite, chert, volcanic rocks, quarts, and quartzite • “Fat” mortar • Higher amount of quartz
3	3A	RED-M2	<ul style="list-style-type: none"> • Lime and earthen mortar mixture • Heterogeneous binder • Fairly well sorted
		RM-M1	<ul style="list-style-type: none"> • Fine sand to silt • Contain quartz, micas, phyllosilicates, and chlorite • Higher amount of lime binder

	3B	AR-M12	<ul style="list-style-type: none"> • Lime and earthen mortar mixture • Heterogeneous binder • Fairly well sorted • Fine sand to silt • Contain quartz, micas, phyllosilicates, and chlorite • Higher amount of clay
Outliers		AP-M1	<ul style="list-style-type: none"> • Presence of <i>cocciopesto</i> • Homogeneous lime-binder • Sparitic binder structure • High amount of lime lumps
		LEO-M5	<ul style="list-style-type: none"> • Very lean mortar • High porosity • Presence of carbonate clasts, chert, volcanic rocks, quartz and quartzite, granitoids • Poorly sorted
		COS-M5	<ul style="list-style-type: none"> • Presence of hydromagnesite • "fat" mortar • Homogeneous lime binder • Sparitic binder structure

Table 05. OM results.

7.4. SCANNING ELECTRON MICROSCOPY (S.E.M.)

According to the observations and the results obtained from the previous analyses (Colorimetry, Optical microscopy, and XRPD), a total of 20 samples were selected for analysis under the SEM-EDS. The selection of samples was made in order to include samples extracted from different structural components of the buildings (walls, vaults, foundations...), belonging to all of the different groups obtained from the optical microscopy analysis, and taking into account also the statistical treatment of the XRPD results and the requirement of including at least one sample from the entire population of structures or contexts. The following table reports the selected samples, their belonging groups, the context from which they were sampled, and their selection criteria.

Tags	OM Group	Context	Selection criteria
AR-M7	1	Vaults of the Arena.	Sample selected due to its distinctive grouping in the PCA analysis of the XRPD data.
LEO-M1		Foundation of Porta Leoni.	Sample selected due to its distinctive grouping in the PCA analysis of the XRPD data.
OD-M3		Walls of the Odeum.	Sample selected due to its distinctive grouping in the PCA analysis of the XRPD data.
AR-M11		Sewer system of the Arena.	Sample selected due to a clearly observed lack of dedolomitization, and representativeness of the general group or cluster in the PCA analysis of the XRPD data.
CSP-M1		Foundation of Temple San Castello.	Sample selected due to a clearly observed dedolomitization, and representativeness of the general group or cluster in the PCA analysis of the XRPD data.
OD-M2		Foundation of Odeum.	Sample selected due to its origin or sampled context, and representativeness of the general group or cluster in the PCA analysis of the XRPD data.
AR M13		Arcoballo of Arena.	Sample selected due to origin or sampled context, and representativeness of the general group or cluster in the PCA analysis of the XRPD data.
SGA-M2		Vault of Capitolium and Archeological area Corte.	Sample selected due to a clearly observed dedolomitization, and representativeness of the general group or cluster in the PCA analysis of the XRPD data.
TR-M1		Cena (walls) of the theatre.	Sample selected due to a clearly observed lack of dedolomitization, and representativeness of the general group or cluster in the PCA analysis of the XRPD data.
COS-M4	2	Walls of city walls	Sample selected due to its distinctive grouping in the PCA analysis of the XRPD data.
COS-M7		Walls of city walls	Sample selected due to its distinctive grouping in the PCA analysis of the XRPD data.
LEO-M4		Walls of Porta Leoni	Sample selected due to its distinctive grouping in the PCA analysis of the XRPD data.
COS-M3		Vault of city walls	Sample selected due to its distinctive grouping in the PCA analysis of the XRPD data.
SGA-M1		Walls of Capitolium and Archeological area Corte.	Sample selected due to its distinctive grouping in the PCA analysis of the XRPD data.
COS-M2		Walls of city walls	Sample selected due to its distinctive grouping in the PCA analysis of the XRPD data and characteristics in optical microscopy.
RED-M2	3	Foundation of Torre della Porta	Sample selected due to origin or sampled context, and distinctive characteristics observed under the optical microscope.

AR-M12		Foundation of city walls around the Arena.	Sample selected due to origin or sampled context, its distinctive grouping in the PCA analysis of the XRPD data and characteristics in optical microscopy.
AP-M1	Outlier	Walls of the Curia	Sample selected due to origin or sampled context, its distinctive grouping in the PCA analysis of the XRPD data, and characteristics in optical microscopy.
COS-M5	Outlier	Walls of city walls	Sample selected due to its distinctive grouping in the PCA analysis of the XRPD data and characteristics in optical microscopy.
LEO-M5	Outlier	Walls of Porta Leoni	Sample selected due to its distinctive grouping in the PCA analysis of the XRPD data and characteristics in optical microscopy.

Table 06. Selection of samples for SEM-EDS analysis.

The same methodological procedure of grouping samples according to the individual observations of the thin sections applied in optical microscopy was adopted for the observation and description of SEM-EDS results. In this way, samples demonstrating similar composition were grouped together in three distinctive groups, with additional outliers. Therefore, the subsequent description of the observed characteristics of the groups will provide a general overview of the individual samples contained in it.

Group I:

The first group, containing the largest population, is composed of samples AR-M11, AR-M13, LEO-M1, OD-M2, OD-M3, SGA-M2, TR-M1, COS-M2, COS-M3, LEO-M4, and LEO-M5. Most of the samples present in this SEM group correspond to the optical microscopy groups 1, 2, and one sample outlier (LEO-M5). This group is mainly characterized by the clear presence of reactive rims around aggregates, both from the dissolution of chert, quartz, quartzite, and volcanic clasts and the correspondent dedolomitization of dolomitic limestone. The group is also characterized by the variable composition of the matrix. Although all samples present in this group are composed of a calcium-based binder, due to the previously mentioned interaction with the aggregate fraction, the samples of group I contain a variable amount of silicon, aluminum, and magnesium. In certain areas the concentration of the previously mentioned elements even surpasses the concentration of calcium, indicating the presence of M-S-H phases, and therefore a hydraulic binder. It should be mentioned as well that some of the samples exhibit the presence of secondary calcite deposits, as is the case of LEO-M4 and COS-M3.

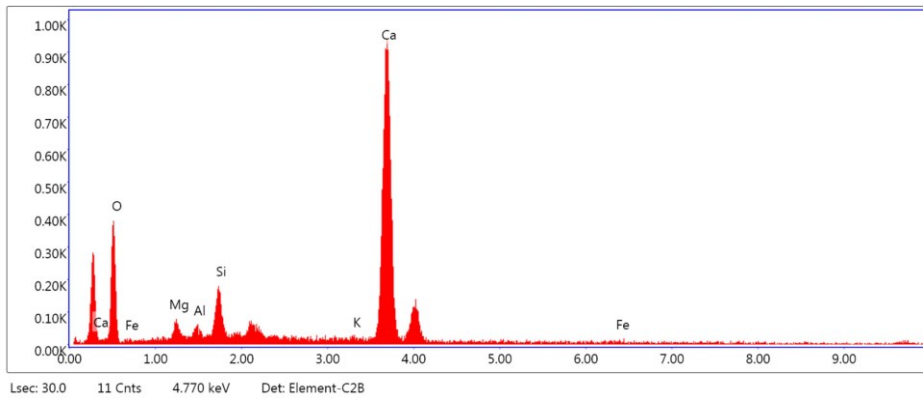
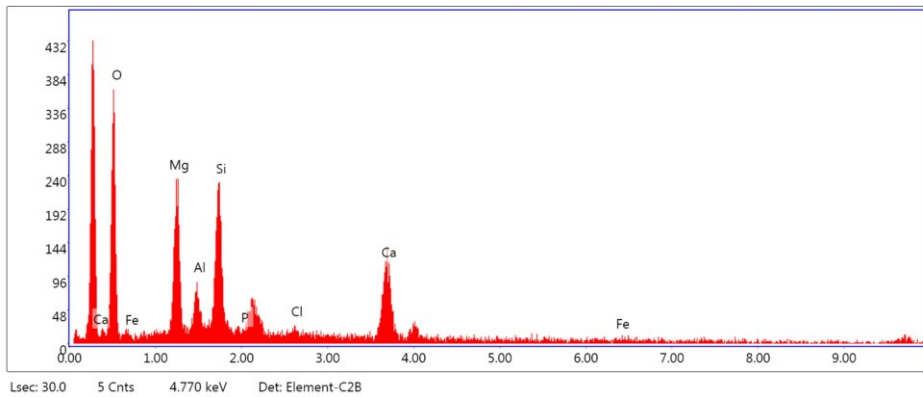
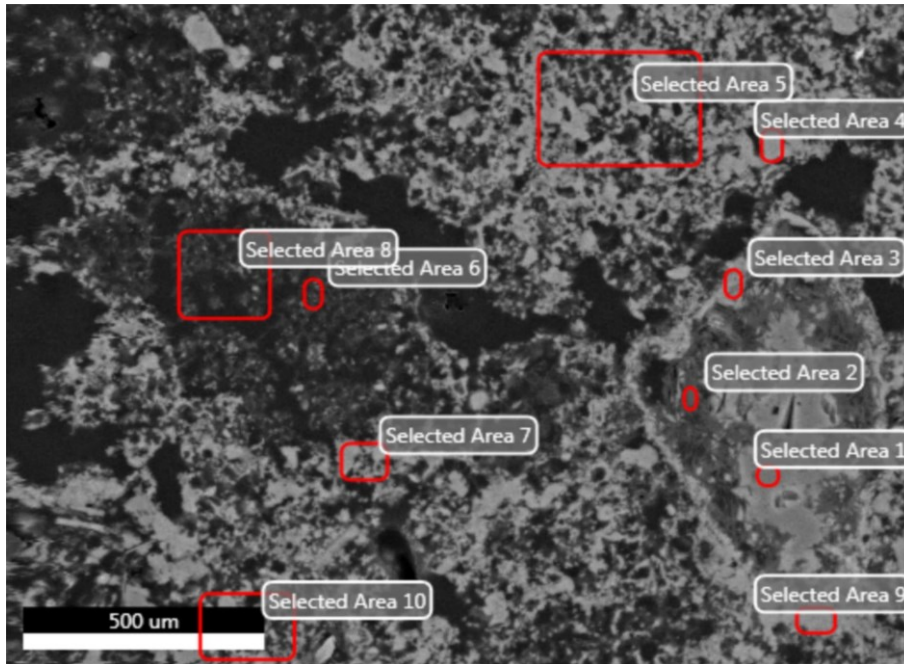


Figure 61. SEM-EDS analysis of sample AR-M13 demonstrating the variation in the composition of the binder in analyzed areas 6 and 7

Group II

This group is composed of samples COS-M4 and SGA-M1, which belong to optical microscopy group N.2. As can be inferred from the previously made observation on the optical microscope, these samples do not display signs of reaction between the aggregate and the binder fraction. The binder, as in the case of group I, is calcium-based. However, due to the lack of reactivity of the components in the mortar, the binder is not altered, and therefore the concentration of other elements such as silicon or magnesium remains at lower values.

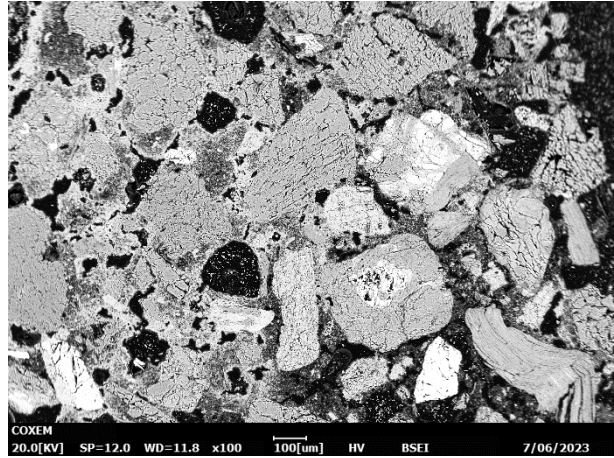


Figure 62 Sample COS-M4 demonstrating the characteristic properties of SEM group II

Group III

The samples corresponding to this SEM group have a clear correlation with the distinction made in the optical microscopy grouping, both samples belonging to OM group N.3. This group therefore comprehends samples AR-M12 and RED-M2. As previously mentioned, this group exhibits a mixture of both lime and earthen binder. In this sense, it does not present any pozzolanic reaction or hydraulic properties of any kind. It should be mentioned as well the lack of reactivity between the binder and the aggregate fraction.

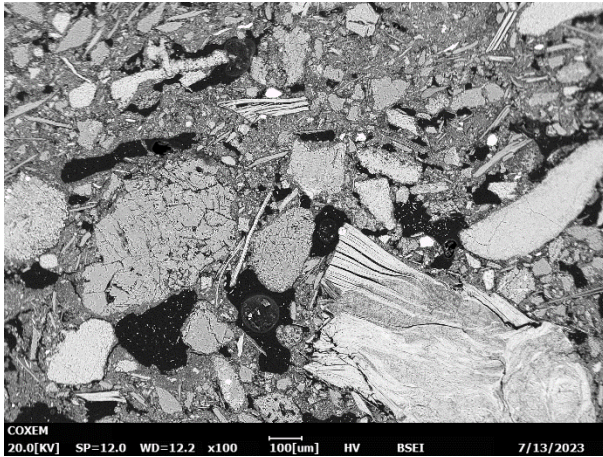


Figure 63 Sample AR-M12 demonstrating the characteristic properties of SEM group III

Outliers:

AR-M7

This sample could be suspected from the results of the XRPD as a highly-hydraulic mortar. Consequently, the composition of the matrix shows a significant variability in the concentrations of calcium, silicon, aluminum, and magnesium, indicating the presence of M-S-H phases. As it has been indicated in the description of SEM group I, this variability in the matrix composition is a consequence of the interaction between the aggregate and the binder fraction, indicated as well by the presence of reaction rims. However, it should be mentioned that due to the presence and elemental analysis of lime lumps, it is possible to identify the original binder mixture, which consisted almost entirely of a calcium-based lime. Moreover, this sample is considered as an outlier not only because of its high levels of reactivity, but also due to the presence of phosphorous in the matrix. This presence has been observed at a higher concentration with respect to the other samples, which could be attributed to the occurrence of ash particles inside the mortar mixture. Finally, the presence of secondary calcite deposits was identified in the pores.

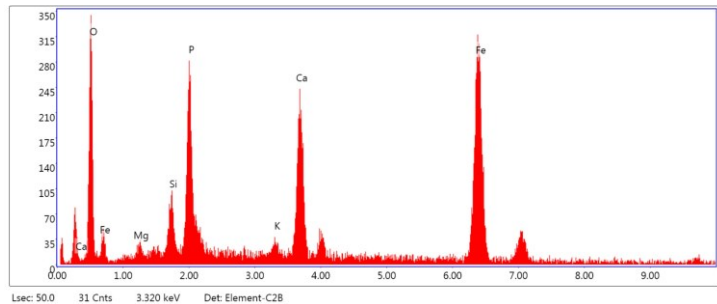
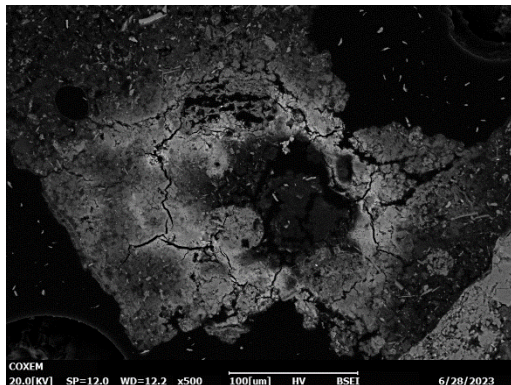


Figure 64 Sample AR-M7 SEM-EDS analysis demonstrating a high concentration of phosphorous in a ash particle.

CSP-M1

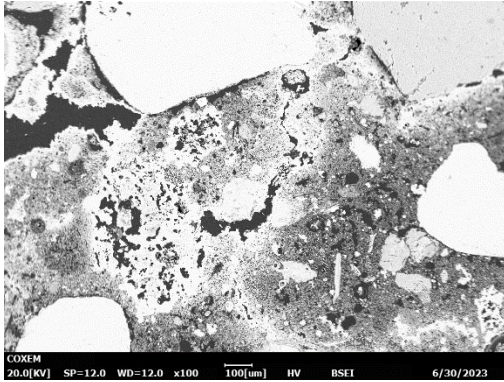


Figure 65 Sample CSP-M1 SEM analysis

Sample CSP-M1 shows pretty similar characteristics as the group I, with a variable elemental concentration in mainly calcitic binder and the presence of reaction rims around aggregates. Nevertheless, the presence of MSH phases is considered common, as the magnesium concentration in the matrix is relatively high.

COS-M7

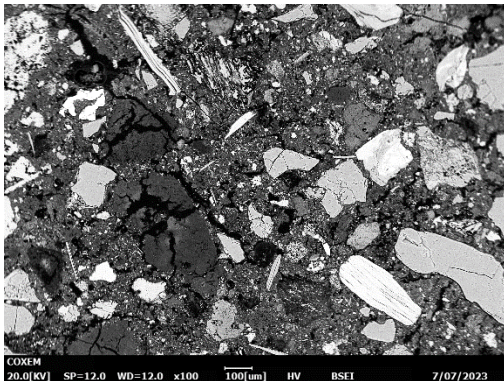


Figure 66 Sample COS-M7 SEM analysis

This sample is composed of a heterogeneous calcitic binder with the presence of M-S-H phases. However, as for the case of sample AR-M7, the presence of lime lumps demonstrates that the initial composition was calcium-based. Furthermore, the analyzed section of the mortar does not show any clear or distinctive reaction of the aggregates.

AP-M1

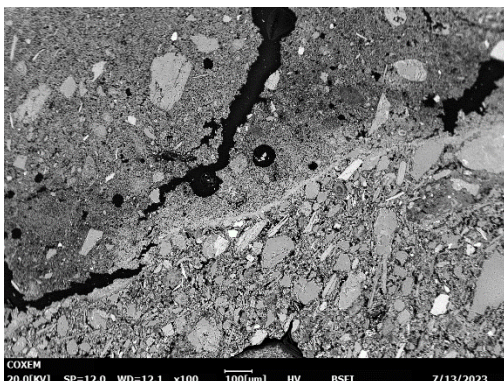


Figure 67 Sample AP-M1 SEM analysis

The sample is characterized by limited reaction rims around the ceramic aggregate fraction. However, it is not reflected in the composition of the binder, which is mainly calcium-based.

COS-M5

Finally, sample COS-M5 demonstrates a clear presence of thin reaction rims caused by the interaction of the binder and the aggregate fractions of the mortar. However, the most representative characteristic of the sample relies on the high concentration of magnesium, which shows the dolomitic nature of the binder.

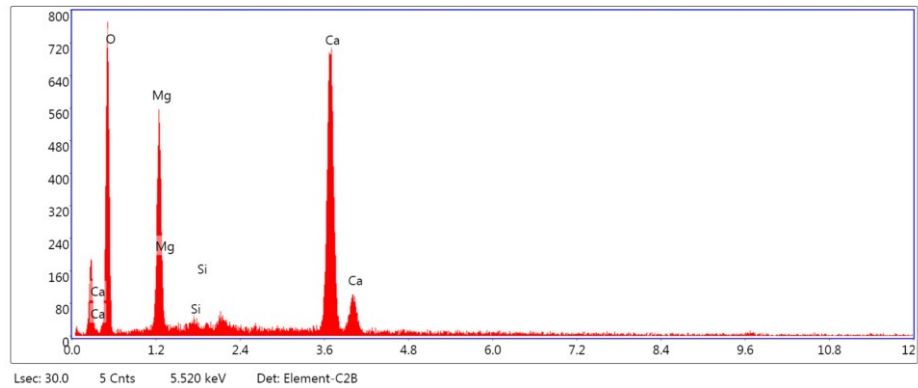
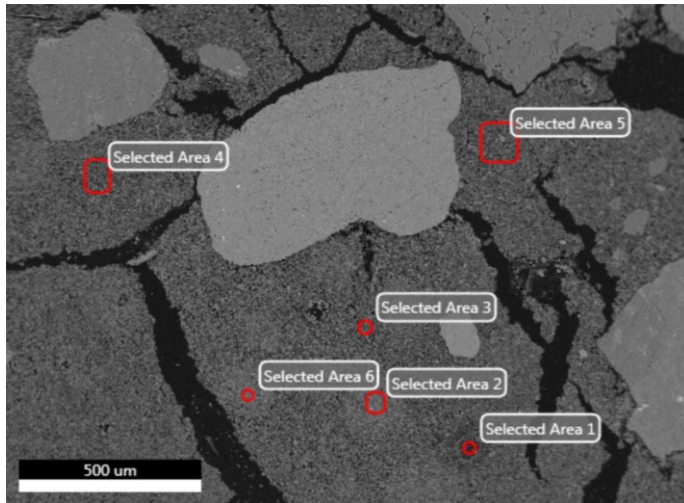


Figure 68 Sample COS-M5 SEM-EDS analysis demonstrating the presence of a dolomitic binder

7.5. BINDER ANALYSIS

7.5.1. X-RAY DIFFRACTION

The previously performed analysis led to the selection of 10 mortar samples to proceed with the separation of the binder and the aggregate fraction and the further characterization of the

binder composition. This procedure is done in order to better comprehend the production processes, material selection, and pozzolanic or parapozzolanic processes taking place inside the binders' matrices. Moreover, the sample selection, following the criteria previously established, aims at considering the individual samples as representative the general properties and characteristics of a mortar group. In this sense, the following table provides the list of selected samples, the groups to which they correspond, their context, and the selection criteria.

Tags	OM Group	Context	Selection criteria
AR-M7	1	Vaults of the Arena.	VERY reactive. High presence of volcanic aggregates, possible presence of ash as an additive
SGA-M2		Vault of Capitolium and Archeological area Corte.	High amount of volcanic clasts from a different building
TR-M1		Cena (walls) of the theatre.	Few amount of volcanic clasts
COS-M7	2	City walls	Only one of the group without volcanic aggregates (at least observed in the sample)
LEO-M4		Walls of Porta Leoni	High amount of volcanic clasts and observed presence of feldspar
RED-M2	3	Foundation of Torre della Porta	Only one from the group observed on the SEM
AR-M12	3B	Foundation of city walls around the Arena.	Only one from the group observed on the SEM
AP-M1	Outlier	Walls of the Curia	Only one with <i>cocciopesto</i>
COS-M5	Outlier	Walls of city walls	Very different. Possible presence of hydromagnesite.
LEO-M5	Outlier	Walls of Porta Leoni	Very lean mortar

Table 07. Gravimetric separation sample selection.

The patterns resulting from the XRD analysis of the selected 10 samples for binder analysis were treated through the use of different softwares such as Highscore Plus, Diffrac.Topas and BGMN-PROFEX in order to retrieve the quantitative data here presented. The following table reports all the identified mineral phases, including the paracrystalline phyllosilicate gel and amorphous phases.

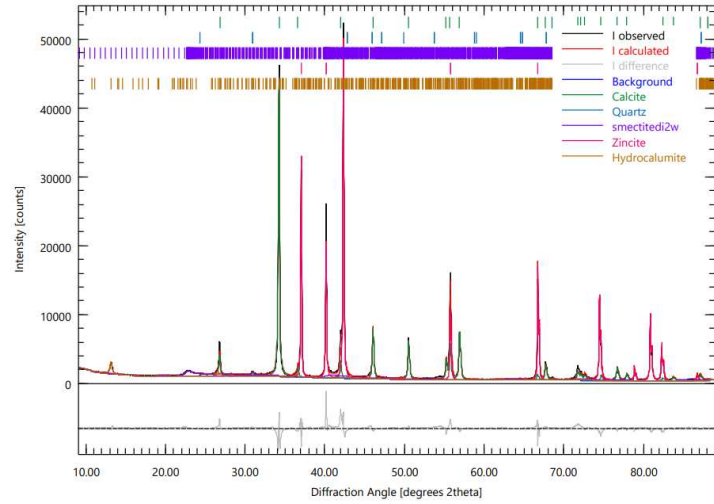
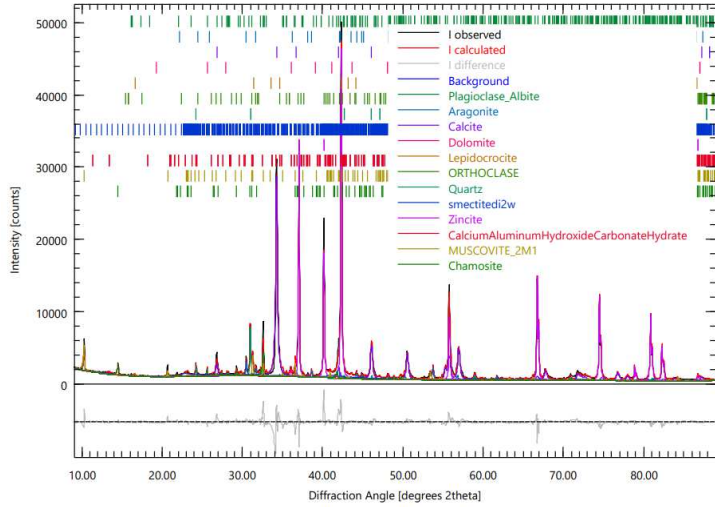


Figure 69. Diffractograms of Samples LEO-M5 and AR-M7 demonstrating the clear difference between the identified mineral phases between the two binders

	Calcite	Aragonite	Dolomite	Ca-AFm phase	Quartz	Plagioclase	K-feldspar	Hematite	Lepidocrocite	Ilmenite	Illite/Micas	Chlorite	Ps gel	Amorphous
AP M1 SG	59.58	0.00	1.45	0.00	1.57	0.00	0.00	0.10	0.00	0.24	2.68	1.25	4.13	29.00
AR M7 SG	49.13	0.00	0.00	3.60	0.67	0.00	0.00	0.00	0.00	0.00	0.00	0.00	21.80	24.80
AR M12 SG	14.92	0.00	5.30	0.00	5.08	1.99	2.83	0.00	0.00	0.00	18.85	8.35	17.18	25.50
COS M5 SG	67.28	0.00	0.46	0.00	1.30	0.00	0.00	0.00	0.00	0.00	5.75	2.82	6.77	15.62
COS M7 SG	71.41	0.00	0.00	3.69	1.01	0.00	0.00	0.00	0.00	0.00	2.27	0.00	5.32	16.30
LEO M4 SG	33.62	0.00	0.00	0.00	0.74	0.00	0.00	0.00	0.00	0.00	1.74	0.00	11.90	52.00
LEO M5 SG	43.50	5.47	1.80	1.27	4.53	3.36	1.38	0.00	0.47	0.00	7.64	2.58	17.70	10.30
RED M2 SG	48.07	0.00	0.00	3.48	2.34	0.96	0.00	0.00	0.00	0.00	7.68	2.01	2.06	33.40
SGA M2 SG	64.56	0.00	0.69	0.97	1.13	0.00	0.00	0.00	0.00	0.00	2.61	2.08	7.34	20.62
TR M1 SG	55.33	0.00	0.00	3.51	1.36	0.00	0.00	0.00	0.00	0.00	0.00	0.00	22.00	17.80

Table 08. XRPD gravimetric separation results.

7.5.2. SCANNING ELECTRON MICROSCOPY (S.E.M.)

The elemental analysis of the binder fraction performed on the SEM-EDS, as previously stated, provided both a quantitative analysis of elements of three randomly selected point analyses per sample, and the elemental mapping. Additionally, the element quantification of the oxide values was further treated to re-scale the values after the exclusion of zinc oxide (due to its nature as an added component) and carbon dioxide (due to poor reliability) from the obtained results. The acquisition of the mean value from the three points for each individual sample then took place to obtain a general idea of the binders' composition. The following table depicts the values obtained after the data were properly treated.

Sample	Na ₂ O	MgO	Al ₂ O ₃	SiO ₂	P ₂ O ₅	SO ₃	K ₂ O	CaO	Sc ₂ O ₃	TiO ₂	MnO	Fe ₂ O ₃
AP-M1	7.87	2.13	6.50	16.54	9.52	0.00	1.03	53.02	0.11	0,23	0,00	3,05
AR-M7	8.68	10.88	4.82	26.76	2.79	0.61	0.58	43.55	0.00	0,00	0,00	1,33
AR-M12	4.92	5.19	19.54	38.47	1.91	0.00	4.00	15.67	0.00	0,75	0,26	9,29
COS-M3	4.33	2.25	8.80	19.84	2.36	0.16	1.48	56.19	0.00	0,16	0,00	4,43
COS-M7	5.39	5.75	6.41	18.61	2.12	0.00	0.91	57.91	0.25	0,12	0,00	2,53
LEO-M4	9.96	11.26	6.70	30.57	6.65	1.14	3.00	28.82	0.00	0,00	0,00	1,89
LEO-M5	4.80	12.87	8.36	30.65	2.04	0.00	1.12	37.14	0.00	0,11	0,00	2,91
RED-M2	4.75	3.72	9.28	40.36	2.00	0.46	1.84	35.27	0.00	0,07	0,00	2,25
SGA-M2	5.92	7.39	5.08	21.60	3.48	0.00	0.76	54.00	0.00	0,00	0,00	1,77
TR-M1	5.68	12.84	5.47	25.07	1.17	0.58	0.52	47.22	0.00	0,00	0,00	1,44

Table 09. SEM-EDS gravimetric separation results.

Moreover, the elemental mapping provided key information on the spatial distribution of the elements present in the binders. It should be highlighted that, due to the extraction process of the binder itself, this procedure was performed not to understand the unaltered spatial distribution of elements as it can be observed in a thin section, in which no modifications of the sample have been done, but to obtain a better comprehension of the correlation between certain elements found in the matrix.

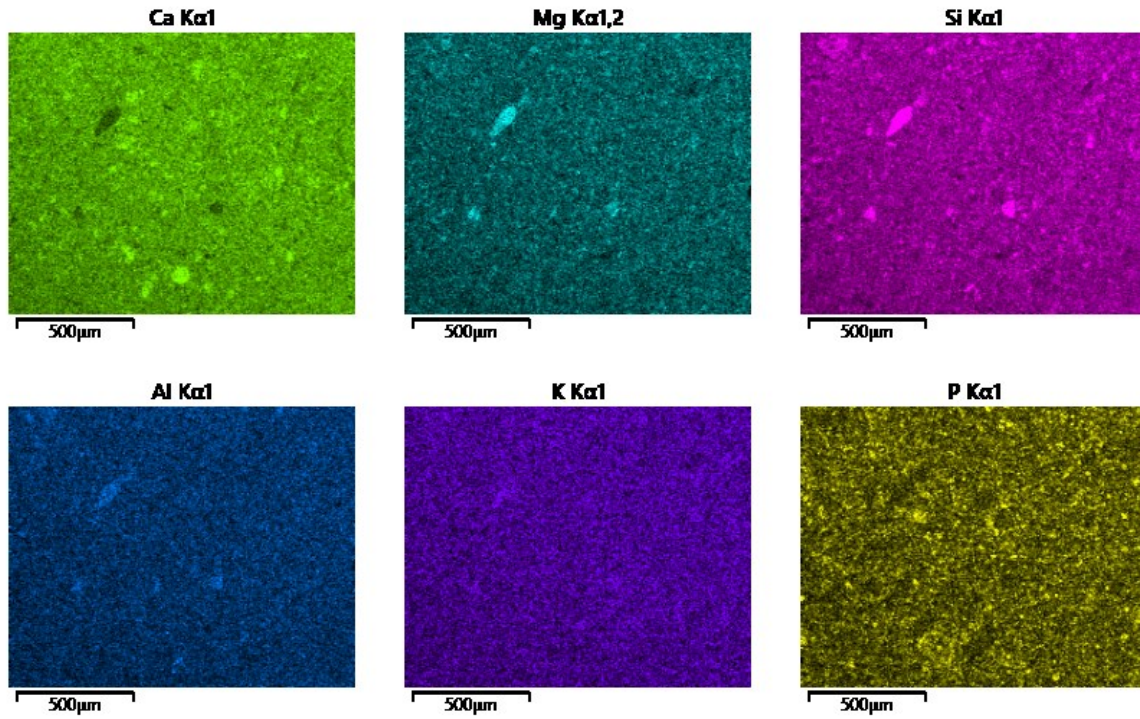


Figure 70. Elemental mapping of sample LEO-M4 depicting spatial distribution of Ca, Mg, Si, Al, P and K.

8. Chapter VIII - Discussion and analysis of the results

There is little information that can be sourced just from the simple observation of the numerical values obtained from the colorimetry analysis. It is, therefore, necessary to perform statistical analyses to obtain a better reading and understanding of the results. For this reason, the study implemented the utilization of a principal component analysis (PCA) as a tool to achieve this objective. A PCA, in statistics, is “a matrix of correlations between all pairs of variables in the original dataset” (Drennan, R. D. 2010). In this sense, and as commented by the aforementioned author, the correlation between the variables will demonstrate a similar behavior between the samples. In this way, the variables showing a similar behavior can be replaced with a single variable, without the significant loss of key information or a loss of the characteristic pattern of the dataset. It is precisely for this reason that this multivariate analysis was selected to proceed with the statistical treatment of the data. In other words, the use of PCA is justified in this dissertation due to its possibility to “reduce the number of variables as much as possible without losing important aspects of the patterning in the original dataset” (Drennan, R. D. 2010).

In this order of ideas, the information obtained by the application of colorimetry was statistically treated through a PCA analysis in order to comprehend the general behavior and variability of the obtained results. This test demonstrated the presence of a major group of samples exhibiting similar color values, with 3 possible sub-groups, and the presence of outliers. The outliers, identified as AP-M1, AR-M8, AR-M12, AR-M13, COS-M4, COS-M5, LEO-M2, and SGA-M8, represent in this way a significant color variation from the general trend. This behavior or color exhibit, as previously mentioned, is directly related to the composition of the mortar. In other words, a variation in the recipe used for the production of the mortar will result in different physical behavior. However, this test by itself does not provide enough information to formulate noteworthy conclusions. It is applied in this case as a starting point, where initial notions, that need to be verified and corroborated with other analytical results, can be noticed.

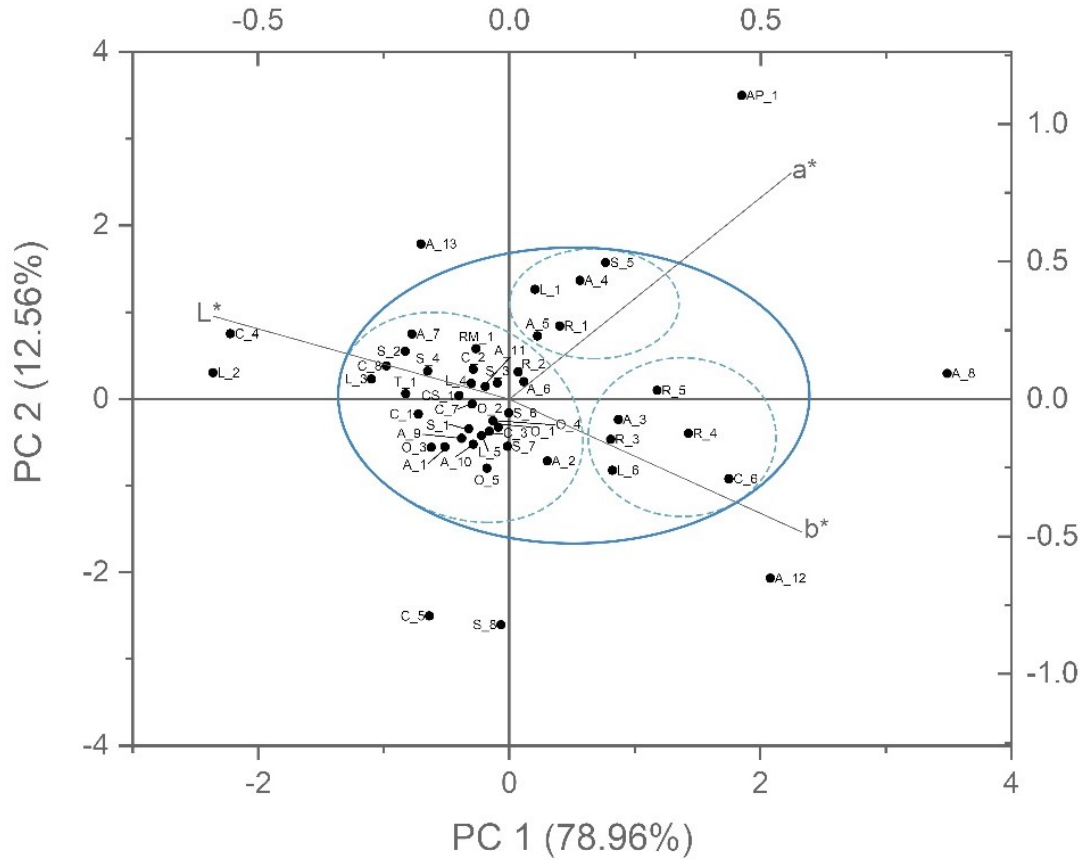


Figure 71 PCA analysis on colorimetry results depicting main group, sub-groups, and outliers.

Complementary to this, according to the quantification of mineral phases present in the samples obtained from the XRPD analysis, it is possible to observe the presence of clear differences between the composition of the samples. This variability can be noticed in the first instance by the presence of certain mineral phases such as dolomite (whose values range from 0 up to 46.89 wt%), amorphous phases (ranging from 4.75 to 49.22 wt%), and calcite (from 14.44 up to 65.43 wt%). It should be noted in this sense that the variability of amorphous phases is due to several different reasons, including the presence of clays and hydraulic phases in mortar samples that due to the small dimensions of their crystals they are not possible to identify with this analytical technique. On the other hand, the variation of calcite, with its noticeable range of 50.99 wt% represents not only the composition of the matrix itself, but also of the calcite-bearing aggregates within mortars. In this way, the identified calcite in the samples, although always present due to the nature of the lime mortars, depicts a great variability of the composition of both matrix and aggregate fractions. Moreover, it should be mentioned that the presence of gypsum and talc in the sample will not be taken into account for the identification of the mineralogical

composition of the samples, since these two phases are normally present in lime mortars as a result of secondary processes, not as part of the initial mortar production.

The following scatterplot (biplot) exhibits the PCA performed on the quantitative XRPD data of the entire population of samples. It should be highlighted that once again that gypsum was not taken into consideration due to its secondary nature. However, in this case, talc aliquots were included since they could be related to the presence of clays or M-S-H phases in the mortars matrix.

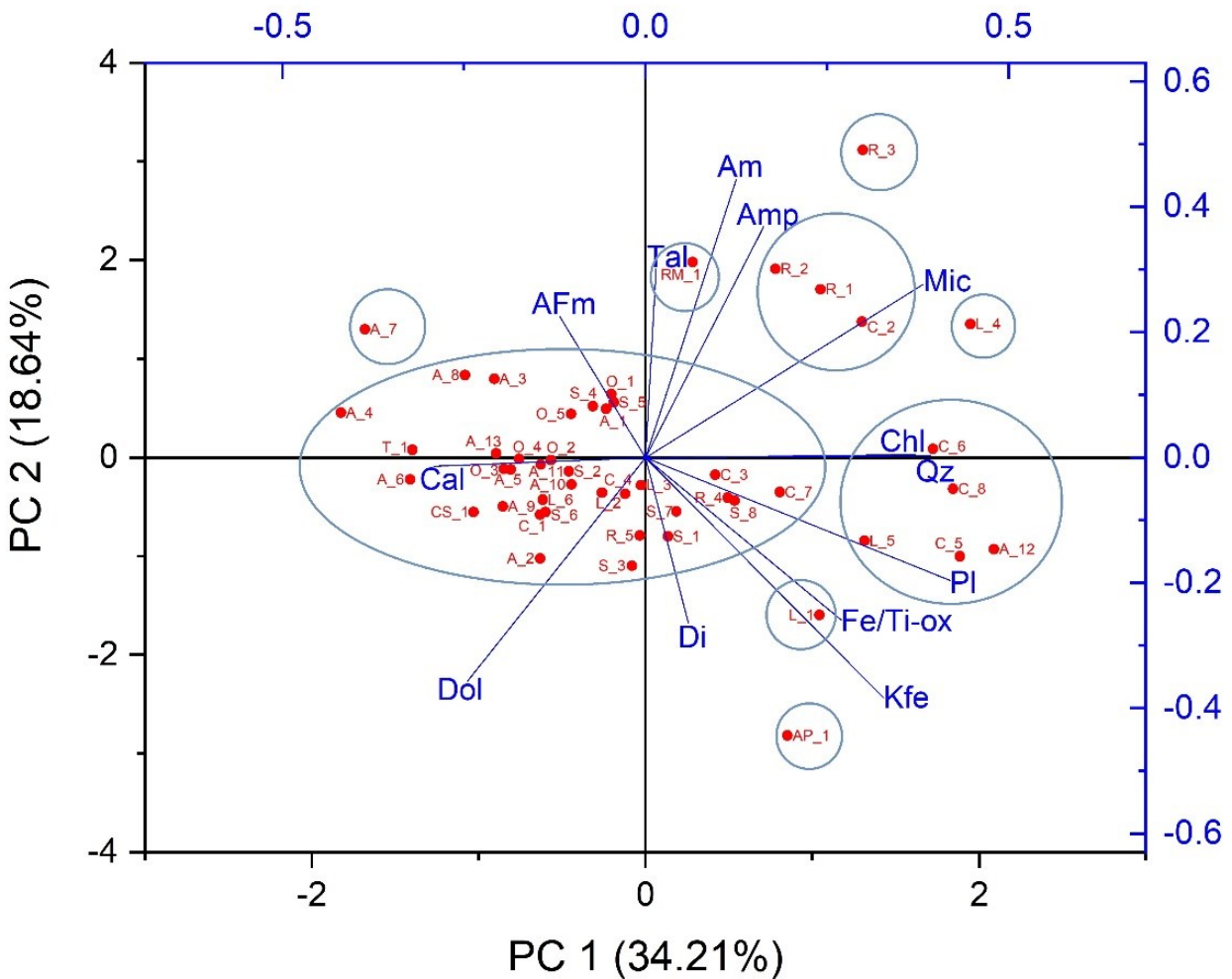


Figure 72 PCA biplot of XRPD results with identified clusters

From the statistical analysis, it is possible to perceive the presence of three main clusters and 5 outliers. The group or cluster with the highest amount of samples depicts, as a general tendency, a higher presence of calcite, dolomite, and AFm phases. On the other hand, cluster number two, containing samples COS-M5, COS-M6, COS-M8, LEO-M5, and AR-12, exhibits a tendency towards a higher presence of chlorite, quartz, and plagioclase, which could be identified as a general tendency towards a higher presence of aggregates and sands from volcanic origin (which would be in accordance to the general composition of sands and aggregates found in the Adige, as described in chapter 4). Furthermore, the third and smallest group, containing samples RED-M2, RED-M1, and COS-M2, shows a higher presence of micas and amorphous mineral phases. This could be an indicator of a higher presence of sands and clays; however, it needs to be confirmed with further analysis. As outliers, it is possible to identify samples AR-M7, AP-M1, LEO-M1, LEO-M4, RED-M3, and RM-M1. Each of these shows its individual characteristics and compositional behavior as can be observed in the scatterplot (biplot).

Moreover, the PCA biplot color tags was altered in order to observe and identify (if any) the possible correlation between the general composition of the mortar samples and their chronology, the individual part of the structure they were collected from (walls, foundations ...), and the construction technique that was applied to the section of the building from which they were sampled. The following table shows in this way all the aforementioned categories in which the population of samples was classified. This is done to recognize if the mortar recipes varied according to the period or the final purpose of the mortar in question (Table 01).

The following treated PCA biplots show analyzed samples and assigned categories for each of the samples chronology, construction technique and structural component.

experimentation during the first construction period. Then, in the course of the second period the production of mortars was mastered, exhibiting a higher hydraulicity and, in this way, a higher resistance and durability. Finally, during the third period, most of the knowledge and techniques were lost, resulting in poorer mortars.

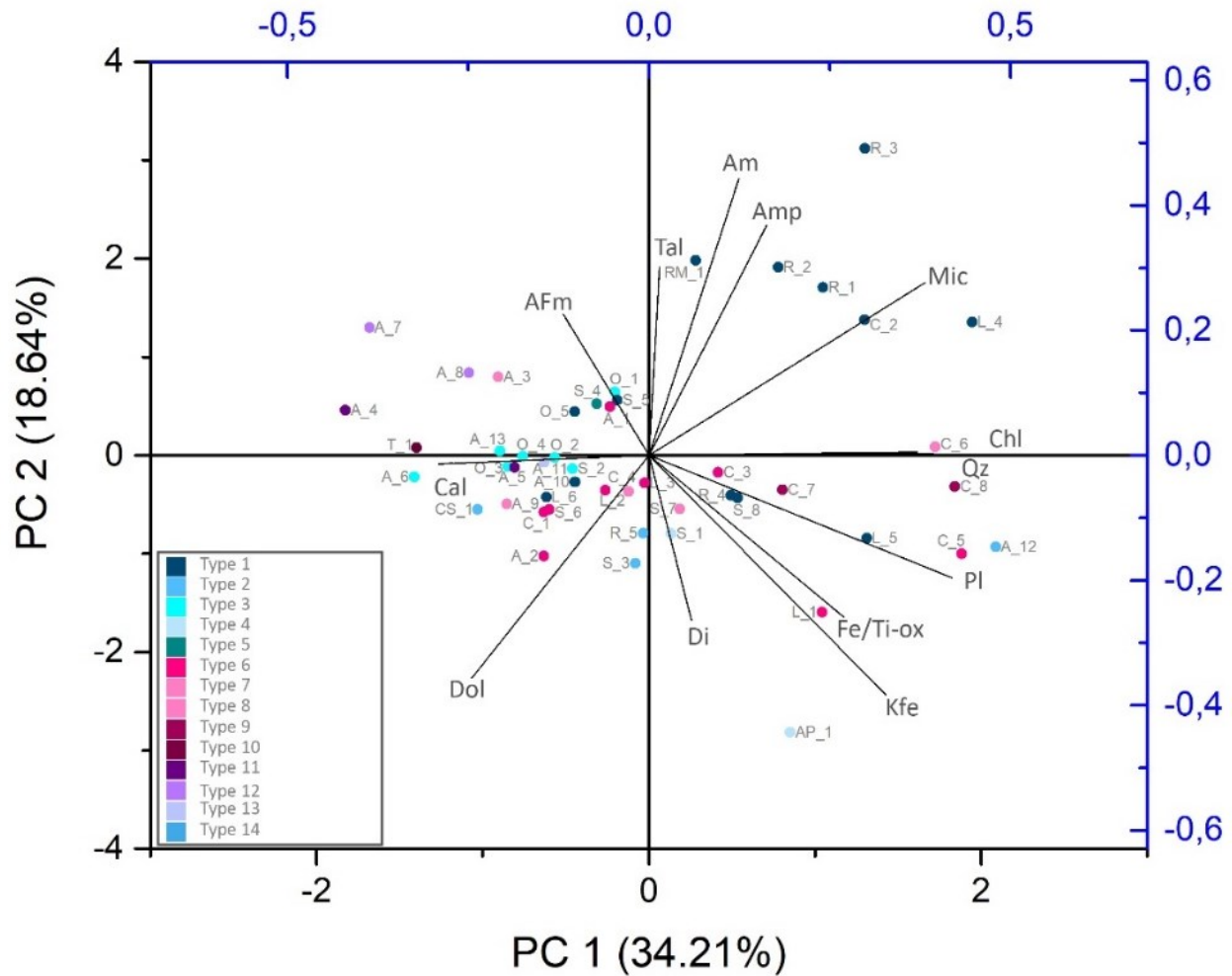


Figure 74 PCA analysis of XRPD of mortar samples exhibiting the structural section from which the sample was extracted

Moreover, when establishing a correlation between the applied construction technique applied and mortar's composition, it is possible to identify that construction type 1 – bricks and bedding mortars – tends to have a higher concentration of micas and amorphous phases. On the other hand, types 2, 11, and 12 (concrete, regular tuff blocks + mortar, and concrete + gravel, respectively) contain a higher amount of AFm phases and calcite. Additionally, samples corresponding to construction techniques type 6, 7, and 8 (pebbles + mortar, irregular tuff blocks + concrete core + layer of bricks and re-used stone blocks + bedding mortar + possible concrete

core), although variable, have a higher content of dolomite, diopside, and K-feldspar and plagioclase. These tendencies are observed regardless of the chronology of the sampled site. It is therefore possible to suggest that the preparation or manufacturing of the employed mortar is also related, in the majority of the cases, to the construction type.

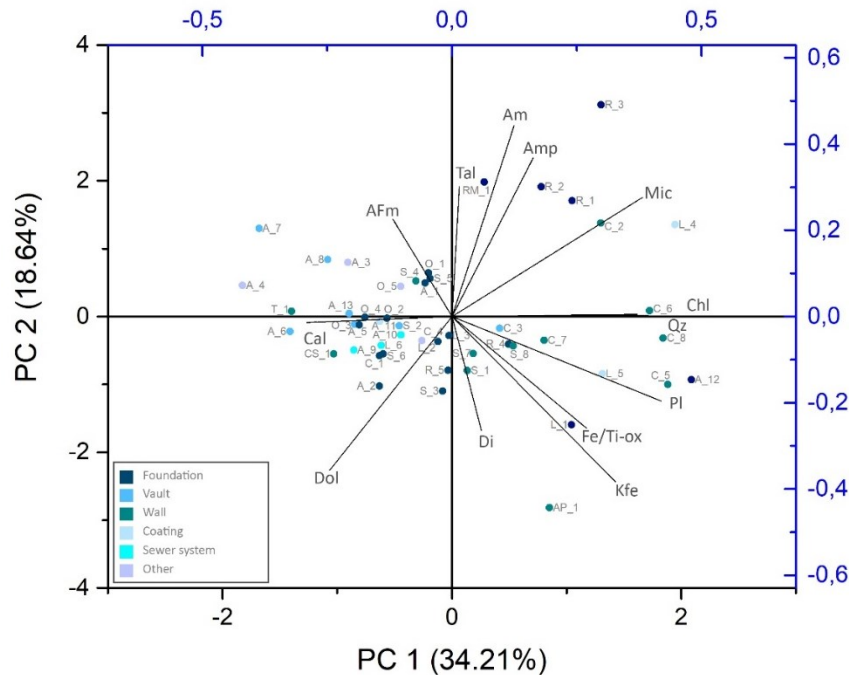


Figure 75 PCA analysis of XRPD of mortar samples exhibiting the function or purpose of the individual analyzed mortar sample

Likewise, when noticing the variation in the composition of mortar samples as regards the individual part of the structure they were collected from (walls, foundations ...) it is possible to observe, once again, an evident correlation. In this sense, samples collected from sewer systems, vaults, and other areas where a higher strength

was required (such as the arcovoli of the Arena or the triangular 'sperone' of the city walls), exhibit a higher hydraulicity. The opposite tendency can be observed for samples collected from coating or finishing layers, in which concentrations of AFm phases are lower. Due to the nature of the structures, samples collected from walls and foundational elements do not demonstrate a clear tendency. However, it can be highlighted from the aforementioned observations the consideration on the utility of mortars., as the structures requiring a higher mechanical resistance or waterproofing demonstrate a higher hydraulicity than samples collected from other structural elements.

Therefore, it can be inferred that the selection of materials and the recipes used for the production of mortars were influenced by the construction technique and the structural element for which the mortar would be used. In other words, the process of mortar production took into account the final purpose of this material in order to use a particular mixture that would satisfy materials'

requirements. This demonstrates a careful planning and execution of mortar production which, as previously mentioned in chapter 2, required more resources and a larger space.

Complementary to the aforementioned information, and as previously described, further mineralogical phase identification of the sole binder fraction of 10 mortar samples was carried out. The PCA analysis of the obtained results was accomplished for a better comprehension of the general tendencies. The following biplot reports the PCA from the previously mentioned results. On it, it is possible to identify the presence of a general group containing the majority of the samples and two outliers, samples AR-M12 and LEO-M5.

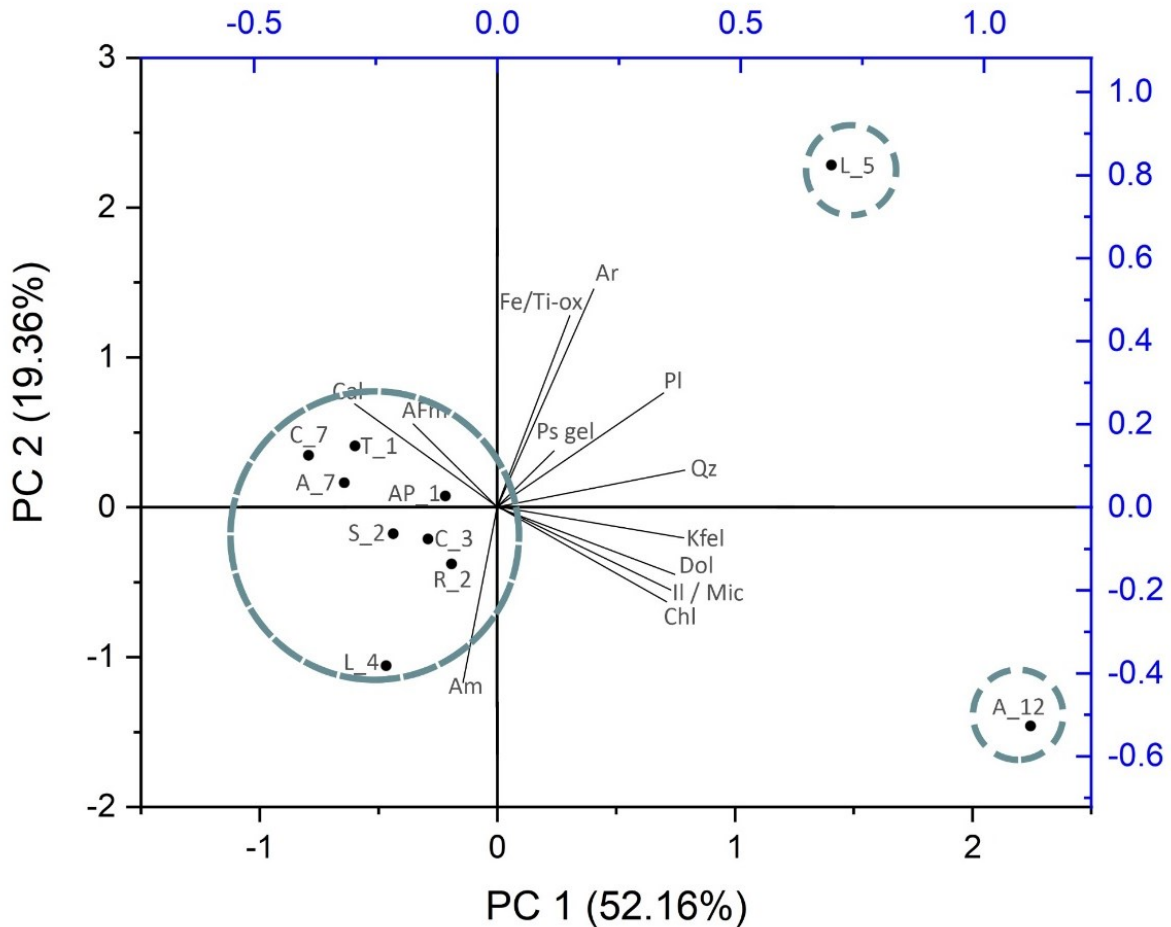


Figure 76 PCA of XRD from binder fraction analysis

In this way, from the mineralogical profile of the binder fraction of sample AR-M12, it is possible to indicate that the sample corresponds to an earthen-based mortar. This can be observed due to the high presence of mineral phases identified as clays, such as smectite and illite, and the remarkably low presence of calcite. This composition could also explain the previously mentioned flocculation encountered during the wet gravimetric separation procedure, since the accumulation of salts within the phyllosilicate layers, when in contact with water, would create a solution rich in alkali ions that would favor the observed phenomena.

On the other hand, sample LEO-M5 exhibits a clear tendency toward an enrichment of paracrystalline phyllosilicate gel. This can be explained due to the high amount of aggregate in the mortar (being this previously described as a very lean mortar when observed under the optical microscope), interacting with the low amount of binder. This mineralogical composition, as is the case of the previously described sample, can explain the causes of the difficulties encountered when separating the binder fraction. In this case, it is possible to hypothesize a relevant occurrence of dissolved alkali ions in solution released from the volcanic aggregates interacting with the binder, causing the observed flocculation.

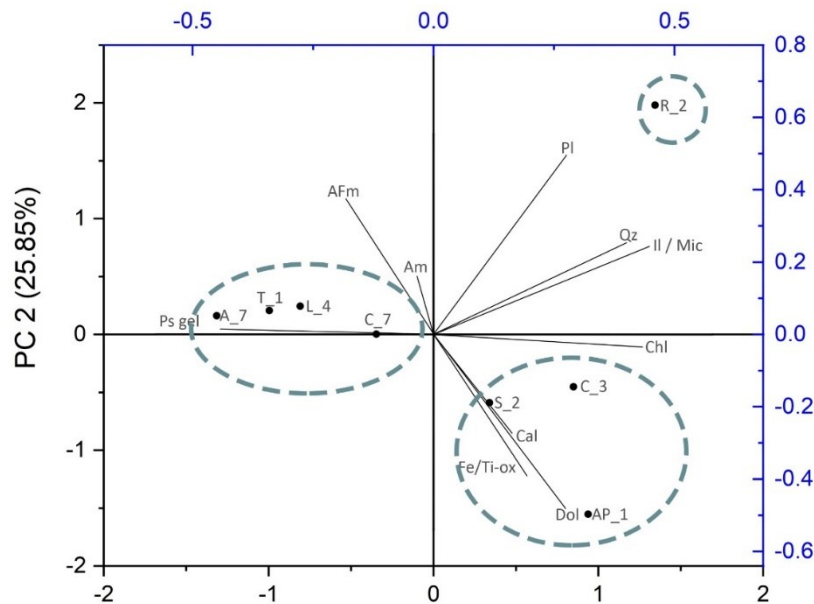


Figure 77 PCA from subgroup XRD binder fraction analysis

Moreover, a different PCA was performed excluding the two previously mentioned outliers to obtain a better reading of the mineralogical composition of the remaining eight mortar samples. On it, it was possible to observe the presence of three clearly different clusters.

The first cluster, containing samples AR-M7, TR-M1, LEO-M4, and COS-M7 demonstrates an evident inclination toward a higher presence of paracrystalline phyllosilicate gel and AFm phases, being it a clear indication of the formation of hydraulic phases as a cause of pozzolanic or parapozzolanic reactions taking place in the binders' matrices. Moreover, the second cluster containing samples AP-M1, COS-M3, and SGA-M2, depicts a higher presence of both dolomite and calcite mineral phases. This is an indication of a low hydraulicity, typical for aerial mortars. Finally, sample RED-M2 contains a higher amount of plagioclase and quartz demonstrating, as in the case for LEO-M5, the presence of silt/clay sediments within the matrix. Thus, it is possible to identify the aforementioned sample as an earthen and lime based mortar.

Complementing the mineralogical data, as previously mentioned in Chapter 7, samples studied under the optical microscope were grouped according to their observed properties, confirming the previously mentioned observations in regards to the binder's composition. This grouping, as for the clustering of the results of the previously performed analyses, allows for the identification of specific groups based on mortar composition and manufacturing process, being this the one that governs the presence and reactivity of the different aggregates and admixtures in the mortar. In this way, it is possible to obtain some key information regarding the composition and properties of the mortar samples from the observations performed on the optical microscope.

For instance, in the first group, it is possible to observe a high grade of interaction between the aggregate and the binder fraction, as suggested by several factors and characteristics, such as the variability of the binder, being this heterogeneous, and the observed reaction rims. This can be corroborated once again by the identified presence of AFm phases and amorphous phases and phyllosilicate gels and corresponding to C-S-H or M-S-H, respectively, in the previously mentioned binder's XRD results. Furthermore, due to these same characteristics, as well as for the low quantity of lime lumps, voids, and cracks present in the matrix, it would be possible to hypothesize the use of hot lime mixing as a slaking technique for the production of the aforementioned mortars.

As previously mentioned, all changes or variations in the production of a mortar will derive in significantly different resulting materials, being the slaking procedure one of the most important steps during this process. Several different techniques have been adopted throughout history, depending mostly on the geographical region and the available knowledge or technology for its

production. Each technique has different requirements and logistics, as can be observed in the case of hot lime mixing. In general terms, it consists of the slow hydration of lime, creating an exothermic reaction (from which the name 'hot lime' is obtained) to produce a dry powder. However, as described by Pavía, S., et al. (2023) two drastically different procedures for hot lime mixing production can be applied. The first one involves the dry mixing of sand and quicklime, resulting in a powder lime mixture to which water is progressively added. The obtained mortar can then be either stored or used immediately. The second procedure involves the mixing of wet sand and quicklime. The water previously retained by the sand will slowly hydrate the lime, resulting in this way in the slow exothermic reaction formerly described. This technique allows for an additional step to take place, where sieving of the mixture is done in order to remove unwanted particles such as remaining ash or lime lumps from the mortar mixture. In this case, as it was for the previous one, the resulting mortar can be used or stored. Nevertheless, a longer period of storage and maturation of the mixture is highly encouraged, since it will derive in a more reactive, stronger, and more resisting mortar. This is the case since, as explained by Pavía, S., et al. (2023), "time is needed to ensure full slaking and avoid late hydration".

Furthermore, due to the hydration of lime in the mixing phase, mortars will display a higher reactivity between the aggregate and the binder fraction. This is due to the fact that hot lime mixing commonly triggers both alkali-carbonate reaction (ACR) and an alkali-silica reaction (ASR) (Pavía, S., et al. 2023). The ACR is a chemical and physical process defined by Štukovnik, P., et al. (2019) as a "combination of various processes (i.e. the alkali silicate reaction (ASR) caused by silica minerals, dedolomitisation of aggregate grains, and carbonate halo formation)". This process is also referred to as a chemical reaction that can occur between some carbonate minerals and alkalis (such as sodium and potassium). In this sense, as it has been described in literature, the ACR is mainly governed by both the dedolomitization process and the dissolution and further precipitation of CaCO_3 (Katayama, T. 2010).

For the above mentioned reaction to take place, a series of conditions must have been met. Initially, and as it must be evident, dolomite aggregates may be present in a CSH-rich matrix. Additionally, a wet environment is required, since it will provide the means for the alkaline $\text{Ca}(\text{OH})_2$ dissociation and the ion diffusion. Furthermore, the presence of certain aggregates will trigger the occurrence of ACR, as alkalinity can be highly influenced by certain aggregates,

especially those containing potassium and sodium or the necessary silicate (such as quartz or chert) (Štukovnik, P., et al. 2019). Moreover, volcanic glass and K-rich aluminosilicate glass are also mentioned by Secco, M., et al. (2020) as a triggering factors by containing both potassium and silica.

The process of dedolomitization, as previously mentioned in Chapter 2, can be defined as the reaction between hydroxide ions (derived from C-S-H in the matrix) with dolomite crystals resulting in both the intergrowth of brucite and calcite and the release of calcium ions (Stukovnik, P., et al. 2020). In this way, the aggregate reacts with the matrix in the so-called dedolomitised region, forming a rim of reaction. In it, dolomite crystals ($\text{MgCa}(\text{CO}_3)_2$) and hydroxide (OH^-) will form a pseudomorph structure of both brucite ($\text{Mg}(\text{OH})_2$) and calcite (CaCO_3). The release of CO_3^{2-} leached into the matrix is also a result of the dedolomitization process that will cause the further precipitation of a carbonate halo (Stukovnik, P., et al. 2020). According to the aforementioned author, “the reaction of C-S-H gel with CO_3^{2-} ions causes another crucial consequence: the release of soluble silicate ions, $\text{H}_2\text{SiO}_4^{2-}$. This $\text{H}_2\text{SiO}_4^{2-}$ is partially consumed for the C-S-H regeneration and partially released into the surroundings, where, due to the concentration, gradient diffuses toward decaying aggregate”. This will later interact with brucite and Si ions from the matrix to form a Mg-Si gel. In addition to the above-mentioned process, and as stated by Katayama, T. (2010), the CO_3^{2-} ions will then interact with the matrix absorbing aluminate ions.

In this way, the resulting mortar will demonstrate a specific behavior that depicts its microscopic structure. On one side, Lanas, J., et al. (2006) mentions an increase in porosity and crack presence, as well as a general loss of strength and durability. However, the abovementioned properties usually apply to modern concretes. For historical, lime-based mortars the resulting properties have been described as an increase in strength, water resistance, and durability and a considerable decrease in porosity (Stukovnik, P., et al. 2020). This is because ASR gel interacts with the binder through a parapozzolanic reaction forming C-S-H and M-S-H phases (if magnesium is present). Lanas, J., et al. (2006) refers to this process as follows: “The newly formed calcite through ACR and the brucite crystallization improve the strength further than similar aerial lime-based mortars”. Moreover, the presence of secondary calcite formed on the pores of the mortar (and possibly related to the presence of gypsum as a secondary product (Liu, X., et al.

2022)) is an evident cause of ACR taking place inside a lime-based mortar (Štukovnik, P., et al. 2015).

In this way, it is possible to formulate the hypothesis of ACR taking place in the mortar samples of OM group N.1 due to several reasons. For instance, the previously stated hypothesis of the utilization of a hot lime mixture correlates accurately with it, since, as previously mentioned, the aggregates demonstrate a high reactivity and general low presence of lime lumps. Furthermore, the distinctly identified presence of reaction rims around dolomitic aggregates with the characteristic halo (corresponding to the brucite halo) is considered a defining indicator of this reaction. In addition to this, the aggregate composition of the sample, specifically the presence of volcanic clasts, quartz, quartzite, and K-feldspar provides the perfect conditions, being the source of both Si and alkalis for an ACR to take place. In the same way, the identification of secondary calcite observed on the voids of the mortar samples corroborates as well the incidence of ACR.

Notwithstanding, both OM groups N. 2 and N.3 do not show any properties that could indicate neither the implementation of hot lime mixing for its production nor the ACR taking place inside the samples. It is possible to state this since samples in both groups show low reactivity of the aggregate fraction, a homogeneous binder matrix (as a result of the low reactivity), and a higher presence of lime lumps. Additionally, definition of binders belonging to this groups as aerial lime binders and earthen based or earthen and lime based binders demonstrates the lack of C-S-H and M-S-H phases present in samples where ACR occurs. The high presence of dolomite in the previously mentioned XRD analysis of the binder demonstrates as well this lack of interaction. Furthermore, the mixture of earthen and lime mortars in group N.3 could indicate that the lime used for the production of the final products did not have a special slaking procedure nor a long curing time, since these are considered rigorous complex procedures, which would not be implemented for lime binders mixed with soil fractions.

AP-M1, which is considered an outlier due to the presence of *cocciopesto* in its matrix, demonstrates as well little to no reactivity. This is indicated not only by the lack of reaction rims surrounding the ceramic fragments present in the mortar, but also by the high presence of calcite identified in the XRD of the binder fraction. This could lead to the identification of a wet slaking process taking place, rather than a hot lime mixture. In the same way, the high amount of lime lumps and the high number of planar voids present in the sample as a result of cracking during

drying or hardening of the mortar would suggest the implementation of this hydration method. In addition to this, the low reactivity of the sample can be explained by the size of the cocciopesto found in AP-M1, since particles with bigger dimensions will tend to a lower reactivity.

In the same way, sample COS-M5 demonstrates a high presence of planar voids and lime lumps, and a homogeneous binder matrix, indicating as well the use of wet slaking rather than a hot lime mixture. However, the observed existence of hydromagnesite in the matrix suggests the use of a dolomitic-based binder, rather than a pure calcic one. If this is the case, and as previously described, the presence of planar voids could be observed as a consequence of the high reactivity of the binder to water presence, typical for magnesian binders due to a delayed hydration of magnesium oxide during setting and hardening.

Finally, and in contrast to the aforementioned outliers, sample LEO-M5 demonstrates a higher affinity towards a hot lime mixture and the occurrence of ACR. This can be suggested by the heterogeneity of the binder's matrix and the identified aggregates. This can be confirmed by the previously observed mineralogical profile of the binder fraction demonstrating a significantly high amount of phyllosilicate gels. In this way, the high amount of vughs could represent a contradictory evidence, since vughs are commonly found in mortars as a consequence of entrapped water leaving the material as it hardens, attesting for a water saturated slaking. Nevertheless, is justified by the low amount of binder present in the sample. In this sense, the high porosity is a cause of the low presence of binder, rather than a consequence of the slaking techniques.

Having said that, the observed reaction of the aggregates and possible presence of C-S-H and M-S-H (or C-A-S-H and M-A-S-H) is further corroborated by the SEM-EDS results. In this way, the result obtained from SEM-EDS analysis will serve to better clarify the previously stated hypothesis regarding the use of hot lime mixture as a slaking technique and the consequent ACR for samples in group N.1. Furthermore, the detailed analysis of the aggregate and binder fractions, as well as the identification of the composition of the matrix for samples present both in groups N.2 and N.3, will provide a better comprehension of production techniques and general composition. Finally, the elemental analysis of outliers will provide a better understanding of the particular composition and reactions occurring in these samples.

In this way, it is possible to observe the correspondence of certain evidences in the SEM-EDS analysis of group N.1 to those observed through both XRPD and OM analyses. Firstly, the

parametrization of the dedolomitization process was carried out in further detail. Indeed, it was possible to distinguish the unaltered portions of dolomite grains (due to the presence of calcium and magnesium) and the calcium-rich halo around the aggregate (surrounded by a brucite halo). Furthermore, the elemental analysis of the samples demonstrated a higher presence of calcium in the matrix surrounding the reacted dolomite aggregates. On the other hand, the high reactivity of other aggregates such as quartz or volcanic rocks observed and chemically identified with this technique attests not only to the high reactivity of the binding system but also to the release of silica and potassium in solution. These evidences strengthen the hypotheses of utilization of an hot lime mixing technique and the relevant incidence of alkali carbonate reactions. Moreover, the analyzed matrices consistently show significant chemical variability, especially regarding calcium, silicon, and aluminum. This variability can be explained by the enrichment of a certain element in specific areas (i.e.: the previously mentioned enrichment of Ca surrounding the dedolomitized aggregates). It should be mentioned as well the occurrence of significant potassium aliquots both in the binder matrix and in K-feldspar-rich aggregates (which is thought to be the source of the leached potassium). This is an essential key in the understanding of the ACR phenomena, since, as previously explained, a higher quantity of active alkalis caused by the presence of potassium inside the matrix will trigger the reactivity of the carbonate aggregates. In this sense, it is possible to imply that the highly reactive binder produced by the hot lime mixture caused the reaction of aggregates such as quartz, volcanic rocks, and K-feldspars, and the dissolution of both Si and K into the matrix. This dissolution provided the ideal conditions for the alkali carbonate reaction to take place, which then caused the dissolution of calcium into the matrix. The interaction of the portlandite in the binders' matrix with both the silica and the calcium released by the aggregates caused in this way a parapozzolanic reaction producing the occurrence of C-S-H phases. A similar process can be observed for the formation of M-S-H phases, through the uptake of magnesium released by the dedolomitization process.

In addition to the previously mentioned characteristics obtained through SEM observations of the samples belonging to group N.1, the presence of secondary calcite is also noted. This occurrence could be a consequence of both the ACR (as calcite is released from dolomite) and a decalcification process occurring in the binding matrices. Decalcification is a series of secondary chemical reactions involving the dissolution and precipitation of calcite in lime-based binders subjected to humid environments. In this sense, and as described by Frankeová, D., et Koudelková,

V. (2020) “In a hydraulic binder exposed to long-term variable humidity, the calcium carbonate progressively dissolves and migrates via the solution through the porous network of the mortar. Under specific conditions, it re-precipitates in cracks and onto pore walls”. Therefore, the decalcification process depends on both the environmental conditions to which the mortar is subjected and the mortar composition (Liu, X. et al. 2022). However, the environmental conditions are defined not only by the moisture, being this the cause of solubility of calcium and the mean In which it is transferred (Thomson, M. L., et al. 2004), but a certain pH level and the possible presence of chloride and sulfate ions will either trigger or limit the calcium leaching. For instance, Liu, X., et al. (2022) mentions “Higher pH is favorable to resist calcium leaching”. In addition, the presence of silica can also limit the loss of Ca^{2+} (Liu, X., et al. 2022).

The resulting mortar, due to the loss of calcium, will present a tendency towards a higher presence of pores and as a consequence, a lower strength and resistance. However, due to the deposition of secondary calcite in both pores of higher dimensions and the external layers of mortars, they will develop a higher resistance to moisture or water damage (Makhloufi, Z., et al. 2014). In regards to the mortar composition, the dissolution of calcium from C-S-H phases present in the binder will result in the formation of a silica-gel structure, as it has been described by Perlot, C., et al. (2013).

In this way, both processes could eventually result in the presence of secondary calcite in the mortar's pores. The variability of calcium inside the matrix, as previously explained, is not able to provide further clarifications (due to the presence of variable amounts of Si, Al, and K leaching from the aggregate components). Furthermore, the amount of secondary calcite is substantially high if its only source is considered the calcium dissolution in the ACR.

Notwithstanding, considering the aforementioned consequences, the samples in group N.1 do not show high porosity, which would contradict the decalcification hypothesis. However, this can be explained by the observed presence of M-S-H phases in the binding matrices.

Mortar samples of group N.1 are characterized a variable but considerably high amount of magnesium, indicating to the presence of M-S-H or MASH phases in the binder $((\text{MgO})_x - (\text{SiO}_2)_y - (\text{H}_2\text{O})_z)$. These phases, as mentioned by Ponce-Antón, G., et al. (2020), “show a layer structure similar to phyllosilicates” and derive from the reaction between a magnesian quicklime ($\text{CaO} +$ minor MgO) and silicon (and aluminum for M-A-S-H phases), or through the autogenous reaction

of Mg-rich aggregates and amorphous silica in presence of calcic lime as alkaline activator (Secco, M., et al. 2022; Roosz, C., et al 2015). Moreover, according to Ponce-Antón, G., et al. (2020), differently from C-S-H phases, “Like phyllosilicates, M–S–H phases are stable in an alkaline environment at pH up to 10”, making them a suitable option for the alkaline environment in which the ACR takes place. It should be highlighted that both M-S-H and M-A-S-H phases are not easily identified through the use of XRD, due to the low crystallinity displayed by the material, which ranges between 2 to 5 nm according to Roosz, C., et al. (2015).

In this sense, the observed prevalence of M-S-H over CSH phases could be related either to a preferential incorporation magnesium over calcium when silicate hydrate formation takes place, or to the previously described instability of C-S-H phases in lime-based mortars. It is therefore probable that both alkali carbonate reaction and decalcification processes took place at the same time, resulting in the observed presence of calcite crystals in the pores of the sample and high presence of M-S-H phases.

Furthermore, SEM analyses on samples AR-M7 and CSP-M1, originally belonging to OM group N.1, highlighted significant microchemical variations that led to consider them as outliers. On one hand, elemental analyses on CSP-M1 sample demonstrate a considerably higher presence of magnesium with respect to the other samples in the aforementioned group. This evidence can suggest the utilization of a lime binder with a higher concentration of magnesium as a sourcing material, or a lower diffusion of calcium resulting from the ACR. On the other hand, differently from the rest of the samples, SEM analyses on sample AR-M7 shows the presence of relevant pozzolanic and parapozzolanic reactions likely triggered by the presence of ash (fig. 78). It is possible to identify the presence of ash in the matrix due both to the observation of ash particles and to the significant phosphorous content throughout the matrix. The presence of ash particles in mortars as an additive is discussed by Lancaster, L., (2012), who

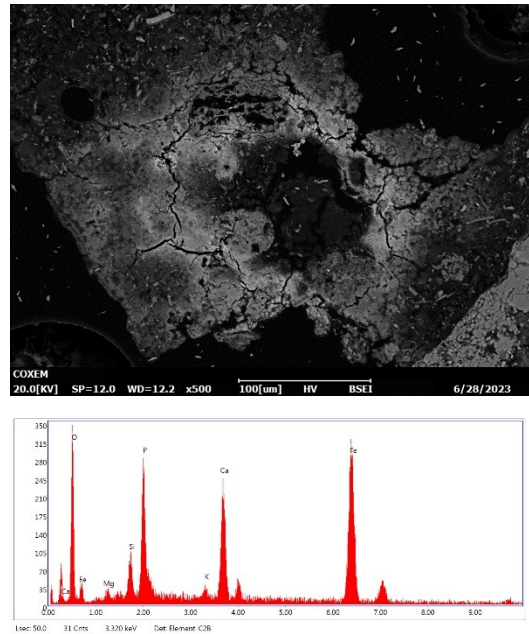


Figure 78 Sample AR-M7 EDS elemental analysis exhibiting the high presence of phosphorous

describes this particle's composition as “mainly siliceous aluminous in composition with associated calcium, magnesium, phosphorous, alkalis, iron, chlorine, and titanium”. The aforementioned author mentions as well the pozzolanic reactivity of the material in an alkaline matrix, such as the one present in AR-M7. Furthermore, Karim, M. E., et al (2017) suggests a possible source of ash derived from herbivores' manure combustion, which, according to Pliny, it was commonly utilized in the Po Valley (corresponding to the location of Verona) for agricultural purposes. In this order of ideas, it is possible to hypothesize the addition of ash to the original mix to promote better strength and resistance in the mortar.

SEM-EDS analyses on samples belonging to group N.2 highlighted significantly different characteristics with respect to those of the previous group. Indeed, no reaction between the aggregate and the binder fraction was observed in the samples, consistently to the optical microscope observations. Furthermore, analyses on the binder's matrices showed a low variability of calcium, together with a low content of silicon and magnesium. In this way, it is possible to hypothesize the lack of use of hot lime mixing technology and the absence of ACR. Nevertheless, the variability of the properties of the binder matrices between the two groups do not rely on the source material, since the samples belonging to both groups contain similar raw materials, but it is likely related to different production processes.

Sample COS-M7, which was previously considered as part of OM group N.2, is considered an outlier after SEM-EDS analysis was performed. This is due to the identification of a higher amount of magnesium, silica and, in certain cases, aluminum, in the binder matrix. In this sense, this sample, although demonstrating similar characteristics to the ones depicted by samples belonging to group N.2, suggests the possible presence of M-S-H phases.

Moreover, the SEM-EDS analyses on samples RED-M2 and AR-M12 belonging to group N.3 corroborate the previously proposed mortar composition. The elemental analysis of lime lumps demonstrated the presence of a calcic lime-based binder. In addition, elemental analyses confirmed the addition of soil aliquots in the binding mixtures. Hence, consistently with the results of the XRD analysis on the binder fraction, it is possible to confirm the use of both lime and earth mixed together for sample RED-M2, to produce a mortar with significantly low reactivity.

The peculiar characteristics of samples AP-M1 and COS-M5 were confirmed by SEM-EDS analyses. Sample AP-M1, differently from what it had been observed through OM, showed

a small reaction between the binder and the *cocciopesto* aggregates. Nevertheless, the binder composition is mainly Ca-based, with only a limited presence of magnesium. Therefore, it is possible to confirm the the previously established hypothesis that the mortar, although containing typically reactive products, does not show much reactivity possibly due to the production techniques implemented for its manufacturing. On the other hand, the previously observed hydromagnesite presence on sample COS-M5 was confirmed through elemental analysis. This fact, in addition to the high concentration of magnesium in the binder, indicates the use of a dolomitic quicklime, rather than a calcic binder, as is the case for the rest of the analyzed samples.

Moreover, as a complement of the XRD results, chemical analyses by SEM-EDS on the 10 selected binder-separated samples were performed in order to obtain a better understanding of their composition. The quantification of certain oxides present in the samples, such as CaO, SiO₂, or MgO, demonstrated a great variability due to the nature of the mortar (previously classified as aerial, hydraulic, or earthen). This analysis also allowed the observation of aliquots of P₂O₅ in the entire population of samples, although highly variable (having a standard deviation value of 56.28). It is precisely the presence of this oxide (even in low quantities) in the earthen and aerial mortar that led to the refutation of the previously established hypothesis of the intentional addition of ashes from animal dung as an additive to enhance the hydraulicity of the samples. Therefore, the presence of P in volcanic aggregates is proposed as a hypothesis for the origin of phosphorous in the analyzed mortar samples.

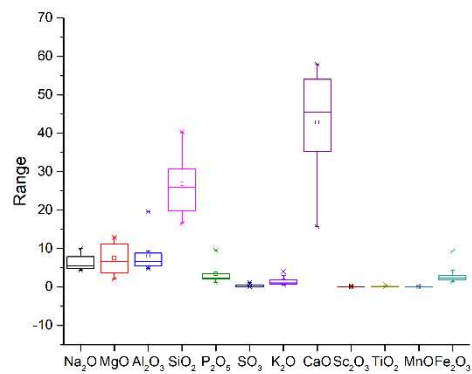


Figure 79. Graph of boxes and whiskers demonstrating the variability of the elemental quantification in oxides

According to Ma, C., et al. (2022) “Igneous rocks are the main carrier of P migration from the deep Earth to the surface”. Ma, C., et al. (2022; 2023) mention as well the presence of P_2O_5 in

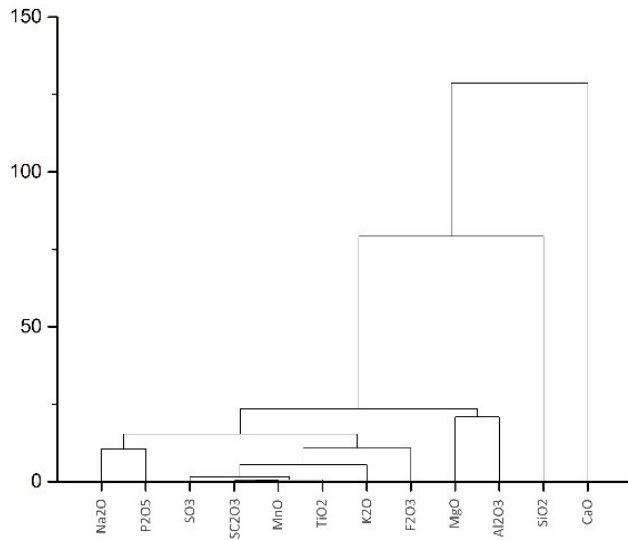


Figure 80. Dendrogram showing the heriarchical relation between the elements found in the mortar samples' binder

volcanic rocks, and their transport throughout the crust as a consequence of rock weathering. Furthermore, the aforementioned literature highlights the association of phosphoric acid with felsic volcanics, such as the observed and previously described K-feldspar-rich aggregates found in the mortar samples. However, due to the complex cycle of P, being highly influenced by CO_2 presence, redox conditions, weathering patterns, and vegetation and animal presence, there has not been an extensive study of phosphorous

presence in sediments (Hartmann, J., et Moosdorf, N. 2011). In this way, and following the observed correlation between the oxides found in the analyzed samples (Fig. 80), it is possible to stipulate that the observed volcanics account for the presence of phosphorous. Moreover, it is possible to speculate that the lack of information concerning the presence of P in the sediments of the Adige River can be explained due to the complex cycle that the element is subjected to and to a generalized lack of scientific knowledge in the topic.

Furthermore, it should be mentioned that the use of phosphorous has been experimentally implemented in cement to enhance the hydraulicity of the material (Mehdizadeh, H., et al. 2022; Qi, G. H., et Peng, X. Q. 2011). In this case, the studies showed the dissolution of silica gels and a clear formation of C-S-H gels in the matrix. However, and as previously mentioned, this reaction is performed in modern cement materials, and no previously performed studies demonstrated the use of P_2O_5 as an additive in a historical context.

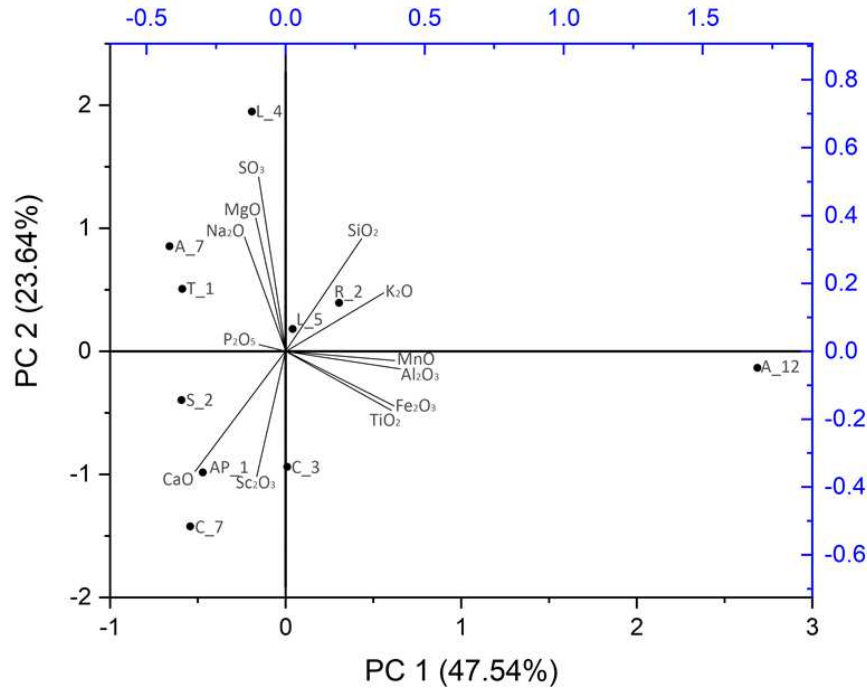


Figure 81 PCA biplot depicting elemental composition in oxides of binders' analysis

In addition to these observations, a statistical treatment of the data through PCA was performed. The analysis allowed to identify, once again, sample AR-M12 as an outlier. In this way, the elemental characterization of the binder demonstrates as well the earthen nature of the mortar.

Furthermore, the same statistical analysis was performed excluding the results of AR-M12. Additionally, the values of scandium and manganese oxides were neglected due to their considerably low values, and values of carbon oxide due to the poor reliability of its results. On the resulting scatterplot (biplot) of the PCA of the subgroup is not possible to observe clear groups, as could be observed in the XRD analysis of the binder. However, the elemental composition of the individual samples corresponds to the expected ones, taking into consideration their nature and their previously defined properties.

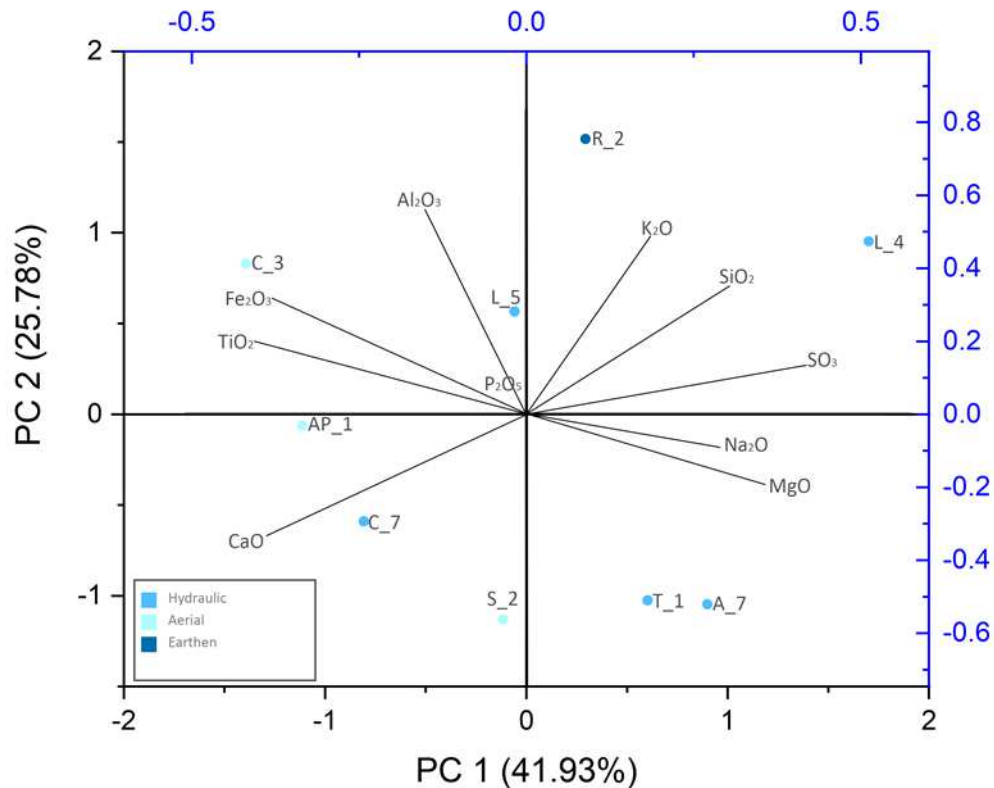


Figure 82. PCA biplot depicting elemental composition in oxides of binders analysis of subgroup with mortar type classification

In this way, it is possible to observe some clear tendencies regarding the type of binder. Samples previously defined as aerial show a higher presence of CaO, as can be seen on AP-M1, COS-M3, and SGA-M2. On the other hand, sample RED-M2, an earthen and lime mortar mixture, exhibits a higher presence of potassium, aluminum, and silicon. These elements correspond to the ones that can be commonly found in clays, reflecting, once again, the characteristic composition of its mortar type. Samples COS-M7, TR-M1, and AR-M7, previously categorized as hydraulic mortars, demonstrate a high content of MgO, which, as previously commented when defining the ACR process, can be found due to the formation of M-S-H and M-A-S-H phases. The lower values of CaO in comparison to those of the aerial mortars respond as well to the ACR and the previously described decalcification phenomena. Finally, sample LEO-M5 demonstrates a different elemental composition, due to the lower binder/aggregate ratio.

9. Chapter IX - Conclusions

The analytical process carried out in this thesis provided a clear overview of the different procedures for mortar production taking place in the city of Verona during the Roman era. It was possible to identify, according to the observation and analysis of the results, the application of three different mortar types: aerial lime mortars, hydraulic lime-based mortars, and a mixture of earthen and lime mortars. The identification of these three general groups was achieved by both the observation of the textural properties of the mortar samples (through the petrographic analysis and SEM observation) and their mineralogical and chemical composition (through XRPD and EDS analyses). It should be mentioned, however, the presence of samples exhibiting unique behaviors, such as the addition of a certain aggregate or a remarkably high reactivity, within the general groups.

The earthen and lime mortar mixtures (with variable proportions of the aforementioned parts) and the aerial mortars did not demonstrate much reactivity between the aggregates and the binder, even when potentially reactive aggregates such as cocchiopesto were added. Nonetheless, the hydraulic mortars showed clear signs of high reactivity between the binder and the aggregate fractions distinctively identified by the observation under the polarized microscope and SEM-EDS.

It is precisely because of this reactivity and the observations of their distinctive characteristics that it is possible to hypothesize the implementation of a hot lime mixing technology during the manufacturing process. This is testified by the identified dedolomitization, the low quantity of lime lumps, voids, and cracks present in the matrix as well as the high level of interaction between the aggregate and the binder. This peculiar production procedure, together with the constant presence of volcanic rocks high in silica and alkalis, provided the means for the alkaline-carbonate reaction to occur, allowing the formation of both C-S-H and M-S-H phases. Moreover, the ACR in conjunction with a decalcification phenomenon resulted in the formation of secondary calcite in the surface of the mortar's voids, which provided the mortar with a water-coating effect as extensively described in the literature. It should be remarked that the decalcification of the binder did not represent a significant loss of strength in the analyzed samples,

as the loss of C-S-H phases is counterbalanced by a relevant formation of M-S-H phases. This process suggests a favorable role of magnesium rather than calcium for the formation of more stable hydrated silicate mineral phases in the mortars' binder.

Additionally, according to the correlation between the mineralogical profiles and the individual context of the samples, it was possible to establish a general conception of the development of technical knowledge for mortar manufacturing in Verona. In this way, a clear development of the techniques was observed, with samples demonstrating better hydraulicity during the second construction period, after the experimentation phase of the first period was finalized. Furthermore, the correlation between the level of hydraulicity (or in general terms the strength and resistance) of mortars and their specific use demonstrates a clear intentionality in the process. In this way, the implementation of certain methods and the addition of aggregates in the manufacturing process of mortars led to a higher quality of the material when required, depicting a conscious manufacturing process.



Figure 83. Sampling location defensive walls on Via del Redentore taken by PhD student Eliana Bridi

The present study was able to provide insightful information regarding the manufacturing procedures and techniques implemented for mortar production of the most representative structures of Roman Verona, however, some of the findings should be further analyzed. In a first instance, the preference for the formation of M-S-H phases over C-S-H phases, observed by SEM-

EDS analysis, should be further investigated. Although a preference for magnesium in the silicate hydrate phase formation was noticed, the decalcification phenomena, as previously commented, is partially accounting for the higher presence of M-S-H.

In addition to this, some unresolved questions arose as a consequence of the high content of phosphorous in the analyzed mortar samples. On one hand, the question regarding the origin of phosphorous and its chronological variability originates. Although the suggestion of a volcanic origin of the aforementioned element was made, no previous geological studies on the sediments of the Adige River mention its occurrence. On the other hand, the possible effect of phosphoric acid as a catalyzer of alkaline-carbonate reaction in historical mortars should be further developed. The presence of P₂O₅ in mortar samples with addition of ashes from animal dung origin is commonly accompanied by the pozzolanic reaction (due to the high silica content in the aforementioned additives). Nevertheless, the question regarding the consequence of phosphoric acid as a part of the reaction process should be developed in further detail.

10. Chapter X - Bibliography

Adam, J. P. (2005). *Roman Building. Materials and Techniques*. London, U.K. Taylor & Francis Group. London, U.K.

Alfieri, P. V. et al. (2020). Non-destructive diagnose of the biodeterioration of heritage assets through an optical microscopy. *Journal of Cultural Heritage* 43 (2020) 249–254. <https://doi.org/10.1016/j.culher.2019.11.013>

Arandigoyen, M., et al. (2006). Variation of microstructure with carbonation in lime and blended pastes. *Applied Surface Science*. 252 (2006) 7562–7571

Arizzi, A., et Cultrone, G. (2021). Mortars and plasters—how to characterise hydraulic mortars. *Archaeological and Anthropological Sciences*. 13: 144. DOI: <https://doi.org/10.1007/s12520-021-01404-2>

Artioli, G. (2010). *Scientific Methods and Cultural Heritage. An introduction to the application of materials science to archaeometry and conservation science*. Oxford University Press. Oxford, U. K.

Artioli, G., et al. (2019). The Vitruvian legacy: mortars and binders before and after the Roman world. *EMU Notes in Mineralogy*, Vol. 20 (2019), Chapter 4, 151–202

Baker, I. (1969). Petrology of the volcanic rocks of Saint Helena island, South Atlantic. *Geological Society of America Bulletin*, 80(7), 1283-1310.

Bakolas, A., et al. (2008). Evaluation of Pozzolanic activity and physico-mechanical characteristics in ceramic powder-lime pastes. *Journal of Thermal Analysis and Calorimetry.*, Vol. 92 (2008) 1, 345–351

Basso, P. et al. (2019) *Verona e le Sue Strade: Archeologia e valorizzazione*. Sommacampagna (VR), Veneto: Cierre edizioni.

Beschi, L. (1960) *Verona e il Suo Territorio: Vol. 1*. Verona, Italy: Istituto per Gli Studi Storici Veronesi.

- Bieber, M. (1961). *The history of greek and roman theater*. Princeton university press.
- Böke, H. D., et al. (2006). Characteristics of brick used as aggregate in historic brick-lime mortars and plasters. *Cement and Concrete Research*. 36 (2006) 1115–1122
- Bolla, M. (2006). *Museo archeologico del teatro romano di Verona*. Ufficio scolastico regionale per il Veneto.
- Bolla, M. (2010). *Il teatro romano di verona e le sue sculture*. Comune di Verona Direzione Musei d'Arte e Monumenti.
- Bolla, M. (2012). *Gli edifici da spettacolo nell'Iconografia rateriana. L'archetipo e l'immagine tramandata*. 2012.
- Bolla, M. (2012). *L'arena di Verona*. Verona: Cierre Edizioni. 2012
- Bolla, M. (2014). *Il luogo di culto alle divinità egizie a Verona. Prospettive di ricerca e indagini sul campo (Antichistica 6; Serie di studi orientali, 2)*, Atti del III Convegno Nazionale Veneto di Egittologia, a cura di E.M. Ciampini, P. Zanovello, Venezia 2014, pp. 119-140
- Bolla, M. (2014). *Verona Romana*. Cierre Edizioni.
- Bolla, M. (2016). *Il teatro romano di verona*. Verona, Italy: Cierre Edizioni. 2016.
- Bonetto, J. (2009). *Veneto*. Libreria dello Stato. Roma: Libreria dello Stato. 2009.
- Borges, C., et al. (2014). Durability of ancient lime mortars in humid environment. *Construction and Building Materials*, 66, 606-620. DOI: <http://dx.doi.org/10.1016/j.conbuildmat.2014.05.019>
- Brondi, A., et al. (1976). *Commento al foglio geologico 027, Bolzano 1 : 50.000*. Studi Trentini di Scienze Naturali. Vol. 53. N. 6A, 1976. Pag. 107-218. Trento, Italia.
- Brunella, B., et al. (2013). *Il teatro romano*. Notizie di archeologia del Veneto.
- Bruno, B., et al. (2014) *Anfiteatro Arena*. Indagini archeologiche negli arcovoli. Dati preliminari. NAVE. *Notizie di Archeologia del Veneto*.
- Calcagni, A.C. (2005) *Le Mura di verona: La Città e le Sue difese Dalla Fondazione Romana All'unità d'italia*. Caselle di Sommacampagna (VR), Veneto: Cierre.

Cameron, C. et Herrmann, J. (2018). Guidance and capacity building for the recognition of associative values using world heritage criterion. Final report. World heritage centre. (2018).

Cavalieri Manasse, G. (1987). Il Veneto nell'età romana II: Note di urbanistica e di archeologia del territorio. Banca Popolare di Verona.

Cavalieri Manasse, G. (1994). L'odeon di Verona. In *Antichità Altoadriatiche XLI* (1994). Spettacolo in Aquileia e nella Cisalpina Romana. Centro di Antichità Altoadriatiche. Casa Bertoli Aquileia.

Cavalieri Manasse, G. (2003). *Luoghi e tradizioni d'Italia: Veneto. Vol.2*. Editalia. Roma: Editalia.

Cavalieri Manasse, G., et Fresco, P. (2012). Verona: Castel San Pietro, indagini 2007-2012. NAvE: *Notizie di Archeologia del Veneto*, 1, 2385-2356. Firenze: All'insegna del giglio. Retrieved from <http://digital.casalini.it/10.1400/225844>

Cizer, O., et al. (2008). Blended lime-cement mortars for conservation purposes: Microstructure and strength development. In *Structural analysis of historic construction* (pp. 965-972). London: Taylor & Francis Group.

Clydesdale, F. M., et Ahmed, E. M. (1978). Colorimetry—methodology and applications. *Critical Reviews in Food Science & Nutrition*, 10(3), 243-301.

Courtois, C. (1989). *Le bâtiment de scène des théâtres d'Italie et de Sicile. Étude chronologique et typologique*. Arts and Archaeology Publications.

Cresci Marrone, G., et al. (2020) 'Il dono di Altino', *Antichistica* [Preprint]. doi:10.30687/978-88-6969-380-9.

Dal Forno, F. (1975). *Il teatro romano di Verona*. Edizioni di Vita Veronese.

Dal Ronco, Nicoletta. (2015). *Identificazione strutturale del teatro romano di Verona mediante monitoraggio statistico e dinamico*. Tesi di Laurea. Università degli Studi di Padova. Dipartimento di Ingegneria civile edile ambientale.

Davidson, M. W. et Abramowitz, M. (2002). Optical Microscopy. In *Encyclopedia of Imaging Science and Technology*, edited by Hornak, J. P. (2002). <https://doi.org/10.1002/0471443395.img074>

DeLaine, J. (2021). Production, transport and on-site organisation of Roman mortars and plasters. *Archaeological and Anthropological Sciences* (2021) 13: 195

DOI: <https://doi.org/10.1007/s12520-021-01401-5>

Delgado Rodrigues, J. (2020). Practical evidence and experimental demonstration of the Liesegang phenomenon in the carbonation process of lime mortars in exposed masonries. *Journal of Cultural Heritage* 45 (2020) 169–179. DOI: <https://doi.org/10.1016/j.culher.2020.02.015>

Domagalski, J., et Saleh, D. (2015). Sources and transport of phosphorus to rivers in California and adjacent states, US, as determined by SPARROW modeling. *JAWRA Journal of the American Water Resources Association*, 51(6), 1463-1486.

Donais, M. K., et al. (2020). Energy dispersive X-ray fluorescence spectrometry characterization of wall mortars with principal component analysis: Phasing and ex situ versus in situ sampling. *Journal of Cultural Heritage* 43 (2020) 90–97. DOI: <https://doi.org/10.1016/j.culher.2019.12.007>

Drennan, R. D. (2010). *Statistics for archaeologists*. New York: Springer.

Dunlap, M. et Adaskaveg, J. E. (1997). *Introduction to the Scanning Electron Microscope*. (Davis, U. C.). Facility for Advanced Instrumentation.

Elsen, J. (2006). Microscopy of historic mortars—a review. *Cement and Concrete Research*.36 (2006) 1416–1424

Ergenç, D., et al. (2021). Mortars and plasters—How to characterize aerial mortars and plasters. *Archaeological and Anthropological Sciences* (2021) 13:197. DOI: <https://doi.org/10.1007/s12520-021-01398-x>

Falchi, L., et al. (2013). Influence and effectiveness of water-repellent admixtures on pozzolana–lime mortars for restoration application. *Construction and Building Materials*, 49, 272-280. DOI: <http://dx.doi.org/10.1016/j.conbuildmat.2013.08.030>

Felitsyn, S. B., et Kirianov, V. Y. (2002). Mobility of phosphorus during the weathering of volcanic ashes. *Lithology and Mineral Resources*, 37, 275-278.

Al-Hasani, N. R., et al. (2022). The morphological analysis of crystalline methadone: a novel combination of microscopy techniques. *ScienceRise: Pharmaceutical Science*, (4 (38)), 44-52.

- Frankeová, D., et Koudelková, V. (2020). Influence of ageing conditions on the mineralogical micro-character of natural hydraulic lime mortars. *Construction and Building Materials*, 264, 120205. DOI: <https://doi.org/10.1016/j.conbuildmat.2020.120205>
- Franzini, M., et al. (2000). A procedure for determining the chemical composition of binder and aggregate in ancient mortars: its application to mortars from some medieval buildings in Pisa. *Journal of Cultural Heritage* 1 (2000) 365–373. DOI: 10.1111/j.1475-4754.2010.00565.x
- Franzoni, L. (1961). La Grotta di S. Siro al Teatro Romano di Verona in «Vita Veronese», 10, ottobre 1961, pp. 397-398
- Fusade, L. et Viles, H. A. (2019). A comparison of standard and realistic curing conditions of natural hydraulic lime repointing mortar for damp masonry: Impact on laboratory evaluation. *Journal of Cultural Heritage* 37 (2019) 82–93. DOI: <https://doi.org/10.1016/j.culher.2018.11.011>
- G.W. Brindley, et D. Brown (1980), *Crystal Structures of Clay Minerals and Their X-Ray Identification*, Mineralogical Society, London, pp. 125–196.
- Gameiro, A., et al. (2014). Physical and chemical assessment of lime–metakaolin mortars: Influence of binder: aggregate ratio. *Cement and Concrete Composites*, 45, 264-271.
- Gandolfi, G., et al. (1982). Composition and longshore dispersal of sands from the Po and Adige rivers since the pre-Etruscan age. *Journal of Sedimentary Research*, 52(3), 797-805
- Ganiatsas, V. (2011). Heritage as ethical paradigms of balancing identity and change aimed socio-cultural development. ICOMOS. (2011).
- Gegenfurtner, K. R., et Kiper, D. C. (2003). Color vision. *Annual review of neuroscience*, 26(1), 181-206.
- Getty conservation institute. (2017). *Values in Heritage Management. Emerging Approaches and Research Directions*. Edited by Avrami, E., Macdonald, S., Manson, R., Myers, D. Los Angeles.
- Gigan, S. (2017). Optical microscopy aims deep. *Nature Photonics*, 11(1), 14-16.
- Gilchrist, A., et Nobbs, J. (2017). Colorimetry, theory. *Encyclopedia of spectroscopy and spectrometry*, 328-333.

Hartmann, J., et Moosdorf, N. (2011). Chemical weathering rates of silicate-dominated lithological classes and associated liberation rates of phosphorus on the Japanese Archipelago—Implications for global scale analysis. *Chemical Geology*, 287(3-4), 125-157.

Hiller, G. (2019). Book five of color management - datacolor. Datacolor. <https://www.datacolor.com/wp-content/uploads/2022/06/color-management-ebook-5-en.pdf>

ICOMOS. (2004). International charters for conservation and restoration. Second edition. Munchhen, ICOMOS. (2004).

ICOMOS. (2008). Criteria for the conservation of built heritage. ICOMOS.

International coalition of sites of conscience. (2018). Interpretation of sites of memory. UNESCO.

Izaguirre, A., et al. (2010). Ageing of lime mortars with admixtures: Durability and strength assessment. *Cement and Concrete Research* 40 (2010) 1081–1095. DOI: 10.1016/j.cemconres.2010.02.013

Jokilehto, J. (2006). Considerations on authenticity and integrity in world heritage context. *City & Time* 2 (1). (2006). <http://www.ct.ceci-br.org>

Jokilehto, J. (2006). Preservation theory unfolding. *Future Anterior* Volume III, Number 1. (2006).

Karim, M. E., et al. (2017). Effect of salinity of water in lime-fly ash treated sand. *International Journal of Geo-Engineering*, 8, 1-12.

Katayama, T. (2010). The so-called alkali-carbonate reaction (ACR)—Its mineralogical and geochemical details, with special reference to ASR. *Cement and Concrete Research*, 40(4), 643-675.

Keppert, M., et al. (2020). Kinetics of pozzolanic reaction and carbonation in ceramic–lime system: Thermogravimetry and solid-state NMR spectroscopy study. *Journal of Building Engineering*, 32, 101729.

Kerr, J. S. (2013). Conservation plan. A guide to the preparation of conservation plans for places of european significance. ICOMOS Australia.

Klosek-Kozłowska, D. (2002). The protection of urban heritage: The social evaluation of the space in historic towns - Local intangible values in a globalised world. In: *Estrategias relativas al*

patrimonio cultural mundial. La salvaguarda en un mundo globalizado. Principios, prácticas y perspectivas. 13th ICOMOS General Assembly and Scientific Symposium. Actas. Comité Nacional Español del ICOMOS, Madrid, pp. 87-89.

Kuehni, R. G. (2012). *Color: An introduction to practice and Principles*. Wiley.

Lanas, J., et al. (2006). Mechanical properties of masonry repair dolomitic lime-based mortars. *Cement and Concrete Research*, 36(5), 951-960.

Lancaster, L. (2019) Pozzolans in Mortar in the Roman Empire: An Overview and Thoughts on Future Work, in: I.F. Ortega, S. Bouffier (Eds.), *Mortiers et hydraulique en Méditerranée antique*, *Archéologies Méditerranéennes* 6, Presses Universitaires de Provence, Aix-en-Provence, pp. 31–39.

Lancaster, L., (2012). Ash mortar and vaulting tubes: agricultural production and the building industry in North Africa, in: Camporeale, S., Dessales, H., Pizzo, A., *Arqueología de la construcción* III. Los procesos constructivos en el mundo romano: la economía de las obras, Ecole Normale Supérieure (Paris, 10-11 diciembre 2009), Consejo Superior de Investigaciones Científicas, Madrid Merida, pp. 145–160

Lindqvist, J. E., et Sandström, M. (2021). Quantitative analysis of historical mortars using optical microscopy. *Materials and Structures/Matériaux et Constructions*. Vol. 33, December 2000, pp 612-617

Liu, X., et al. (2022). Decalcification of calcium silicate hydrate (CSH) under aggressive solution attack. *Construction and Building Materials*, 342, 127988.

Ma, C., et al. (2022). Global tectonics and oxygenation events drove the Earth-scale phosphorus cycle. *Earth-Science Reviews*, 104166.

Ma, C., et al. (2022). Mechanisms for phosphorus fluctuation in Phanerozoic volcanic rocks. *Lithos*, 424, 106764.

Ma, C., et al. (2022). Phosphorus variations in volcanic sequences reveal the linkage between regional tectonics and terrestrial biota evolution. *Geochemistry, Geophysics, Geosystems*, 23(8), e2022GC010536.

- Ma, C., et al. (2022). Volcanic phosphorus spikes associated with supercontinent assembly supported the evolution of land plants. *Earth-Science Reviews*, 232, 104101.
- Ma, C., et al. (2023). Volcanic phosphorus supply boosted Mesozoic terrestrial biotas in northern China. *Science Bulletin*.
- Makhloufi, Z., et al. (2012). The strength of limestone mortars with quaternary binders: Leaching effect by demineralized water. *Construction and Building Materials*, 36, 171-181. DOI: <http://dx.doi.org/10.1016/j.conbuildmat.2012.04.112>
- Makhloufi, Z., et al. (2014). Durability of limestone mortars based on quaternary binders subjected to sulfuric acid using drying–immersion cycles. *Construction and Building Materials*, 71, 579-588. DOI: <http://dx.doi.org/10.1016/j.conbuildmat.2014.08.086>
- Malhotra, V. M., et Kumar Mehta, P. (2017). *Pozzolanic and Cementitious Materials*. Boca ratón, FL. United States of America. CRC Press. Taylor & Francis Group. Boca ratón, FL. United States of America.
- Maravelaki-Kalaitzaki, P., et al. (2003). Physico-chemical study of Cretan ancient mortars. *Cement and Concrete Research*.33 (2003) 651 – 661. DOI: 10.1016/S0008-8846(02)01030-X
- Marchini, G. P. (1978). *Verona romana e paleocristiana*. Banca Popolare di Verona.
- Martínez-Ramírez, S. et Thompson, G. E. (1998). Deterioro de morteros de cemento producido por la "deposición" seca y húmeda de contaminantes atmosféricos. Dry and wet "deposition" studies of the degradation of cement mortars. *Materiales de construcción*. Vol. 48 n.250 abril/mayo/junio 1998.
- Mehdizadeh, H., et al. (2022). Enhancement of early age cementitious properties of yellow phosphorus slag via CO₂ aqueous carbonation. *Cement and Concrete Composites*, 133, 104702.
- Moropoulou, A. et al. (2005). Strength development and lime reaction in mortars for repairing historic masonries. *Cement & Concrete Composites* 27 (2005) 289–294. DOI: 10.1016/j.cemconcomp.2004.02.017
- Moropoulou, A., et al. (2005). Composite materials in ancient structures. *Cement and Concrete Research*. 27 (2005) 295–300. DOI: 10.1016/j.cemconcomp.2004.02.018

Navarro-Mendoza, et al. (2023). Physical and Mechanical Characterization of Lime Pastes and Mortars for Use in Restoration. *Heritage*, 6(3), 2582-2600.

Niglio, O. (2012). Concepto de valor para el patrimonio cultural y diferentes métodos de restauración a nivel internacional. Congreso Internacional sobre Patrimonio Cultural en México, Universidad Autónoma “Benito Juárez”.

Nogueira, R., et al. (2020). Artificial ageing by salt crystallization: test protocol and salt distribution patterns in lime-based rendering mortars. *Journal of Cultural Heritage* 45 (2020) 180–192. DOI: <https://doi.org/10.1016/j.culher.2020.01.013>

O’Donnell, P. M. (2008). Urban Cultural Landscapes and the Spirit of Place. In: 16th ICOMOS General Assembly and International Symposium: ‘Finding the spirit of place – between the tangible and the intangible’, 29 sept – 4 oct 2008, Quebec, Canada.

Ohta, N., et Robertson, A. A. (2006). *Colorimetry: Fundamentals and applications*. John Wiley & Sons.

Oliveira, M. L. S., et al. (2020). Atmospheric contaminations and bad conservation effects in Roman mosaics and mortars of Italica. *Journal of Cleaner Production* 248 (2020) 119250. DOI: <https://doi.org/10.1016/j.jclepro.2019.119250>

Oliveira, M., et al. (2022). Simulation of humidity fields in aerial lime mortar. *Journal of Cultural Heritage* 53 (2022) 35–46. DOI: <https://doi.org/10.1016/j.culher.2021.11.003>

Organización de las Naciones Unidas para la Educación, la Ciencia y la Cultura. (2014). *Gestión del patrimonio mundial cultural. Manual de referencia*. UNESCO. www.unesco.org/open-access/terms-use-ccbyncsa-sp

P. Jobstraibizer et P. Malesani. (1973). *I sedimenti dei fiumi veneti*. Roma, Italia. June 16, 1973.

Pavía, S., et al. (2023). RILEM TC 277-LHS report: How hot are hot-lime-mixed mortars? A review. *Materials and Structures*, 56(4), 87.

Pavía, S., et Caro, S. (2007). An investigation of Roman mortar technology through the petrographic analysis of archaeological material. *Construction and Building Materials* 22 (2008) 1807–1811. DOI: [10.1016/j.conbuildmat.2007.05.003](https://doi.org/10.1016/j.conbuildmat.2007.05.003)

- Pavlík, V., et Užáková, M. (2016). Effect of curing conditions on the properties of lime, lime–metakaolin and lime–zeolite mortars. *Construction and Building Materials*, 102, 14-25. DOI: <http://dx.doi.org/10.1016/j.conbuildmat.2015.10.128>
- Pel, L., et al. (1998). Water absorption in mortar determined by NMR. *Magnetic resonance imaging*, 16(5-6), 525-528.
- Perlot, C., et al. (2013). Diffusivity evolution under decalcification: influence of aggregate natures and cement type. *Materials and structures*, 46, 787-801.
- Pineda, P., et al. (2022). Pore structure and interdisciplinary analyses in Roman mortars: Building techniques and durability factors identification. *Construction and Building Materials* 317 (2022) 125821. DOI: <https://doi.org/10.1016/j.conbuildmat.2021.125821>
- Piovan, S., et al. (2010). Bronze Age paleohydrography of the southern Venetian Plain. *Geoarchaeology: An International Journal*, 25(1), 6-35, 2010.
- Ponce-Antón, G., et al. (2020). Multi-analytical approach for chemical-mineralogical characterization of reaction rims in the lime mortars from Amaiur Castle (Navarre, Spain). *Microchemical Journal*, 152, 104303. DOI: <https://doi.org/10.1016/j.microc.2019.104303>
- Qi, G. H., et Peng, X. Q. (2011). Analysis on the pozzolanic effects of phosphorus slag powder in concrete. *Key Engineering Materials*, 477, 112-117.
- Quaranta, A., et al. (1998). Principal Component Analysis of Ion Beam Induced Luminescence Spectra of River Sands. *Geology*, 116, 13.
- Quinn, P. S. *Composition of Archaeological Ceramics in Thin Section*. (2003). *Ceramic Petrography: The Interpretation of Archaeological Pottery & Related Artefacts in Thin Section*, edited by: Archaeopress.
- Razzante, V. (2022/2023). *Analisi archeometriche di malte storiche: il caso studio della chiesa e del cimitero di San Giovanni Evangelista in Castel Seprio*. (Master's thesis). Università degli Studi di Padova, Dipartimento dei Beni Culturali: Archeologia, Storia dell'arte, del cinema e della musica.

- Riederer, J. (2004). Thin Section Microscopy Applied to the Study of Archaeological Ceramics. *Hyperfine Interactions* 154 (2004) 143–158. <https://doi.org/10.1023/B:HYPE.0000032029.24557.b1>
- Rispoli, C., et al. (2020). Unveiling the secrets of Roman craftsmanship: mortars from Piscina Mirabilis (Campi Flegrei, Italy). *Archaeological and Anthropological Sciences* 12: 8. DOI: <https://doi.org/10.1007/s12520-019-00964-8>
- Roosz, C., et al. (2015). Crystal structure of magnesium silicate hydrates (MSH): The relation with 2: 1 Mg–Si phyllosilicates. *Cement and Concrete Research*, 73, 228-237. DOI: <https://doi.org/10.1016/j.cemconres.2015.03.014>
- Rosso, F. et al. (2022). Urban morphology parameters towards multi-risk scenarios for squares in the historical centers: Analyses and definition of square typologies and application to the Italian context. *Journal of Cultural Heritage* 56 (2022) 167–182. <https://doi.org/10.1016/j.culher.2022.06.012>
- Rubert, S., et al. (2018). Hydration mechanisms of supersulfated cement: The role of alkali activator and calcium sulfate content. *Journal of Thermal Analysis and Calorimetry*, 134, 971-980.
- Sagin, E. U., et al. (2021). Lime mortar technology in ancient eastern Roman provinces. *Journal of Archaeological Science: Reports* 39 (2021) 103132. DOI: <https://doi.org/10.1016/j.jasrep.2021.103132>
- Scaparro, M. et al. (1994). *Teatri greci e romani: alle origini del linguaggio rappresentato*. Edizioni SEAT.
- Schanda, J. (2007). *Colorimetry: Understanding the CIE system*. John Wiley & Sons.
- Schiavon, N., et al., G.A. Mazzocchin. (2009). The Provenance of Sand in Mortars from Roman Villas in Ne Italy: a Chemical-Mineralogical Approach. *The Open Mineralogy Journal*, 2009, 3, 32-39.
- Sear, F. (2006). *Roman theatres: An architectural Study*. Oxford university press.

- Secco et al. (2019). Mineralogical clustering of the structural mortars from the Sarno Baths, Pompeii: A tool to interpret construction techniques and relative chronologies. *Journal of Cultural Heritage* Vol. 40. 265-273.
- Secco, M., et al. (2020). Technological transfers in the Mediterranean on the verge of Romanization: Insights from the waterproofing renders of Nora (Sardinia, Italy). *Journal of Cultural Heritage*, 44, 63-82. <https://doi.org/10.1016/j.culher.2020.01.010>
- Secco, M., et al. (2022). Cementation processes of Roman pozzolanic binders from Caesarea Maritima (Israel). *Construction and Building Materials*, 355, 129128. <https://doi.org/10.1016/j.conbuildmat.2022.129128>
- Shi, Z., et al. (2016). Experimental studies and thermodynamic modeling of the carbonation of Portland cement, metakaolin and limestone mortars. *Cement and Concrete Research*, 88, 60-72. DOI: <http://dx.doi.org/10.1016/j.cemconres.2016.06.006>
- Silva, A. S., et al. (2014). Long-term behavior of lime–metakaolin pastes at ambient temperature and humid curing condition. *Applied Clay Science*, 88, 49-55.
- Stanjek, H. et Häusler, W. (2004). Basics of X-ray Diffraction. *Hyperfine Interactions* 154: 107–119, 2004. <https://doi.org/10.1023/B:HYPE.0000032028.60546.38>
- Stella, G., et al. (2018). Historical building dating: a multidisciplinary study of the Convento de São Francisco (Coimbra, Portugal). *Geochronometria*, 45(1), 119-129.
- Stoops, G. (2003). Guidelines for analysis and description of soil and regolith thin section. (Vepraskas, M. J.). Soil Science Society of America, Inc. Madison, Wisconsin, USA.
- Štukovnik, P., et al. (2015). Influence of alkali carbonate reaction on compressive strength of mortars with air lime binder. *Construction and Building Materials*, 75, 247-254.
- Štukovnik, P., et al. (2019). Detailed investigation of ACR in concrete with silica-free dolomite aggregate. *Construction and Building Materials*, 216, 325-336.
- Štukovnik, P., et al. (2020). Alkali-dolomite reaction in air lime mortar – implications for increased strength and water resistance. *Journal of Cultural Heritage* 45 (2020) 160–168. DOI: <https://doi.org/10.1016/j.culher.2020.02.007>

- Tapete, D., et al. (2014). Petrographic study of lime-based mortars and carbonate incrustation processes of mural paintings in Roman catacombs. *Periodico di Mineralogia* Vol. 82, 3 december 2013, 503.
- Tenconi, M., et al. (2018). Technological and microstructural characterization of mortars and plasters from the Roman site of Qasr Azraq, in Jordan. *Journal of Cultural Heritage* 33 (2018) 100–116. DOI: <https://doi.org/10.1016/j.culher.2018.03.005>
- Theodoridou, M., et al. (2013). New evidence of early use of artificial pozzolanic material in mortars. *Journal of Archaeological Science* 40 (2013) 3263e3269. DOI: <http://dx.doi.org/10.1016/j.jas.2013.03.027>
- Thomson, M. (2005). Properties of lime mortar. *Structure Magazine*, 26-29.
- Thomson, M. L., et al. (2004, July). Porosity of historic mortars. In 13th international brick and block masonry conference Amsterdam.
- Tosi, G. (1994). Gli edifici per spettacolo di Verona. In: *Spettacolo in Aquileia en ella Cisalpina Romana*. Centro di antichità altoadriatiche.
- Tosi, G. (1999). *Teatri e anfiteatri dell'Italia romana nella tradizione grafica rinascimentale*. Commento archeologico. Imprimerie Editrice. Padova: Imprimerie Editrice.
- Tronchin, L. et Bevilacqua, A. (2022). Historically informed digital reconstruction of the Roman theatre of Verona. Unveiling the acoustics of the original shape. *Applied Acoustics*. Volume 185, 1 January 2022. DOI: <https://doi.org/10.1016/j.apacoust.2021.108409>
- Truscott, M. C. (2003). Tradition or invention: Remembering and reviving meaning of places. In: 14th ICOMOS General Assembly and International Symposium: 'Place, memory, meaning: preserving intangible values in monuments and sites', 27 – 31
- Ul-Hamid, A. (2018). *A Beginners' Guide to Scanning Electron Microscopy*. (Springer Cham). Springer Nature. Dhahran, Saudi Arabia. <https://doi.org/10.1007/978-3-319-98482-7>
- Vaia, F. (1965). Ricerche sui depositi sabbiosi del fiume Adige nel tratto dalla sorgente a Bolzano e dei suoi principali affluenti. *Atti dell'Accademia roveretana degli Agiati*. B, Classe di scienze matematiche, fisiche e naturali, 5, 57-67.

Vasanellia, E. et al. (2005). Ultrasonic pulse velocity for the evaluation of physical and mechanical properties of a highly porous building limestone. *Ultrasonics*, Vol. 60. 33-40 (2015). <https://doi.org/10.1016/j.ultras.2015.02.010>

Veiga, R. (2017). Air lime mortars: What else do we need to know to apply them in conservation and rehabilitation interventions? A review. *Construction and Building Materials* 157 (2017) 132 - 140. DOI: <https://doi.org/10.1016/j.conbuildmat.2017.09.080>

Villa, C. F. R., et Blanco-Várela, M. T. (2000). Influencia de tratamientos de hidrofugación en las propiedades de morteros de cal y cal y puzolana.

Vitti, P. (2021). Mortars and masonry—structural lime and gypsum mortars in Antiquity and Middle Ages. *Archaeological and Anthropological Sciences* 13: 164. DOI: <https://doi.org/10.1007/s12520-021-01408-y>

Whittig, L. D. et Allardice, W. R. (1986). X-Ray Diffraction Techniques. In: Klute, A., Ed., *Methods of Soil Analysis, Part 1: Physical and Mineralogical Methods*, American Society of Agronomy, Madison, 331-362.

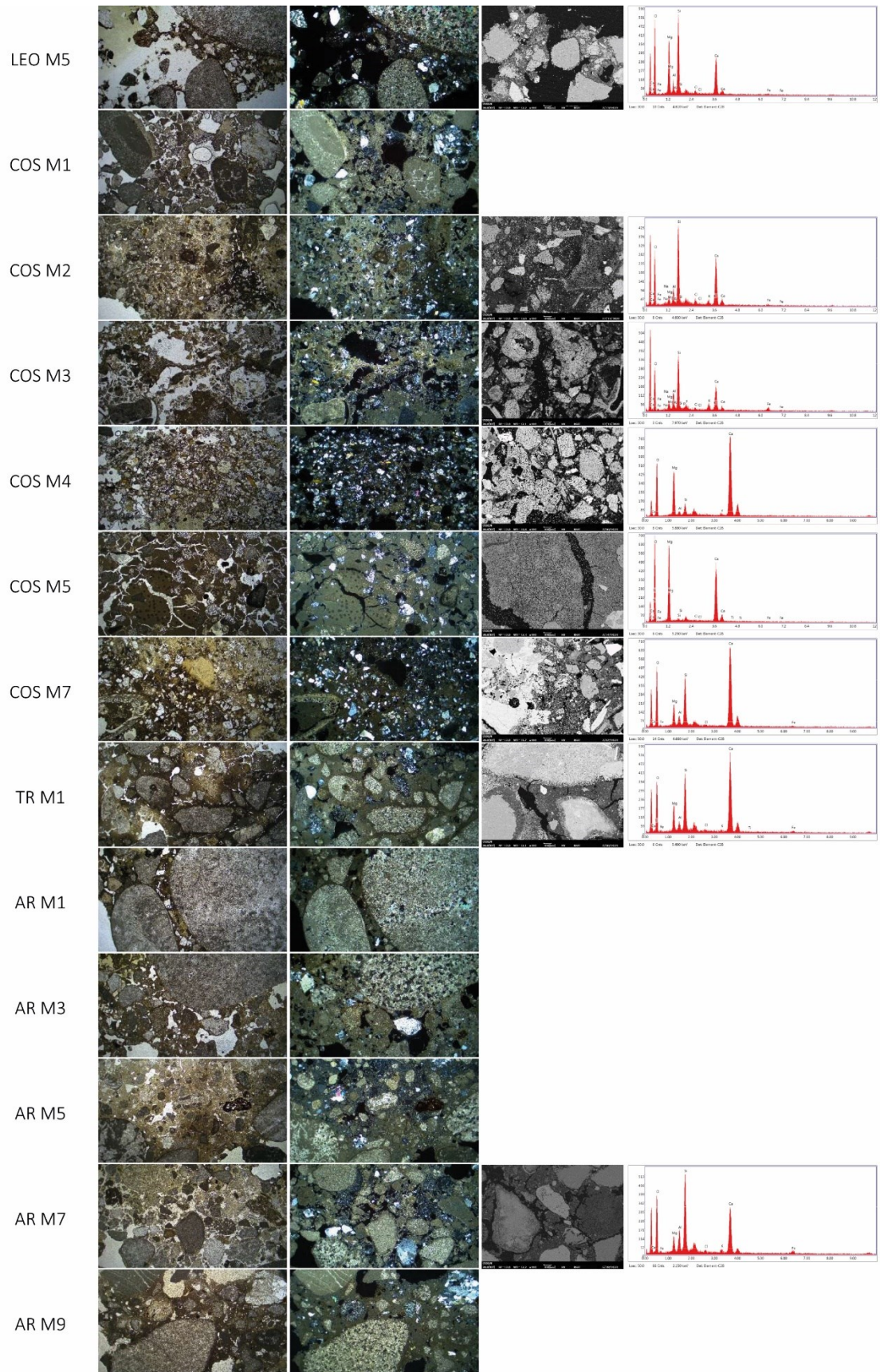
Yurtdas, I., et al. (2013). Influence of alkali silica reaction (ASR) on mechanical properties of mortar. *Construction and Building Materials*, 47, 165-174.

Zendri, E., et al. (2004). Interaction between clay and lime in “cocciopesto” mortars: a study by ²⁹Si MAS spectroscopy. *Applied Clay Science* 25 (2004) 1 – 7. DOI: 10.1111/j.1475-4754.2010.00565.x

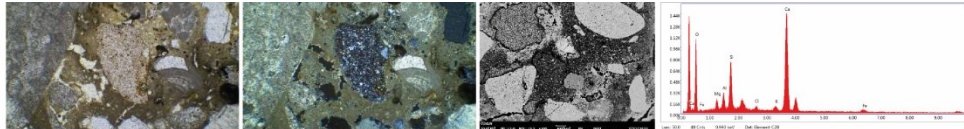
11. Chapter XI - Annex and Appendix

Context / site	Sample	Colorimetry	XRPD	OM	SEM-EDS	XRPD G.S.	SEM-EDS G.S.	NMR
Torre della porta	RED M1	x	x					
	RED M2	x	x	x	x	x	x	
	RED M3	x	x					
	RED M4	x	x					
	RED M5	x	x	x				
Odeum	OD M1	x	x					
	OD M2	x	x	x	x			
	OD M3	x	x	x	x			
	OD M4	x	x					
	OD M5	x	x					
Tempio (castello S. Pietro)	CSP M1	x	x	x	x			
Capitolium and Archeological area Corte	RM M1	x	x	x				
	SGA M1	x	x	x	x			
	SGA M2	x	x	x	x	x	x	
	SGA M3	x	x	x				
	SGA M4	x	x					
	SGA M5	x	x					
	SGA M6	x	x	x				
	SGA M7	x	x					
SGA M8	x	x						
Curia	AP M1	x	x	x	x	x	x	x
Porta Leoni	LEO M1	x	x	x	x			
	LEO M2	x	x	x				
	LEO M3	x	x					
	LEO M4	x	x	x	x	x	x	
	LEO M5	x	x	x	x	x	x	
	LEO M6	x	x					
Defensive walls on San Cosimo	COS M1	x	x	x				
	COS M2	x	x	x	x			
	COS M3	x	x	x	x			x
	COS M4	x	x	x	x			
	COS M5	x	x	x	x	x	x	
	COS M6	x	x					
	COS M7	x	x	x	x	x	x	
	COS M8	x	x					
Theatre	TR M1	x	x	x	x	x	x	x
Arena (amphitheater)	AR M1	x	x	x				
	AR M2	x	x					
	AR M3	x	x	x				
	AR M4	x	x					
	AR M5	x	x	x				
	AR M6	x	x					
	AR M7	x	x	x	x	x	x	x
	AR M8	x	x					
	AR M9	x	x	x				
	AR M10	x	x					
	AR M11	x	x	x	x			
	AR M12	x	x	x	x	x	x	
	AR M13	x	x	x	x			

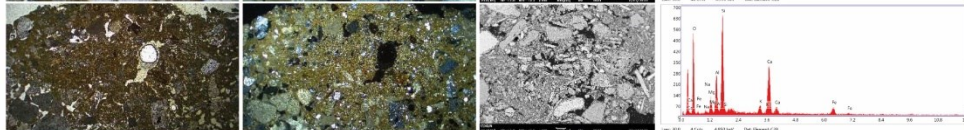
Sample	OM (P.P.)	OM (X.P.)	SEM	EDS
RED M2				
RED M5				
OD M2				
OD M3				
CSP M1				
RM M1				
SGA M1				
SGA M2				
SGA M3				
SGA M6				
AP M1				
LEO M1				
LEO M4				



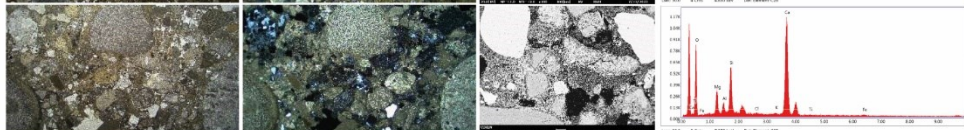
AR M11

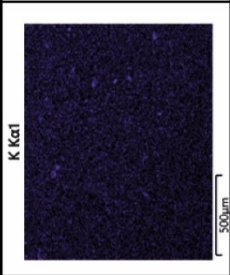
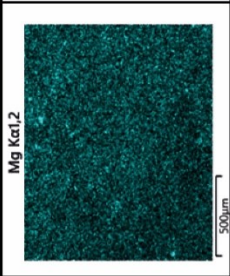
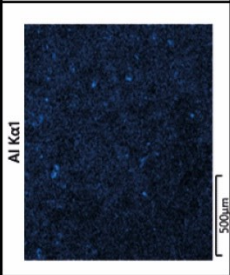
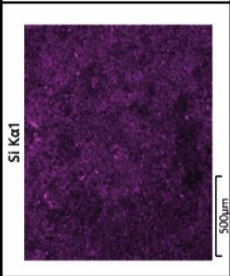
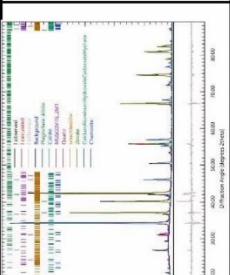
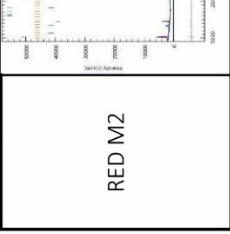
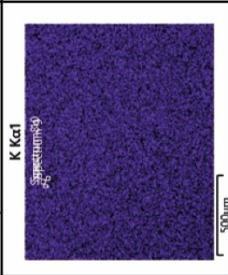
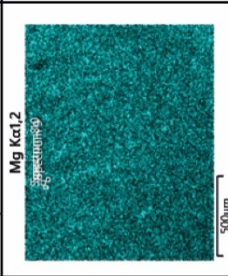
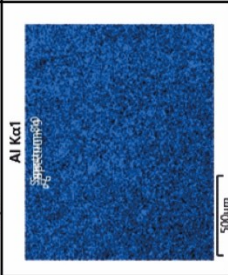
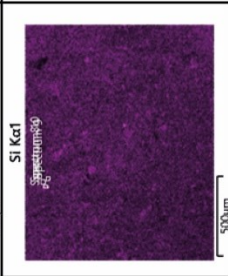
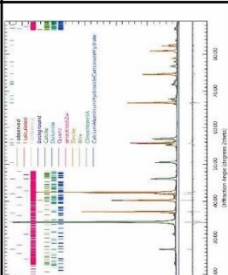
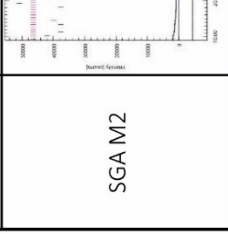
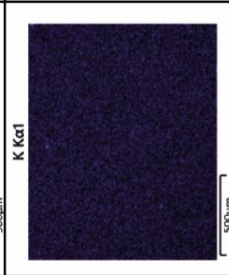
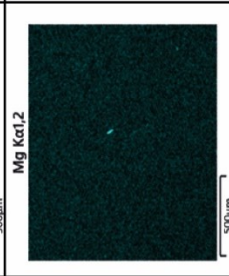
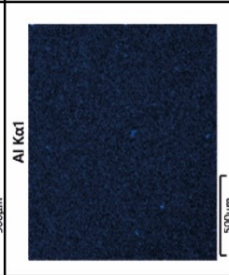
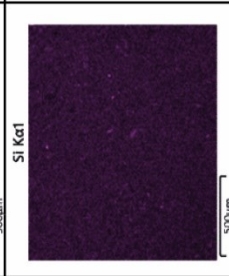
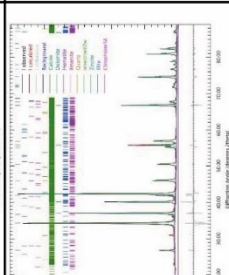
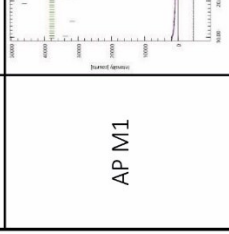
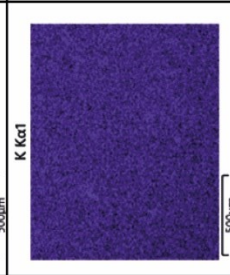
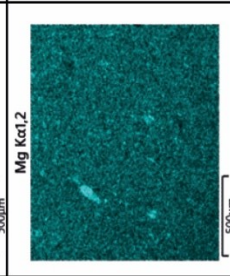
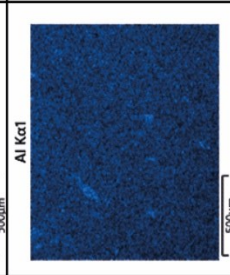
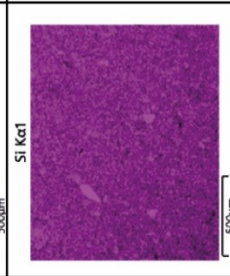
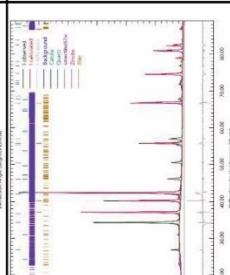
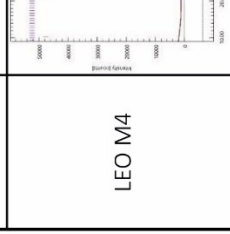


AR M12



AR M13



Sample	XRPD G.S.	SEM-EDS (Si)	SEM-EDS (Al)	SEM-EDS (Mg)	SEM-EDS (K)	SEM-EDS (P)
RED M2						
SGA M2						
AP M1						
LEO M4						
LEO M5	